HOST CELL SIGNALING IN RESPONSE TO RSV INFECTION

by

Ping Liu, MD.

Dissertation
Presented to the Faculty of The University of Texas Graduate School of
Biomedical Sciences at Galveston
in Partial Fulfillment of the Requirements
for the Degree of

Doctor of Philosophy

Approved by the Supervisory Committee

Edward B. Thompson
Roberto P. Garofalo
Stokes Peebles
Kui Li
Allan R. Brasier

April, 2008
Galveston, Texas

Key words: New therapy for RSV infection, Kinase inhibitor

To my dear mother, Zhenru Li,
Who always watches me from the heaven;

To my wonderful wife, Yafei Huang,
who gives me unreserved love and support throughout these years;

To my two precious angels, Marissa and Serena,
who make my life full of joy and surprises.

ACKNOWLEDGEMENTS

First and foremost I would like to give my heartfelt thanks to my mentor, Dr. Allan R. Brasier, who has been my role model as an ingenious and yet hard-working scientist. Before I started graduate school here at UTMB, I was enthusiastic, but quite innocent about scientific research. It was Dr. Brasier who opened the door of scientific research in front of me. Under his direct supervision, I learned a variety of techniques and gained essential skills in molecular biology, such as, PCR. I still remember the day when he himself taught me how to handle the pipette properly under the sterile hood. But much more importantly, I learned from him how to develop independent thinking, how to foster creative ideas, and how to overcome hurdles we may encounter in research. Dr. Brasier has always encouraged me to pursue my own research hypothesis, to test innovative ideas, and to draw my own conclusions. At times when I stumbled or was frustrated at certain project, he would always guide me to sort out the problems and find solutions. Despite his busy work schedule, he has always been there for me whenever I have questions, concerns or need help. His enthusiasm in research, his meticulous attitude in treating scientific findings, and his kindness and generosity towards anyone who is in need have been and will always be a true inspiration for my career and my life.

All past and present members of Dr. Brasier's lab have also provided tremendous help for my research, without which I could not have gotten this far today. In particular, I would like to thank Bing Tian, Muping Lu, Ruwen, Cui, Tieying Hou, Hong Sun, and Tao Hai for their unconditional support throughout the years.

My appreciation also goes to Dr. Roberto R. Garofalo for being the "technical support" for all my RSV study, Dr.Kui Li for being the mentor for all the IRF3 study, Dr. Edward B. Thompson for providing academic and personal guidance during times of difficulties.
.

HOST CELL SIGNALING IN RESPONSE TO RSV INFECTION

Ping Liu, MD.
The University of Texas Graduate School of Biomedical Sciences at Galveston, 2008

Supervisor: Allan R. Brasier

RSV infection is the most important cause of hospitalization of infants, and is also the major cause for admissions in adults with chronic cardiac disease and pulmonary diseases. So far, there is no effective treatment or vaccine against RSV infection. Intensive studies have been performed to understand mechanisms and consequences of RSV-induced host cell signaling. My dissertation project provides three major contributions to this field.

Firstly, I found that retinoic acid-inducible gene I (RIG-I) and Toll like receptor 3 (TLR3) play distinct roles in mediating RSV-induced innate immune responses. Short interfering RNA (siRNA)-mediated RIG-I "knockdown" significantly inhibited the translocation of nuclear factor-kappaB (NF-κB) and interferon response factor 3 (IRF3) to the nucleus at the early phase of viral infection. In contrast, siRNA-mediated TLR3 knockdown did not affect RSV-induced NF-κB binding to DNA but block the activating phosphorylation of NF-κB /RelA at serine residue 276.

Secondly, I first demonstrated that RIG-I was involved in the activation of NIK·IKKα complex, two key noncanonical kinases that induce the protelytic processing of an IκBα-like inhibitor p100 to p52. I also proved that a fraction of RelA was associated with cytoplasmic p100. In addition, the RSV-induced proteolysis of p100 not only produces p52, but also releases RelA and increases its nuclear translocation. This finding suggested that part of the RelA activation in response to RSV infection was induced by the NIK·IKKα complex. Because inhibition of NIK·IKKα does not affect RSV replication but reduces inflammatory chemokine production, this protein complex could be a good target for drug treatment of RSV infection.

Thirdly, our previous study has reported the existence of IKKγΔ, a splicing variant of IKKγ, which excludes exon 5. I compared the function of IKKγ and IKKγΔ in response to ssRNA viruses. I found that in contrast to IKKγ, which is essential for both NF-κB and IRF3 activation, IKKγΔ failed to activate IRF3 in response to either Sendai virus or respiratory syncytial virus (RSV). However, IKKγΔ mediated NF-κB activation was intact. I demonstrated that the missing region of IKKγΔ made it unable to recruit TANK, a key factor that recruits atypical IKKs to activate the IRF3 pathway.

TABLE OF CONTENTS

Page

CHAPTER V: Summary and Future Directions

LIST OF TABLES

LIST OF FIGURES

LIST OF ILLUSTRATIONS

LIST OF ABBREVIATIONS

RSV   Respiratory syncytial virus

URI   Upper respiratory infection

LRTI   Lower respiratory tract infection

NF-κB   Nuclear factor-kappaB

IKK   IκB kinase

IRF3   Interferon response factor 3

TLR   Toll like receptor

Myd88   Myeloid differentiation primary-response gene 88

IRAK   IL-1R-associated kinase

TRIF   TIR-domain-containing adaptor protein inducing IFN-β

TBK1   TANK-binding kinase 1

RIG-I   Retinoic acid inducible gene I

MAVS   Mitochondrial antiviral signaling

TANK   TRAF family member-associated NF-κB activator

CARD   Caspase recruitment domain

TIM   TRAF-interaction domains

Mda5   Melanoma differentiation-associated gene-5

NIK   NF-κB inducing kinase

TRAF   TNF receptor-associated factor 3

ISRE   Interferon response element

STAT   Signal transducers and activators of transcription

CHAPTER I: GENERAL INTRODUCTION

1.1 THE IMPACT AND MAGNITUDE OF RSV INFECTION.

Respiratory syncytial virus (RSV) is a significant human pathogen that produces a variety of respiratory diseases including simple upper respiratory tract infection (URI) such as epiglotitis or laryngitis, and lower respiratory tract infection (LRTI) like acute bronchiolitis or pneumonia (113). Extrapulmonary manifestations are also very common in RSV infected children, and common life-threatening manifestations include central apnea, hyponatraemia associated status epilepticus, ventricular tachycardias and fibrillation, and other cardiac symptoms (34). The major targets of RSV infection are infants, very young children, elderly people and those with a weakened immune system (32,82,83,147). RSV infection is the most common cause of admission to pediatric intensive care units due to respiratory failure in infancy and is also the major cause for admissions in adults with chronic cardiac disease and pulmonary disease(13,113).   A retrospective study, the National Hospital Discharge Survey from the years 1997 to 1999, also found that RSV is the most important cause of hospitalization of infants for any reason (81). This study estimated that a hospitalization rate of 25.2 hospitalizations per 1000 infants. RSV-caused LRTI was responsible for 86,000 hospitalizations, 1.7 M office visits, and an estimated annual direct medical cost of $394 M in the year 2000.

1.2 RSV VIROLOGY

The spread of RSV requires close contact with infected persons or contact with objects contaminated by infected respiratory secretions. Via its surface glycoprotein, RSV attaches to epithelial cells of the nasopharynx and initiates intracellular replication. Incubation time is usually about 2-8 days. RSV is an enveloped, negative-sense single-stranded RNA virus belonging to paramyxovirus family. Two subgroups, A and B, have been identified.

RSV has a 15,222 nucleotide single-stranded, negative-sense RNA genome, which codes for 11 proteins, including transmembrane proteins G, F and SH, nucleocapsid associated proteins N, P, L and M2, the matrix protein M, and non-structural proteins NS1 and NS2 (23,63,102,139).   Each protein has its specific function

1

in the viral life cycle. The development of powerful reverse genetics systems has allowed systematic dissection of the functions of the remaining RSV proteins (93). RSV attaches to target cells via the glycosylated glycoprotein (G), and in mouse models, the G protein has been linked to pulmonary eosinophilia and increased expression of Th2 cytokines (43). F is responsible for viral fusion with cell membranes and is the target for neutralizing antibodies (145). The hydrophobic 1A protein is a low abundance integral membrane protein that participates in cell fusion with the F (fusion) protein. The small 1A protein is found on cell surface, which strongly suggests that it is a counterpart to the SH protein that has been described for simian virus type 5 (108). The virus then enters the cell cytoplasm, uncoats, and the viral RNA serves both as a template for the synthesis of a full-length, positive-sense complementary (c) RNA (a template for transcription of virion RNA), as well as for the positive-sense messenger RNAs (templates for translation of viral proteins). The nucleocapsid (N) protein as well as the acidic phosphoprotein (P) and the L protein are parts of the RNA dependent RNA polymerase complex (51). The nonstructural (NS) proteins NS-1 and –2 are unique to the pneumovirus genus, and inhibit type I interferon reaction in infected cells; NS2 is also found to inhibit minigenome transcription (5,77). The M2 protein is also unique to the pneumovirus genus, and acts as an elongation factor for viral transcription (22). M protein is associated with RSV nucleocapsids and can inhibit virus transcription (46).

1.3 THE DEVELOPMENT OF RSV VACCINE AND TREATMENT

In the 1960s, four groups started clinical trials using formalin-inactivated (FI)-RSV vaccines. These vaccines have been shown to enhance the disease rather than protecting the children from subsequent natural infection (24,50). In one of the studies, 80 percent of children using FI-RSV vaccine required hospitalization and 2 children died, whereas only 5 percent of those who received a control parainfluenza vaccine needed hospitalization. During natural infection, FI-RSV vaccinees usually experienced LRTI, while control vaccinees only experienced rhinitis, pharyngitis and/or bronchitis (74). Autopsy reports from the children who died described a lung infiltrate consisting mostly of neutrophils, with also eosinophils, which suggest the importance of the host

2

inflammatory response in the enhancement of disease (114). Analysis of sera from hospitalized FI-RSV vaccinees revealed production of non-neutralizing antibodies against the F and G proteins. This result suggests that a lack of neutralizing antibodies may contribute to the enhancement of disease by delaying the clearance of virus from the lungs (24).

For a long period of time, the detrimental effects of the FI-RSV vaccine led to reduced efforts in RSV vaccine development and limited the available resources for RSV vaccine research. As a result, the progress in RSV vaccine development has been very slow. In addition, several obstacles somewhat unique for RSV are difficult to overcome. Firstly, the target for vaccination is the neonate. Neonates have an immune system that fails to respond adequately to conventional vaccines. Also, maternal antibodies in these neonates may interfere with the development of active immunity. Secondly, since RSV has two strains, A and B, and since natural RSV infection only leads to protective immunity after re-exposures, it is likely that several vaccinations will be required to induce protective immunity. Thirdly, because there is a lack of fully relevant animal models for pre-clinical trials, testing vaccine candidates in neonate presents significant safety issues. Finally, since RSV enters the body through airway epithelial cells, delivering a RSV vaccine to induce immunity at these mucosal surfaces may be critical.

1.4 RSV TREATMENT

Supportive therapies like supplemental oxygen, nasal suctioning, and fluids to prevent dehydration, are the major treatments for RSV-infected infants with acute bronchiolitis. Hospitalization is required for those who have high risk including those younger than three months and those with a preterm birth, cardiopulmonary disease, immunodeficiency, respiratory distress, or inadequate oxygenation.

Ribavirin is a nucleotide analogue with in vitro activity against influenza A and B, measles, and RSV. Possible benefits include reduced time on ventilator, shortened length of stay, and improved clinical scores (97,116). However, some experts challenged the experimental methods in the study of acute RSV bronchiolitis treated by Ribavirin. In one study of infants on mechanical ventilation for severe RSV infection, the placebo group

received nebulized water, an agent known to cause bronchospasm (136). Thus, the reported advantage of Ribavirin actually may have been caused by adverse effects from the placebo. This interpretation is supported by the lack of significant differences between the treatment and control groups in a later study that used nebulized saline placebo (53). In addition, a meta-analysis concluded there was no evidence to support the use of Ribavirin in the treatment of RSV bronchiolitis (115). The American Academy of Pediatrics (AAP) generally does not recommend Ribavirin treatment for RSV infections and the Agency for Healthcare Research and Quality (AHRQ) classifies Ribavirin as "probably ineffective."

The evidence for use of corticosteroids in the treatment of RSV infection remains controversial. The specific steroid doesn't matter, because there is no difference in benefit from oral prednisolone (49,153), intravenous dexamethasone (10), or budesonide (12). A recent meta-analysis of corticosteroids for bronchiolitis showed small, statistically significant improvements in clinical symptoms, length of stay, and duration of symptoms (45). However, subset analysis for first-time wheezing showed that corticosteroid treatment did not produce significant improvement, and the practical relevance of the small differences between treatment groups is not clear.

RSV is a disease for whick we lack effective vaccines or treatments. Further studies on RSV are required to find new points of attack by drugs. Hence, my research focuses on how RSV activates intracullar cell signaling and discovering new targets for RSV treatment.

1.5 DETECTION OF RSV INFECTION BY AIRWAY EPITHELIAL CELLS

Epithelial cells are known to have at least two distinct mechanisms for detecting the presence of viral replication. The family of Toll-like receptors (TLRs) was first described as an important sensor for detecting foreign pathogens. In 2001, Alexopoulou and colleges reported the recognition of double-stranded RNA (dsRNA) by the TLR3 isoform (4). Since then, TLR3 has been believed to play a critical role on activating innate immune system in response to viral infection. However, this notion has been challenged from the studies using TLR3 deficient mice in which no difference in immune

response was observed, compared to wild type mice, in response to several viruses. This finding resulted in the discovery of a new family of PRRs, cytoplasmic dsRNA receptors. Two Dexd/H box RNA helicases, RIG-I and Mda-5, have been reported to recognize different viruses, especially single-stranded RNA viruses (70,112). The signaling pathways initiated by these two types of sensor have also referred to as "TLR dependent" or "TLR independent" pathways. In the case of RSV infection, the activation of both TLR dependent and -independent pathways have been reported (87,118,119).

TLR dependent pathways

The TLR-family members are pattern recognition receptors (PRRs) that recognize different types of pathogens including LPS, carbohydrate, peptide, double-stranded RNA, single-stranded RNA and DNA. So far, 12 TLR family members have been identified. Interestingly, different TLRs are expressed in different compartments of cells. TLR1 -2 -4 -5 and -6 localize at the cell surface, whereas TLR7 -8 and -9 are contained within the endosomal compartment. The localization of TLR3 is apparently more dynamic, with both cell surface associated and endosomal bound TLR3s having been reported (101,106,146).

TLRs are composed of an ectodomain of leucine-rich repeats (LRRs) which are involved in ligand binding, and a cytoplasmic Toll/interleukin-1 (IL-1) receptor (TIR) domain that interacts with TIR-domain-containing adaptor molecules. Two types of downstream adaptors have been identified to associate with different TLRs. Myeloid differentiation primary-response gene 88 (Myd88) has been shown to interact with most of the TLRs, except TLR3. Downstream of Myd88, IL-1R-associated kinase 1 (IRAK1), IL-1R-associated kinase 2 (IRAK2) and TNFα receptor-associated factor 6 (TRAF6) form a large complex and recruit the IκB kinases (IKKs). The other TLR adaptor, TIR-domain-containing adaptor protein inducing IFN-β (TRIF), is only recruited by TLR3 and TLR4 during signaling transduction. TLR pathways ultimately converge on activation of the latent cytoplasmic NF-κB transcription factor through the IKKs. In addition, the interferon response factor (IRF) pathway is activated only by TLR3 and

TLR4 via a process involving recruitment of TANK-binding kinase 1 (TBK 1) and IKKε to TRIF (106,107). NF-κB and IRF are key transcription factors in activation of type I IFNs.

In response to RSV infection, TLR3 -4 -7/8 and -9 have been reported as RSV sensors in different cell types. In airway epithelial cells, TLR3 and -4 have been shown to interact with RSV, whereas TLR7/8 and TLR9 functions in plasmacytoid dendritic cells (pDCs).

The TLR4 pathway

TLR4 has been reported to recognize bacteria endotoxin (lipopolysaccharide, LPS) and RSV fusion protein (F protein) (80). In unstimulated airway epithelial cells, TLR4 is expressed at very low levels on the cell surface and as a result, are barely responsive to LPS. However, RSV infection increases expression and cell surface translocation of TLR4 (170). Confirming this finding, increased TLR4 expression has been reported in monocytes of RSV infected infants (40). One hypothesis of this finding is that after RSV exposure, TLR4 is increased in airway epithelium and responses to environmental LPS exposure, which increase the happening of asthma (103). The relationship between RSV infection and polymorphism of the TLR4/CD14 complex has also been studied in humans. Nonsynonmous TLR4 ($Asp^{299}Gly$ and $Thr^{399}Ile$) and the noncoding CD14/-159 polymorphisms were analyzed in 99 infants with severe RSV bronchiolitis, 82 ambulatory infants with mild RSV bronchiolitis and 90 healthy adults composed the 2 control groups. This study showed that the $Asp^{299}Gly$ and $Thr^{399}Ile$ mutations were significantly overrepresented in severe RSV bronchiolitis (142). By contrast, studies of TLR4 function in RSV infected animal models have revealed controversial results. One study showed that RSV infection of TLR4 deficient mice (in the C57/BL10ScNCr background) exhibited impaired pulmonary recruitment of $CD14^{+}$ cells, deficient NK cell activity, reduced IL-12 expression, and impaired virus clearance compared to TLR4 expressing mice(58). In contrast, another study using TLR4 defective

6

mice (in BALB/c strain) showed that the absence of TLR4 had no impact on NK cell recruitment or activity, as well as no effect on RSV clearance and recruitment of inflammatory cells. This study also indicated that the C57BL/10ScNCr mice used in previous study had an additional defect in the IL-12R which contributes to the impaired RSV control (33). In a separate study investigating NF-κB activation in the airways of RSV infected BALB/c mice, the role of alveolar macrophages (AMs) and TLR4 were described in mediating two different patterns of NF-κB activation. The first NF-κB response occurs early after RSV inoculation, is AM and TLR4 dependent, and is viral replication independent, whereas the second response involves epithelial cells and/or inflammatory cells, is TLR4 independent, and requires viral replication (55). These data suggest that TLR4 plays a minor (early) role in the RSV induced innate immune response.

Studies of TLR4 function in response to other paramyxoviruses have produced similar conclusions. Sendai virus (mouse parainfluenza type 1) shares many features with RSV, including a structurally and functionally similar F protein. One study showed that in response to Sendai virus, TLR4 mutant and wild type mice showed no difference in pulmonary viral loads, histopathology, cytokine levels and leukocyte influx. As a result, the investigators concluded that TLR4 is not involved in host defense against Sendai virus infection (152). Pneumonia virus of mice (PVM) also shares many similarities with RSV. One study showed that in response to PVM, mouse body weight, pulmonary function values, histopathology, and pulmonary viral loads were no difference between TLR4 wild type and TLR4 deficient mice (36).

All these results suggest that TLR4 may not play such an important role as initially expected. However, RSV is not a natural pathogen of mice, and using mouse models to study RSV induced bronchiolitis might not be relevant. In human clinical trials, TLR4 polymorphisms did associate with severe RSV infection. More work will be required to resolve this issue.

The TLR3 pathway

In airway epithelial cells, RSV replication is necessary for inducing downstream signaling. As a negative single-stranded RNA virus, RSV requires full-length positive-sense RNA for synthesis of new viral RNA, yielding double-stranded RNA intermediates. So it is reasonable to believe that TLR3, the receptor for dsRNA, functions as an intracellular sensor for RSV infection. One study showed that inhibiting TLR3 expression with small interfering RNA decreased synthesis of CXCL10 and CCL5 but did not significantly reduce levels of IL-8 in response to RSV infection (119). Down-regulation of TLR3 did not affect viral replication. They suggested that at least part of anti-viral signaling is mediated by the TLR3 pathway in airway epithelial cells. Interestingly, similar to TLR4, our group and others also proved that in unstimulated airway epithelial cells, most of TLR3 are contained in the endosomal compartment, whereas after viral infection, some of the TLR3s redistribute to the cell surface. The mechanism and function of TLR3 relocalization are not clearly understood (52,87). Our study also showed that the induction of TLR3 expression is a paracrine effect-dependent on RSV-activated interferon beta (IFN-β) signaling. In IFN-β deficient Vero cells, RSV failed to increase TLR3 expression, whereas after adding conditioned-media from RSV-infected A549 cells into Vero cells, TLR3 expression was significantly induced (87). This result not only indicated the essential role of IFN-β for TLR3 induction, but also suggested the existence of other intracellular viral sensors at the early time point for RSV infection.

The animal studies of TLR3 suggested the specific role of this receptor against RSV infection. One study showed that in TLR3 deficient mice, but not wild type mice, an accumulation of eosinophils has been found after RSV exposure. TLR3 deficient mice also produced significant increases in Th2-type cytokines, IL-5, and IL-13, as well as an increase of mucus production compared with wild-type mice after RSV infection. However, RSV clearance is apparently not reduced in TLR3 deficient mice. This data suggested that TLR3 is necessary to maintain the proper immune environment in the lung and protect animals from developing further pathologic symptoms (118).

Together, these studies suggest that the anti-RSV function of TLRs may be not important as initially expected, and the existence of a new signaling pathway to detect RSV infection was indicated.

DExD/H box RNA helicases, ("TLR independent" pathways)

In 2004, retinoic acid inducible gene I (RIG-I), a gene encoding a DExD/H box motif-containing RNA helicase, was identified as an essential regulator for dsRNA-induced signaling (163). Over 100 helicases have been identified in the human genome related to various biological processes such as transcription, translation, mRNA splicing and siRNA processing. The DExD/H box helicases are of interest because they have the potential to unwind dsRNA, and RIG-I in particular, contains two caspase recruitment domains (CARDs) that interact with downstream molecules and result in the activation of transcription factors NF-κB and IRF-3. The RIG-I helicase domain contains ATPase activity and is responsible for dsRNA or ssRNA recognition (20). Another DExD/H box RNA helicase, melanoma differentiation-associated gene-5 (Mda5), also contains two tandems of CARD domains and is the closest relative of RIG-I (68,78). Both RIG-I and Mda5 have the ability to detect RNA viruses and polyinosine-polycytidylic acid (poly I:C)(163). It is now known that RIG-I and Mda5 recognize different types of dsRNAs and are activated by different viruses: RIG-I is essential for the production of type I IFNs in response to most ssRNA viruses including paramyxoviruses, influenza virus and Japanese encephalitis virus, whereas Mda5 is critical for picornavirus detection(71). Recently, another DExD/H box helicase, LGP2, has also been identified. LGP2 lacks the CARD region and does not activate IFN-beta gene expression. Its mRNA is induced by interferon, dsRNA treatment, or Sendai virus infection. LGP2 acts as a feedback regulator inhibiting the recognition of viral RNA by RIG-I and Mda5.

Interestingly, all known DExD/H box RNA helicases converge on the same downstream adaptor. Four different groups have reported this molecule at the same time with different names, mitochondrial antiviral signaling (MAVS), IFN-β promoter stimulator 1 (IPS-1), CARD adaptor inducing IFN-β (Cardif) and virus-induced signaling

adaptor (VISA). MAVS contains an NH2-terminal CARD domain, Proline-rich domain and a COOH-terminal transmembrane domain (TM) (72,79,100,109).

In 2006, our group first reported that RIG-I but not Mda5 is the intracellular RSV sensor. We demonstrated that RIG-I is the primary anti-RSV sensor in airway epithelial cells, and in the later time of infection, other antiviral signaling including TLR3 might be activated (87). Consistent with our study, Seya and colleagues proved that RSV induced IFN-β production is initiated by RIG-I but not the TLR3 pathway. They also showed that NAK-associated protein 1 (NAP1) was involved in the activation of IFN-β downstream of both RIG-I and TLR3 (121).

In summary, previous studies confirmed the role of RIG-I as an initial intracellular sensor for detecting RSV in airway epithelial cells.

1.6 HOST CELL SIGNALING AGAINST RSV INFECTION IN AIRWAY EPITHELIAL CELLS.

The NF-κB pathways

NF-κB is a family of cytoplasmic transcription factors that play a central role as a mediator of inflammation. The NF-κB family contains 5 members including 3 transactivating subunits, RelA, RelB, c-Rel, and 2 DNA binding subunits, NF-κB1 (p50) and NF-κB2 (p52) (135). A group of inhibitory ankyrin repeat-containing proteins, IκBα, IκBβ, IκBε, p100 and p105 are associated with NF-κB and sequester it in the ctyoplasm. Extracellular signaling induces phosphorylation-coupled proteolytic degradation of these inhibitors and releases NF-κB (6). Recently it has been appreciated that NF-κB activation can be controlled by at least two major pathways: the "canonical" and the "non-canonical" pathways.

Canonical Pathway of NF-κB activation

The canonical (or so-called "classical") pathway is rapidly and transiently activated by various stimuli, such as inflammatory cytokines (TNFα and IL1), mitogens

10

and DNA damage. In the example of TNFα stimulation, the activated TNF receptor recruits TNF receptor associated adapter proteins. This process leads to the phosphorylation of IKK, a 700 to 900 kDa multiprotein complex containing at least two catalytic subunits, IKKα and IKKβ, and a regulatory subunit, IKKγ (128). Activation of IKK complex leads to IκBα phosphorylation at specific N-terminal serine residues targeting them for ubiquitination by ubiquitin ligase complex and subsequent degradation by the 26S proteosome (47). This process releases sequestered Rel A•NF-κB1 to undergo modification and translocation to the nucleus where it can bind NF-kB specific promoter sequence and regulate expression of NF-κB dependent genes. My lab has demonstrated that RSV was able to induce the proteolysis of IκBα, and also a NEMO binding domain peptide inhibited RSV induced NF-kB activation in Balb/C mice (55,64). My lab has also identified reviewed the genetic network under NF-κB control in canonical and RSV infection (reviewed in (149)).

Non-canonical pathway of NF-κB activation

In contrast to the activation of canonical NF-κB pathway, the non-canonical pathway liberates Rel B•NF-κB2 complexes to translocate into the nucleus. Specific stimuli, including lymphotoxin β (29,158), CD40 ligand (25), DNA virus infection (157), and B-cell activating factor (BAFF) (21,73) are able to activate this pathway. Interestingly, neither IKKγ or IKKβ, key regulators of the canonical pathway, are required for activation of the non-canonical pathway (131,158). Rather, a kinase complex consisting of NIK and IKKα activates proteolytic processing of the NF-κB2 precursor, p100, into the 52 kDa active DNA binding isoform, p52. Newly formed p52 (NF-κB2) then dimerizes with cytoplasmic Rel B and translocates into the nucleus. In this pathway, NIK serves to activate IKKα as well as providing a docking site to recruit both p100 and IKKα into the complex (157). NIK therefore is an essential component of the non-canonical NF-κB activation pathway.

The interferon response factor (IRF) pathway

In addition to the NF-κB pathway, virus infection also activates the IRFs, a family of transcription factors controlling type I IFN expression, a group of cytokines inhibiting viral replication in airway epithelial cells (75). So far, nine human IRFs have been reported (IRF1-9); of these, IRF3 and -7 are the key regulators of type 1 IFN gene expression in response to viral infection (92,95).

IRF3 is constitutively expressed in the cytoplasm. In response to viral infection, IRF3 is phosphorylated, inducing dimerization and nuclear translocation (86,124). By contrast, IRF7 is expressed at a low level in most of cell lines and is strongly induced in response to viral infection. The virus-induced phosphorylation, dimerization and nuclear translocation of IRF7 are similar to the activation of IRF3 (92,123). Because IRF7 is strongly induced by type I IFN by an ISRE binding site in its promoter (89), a two-phase model of secretion of type I IFN in response to viral infection has been proposed. The first phase involves the detection of virus by cytoplasmic PRRs, activation of IRF3 and initial production of IFN-β/IFN-α4. Activated IRF3 or the secreted type I IFN increases IRF7 transcription. The second phase includes the activation of IRF7 and the induction of other type I IFNs. The IRF-controlled second phase of IFN secretion ensures a maximum antiviral response from host cells (133).

RSV-induced IRF activation was described by Casola and colleagues, showing IRF1 and -7 induction in response to RSV infection. They showed that signal transducers and activators of transcription (STAT) was a necessary factor for IRF induction. In addition, they also demonstrated that RSV-induced reactive oxygen species (ROS) is required for the activation of STAT. Using NADPH oxidase inhibitors, BHA and DPI, they successfully blocked the production of ROS, inhibited the phosphorylation of STAT, and consequently down-regulated the induction of IRF1 and IRF7 (88). Collins laboratory reported IRF3 activation in response to RSV infection. Their study showed that the two nonstructural proteins of RSV, NS1 and NS2, have the ability to inhibit IRF3 activation (138). The vaccine candidates using recombinant human RSVs without NS1, NS2 or both NS1 and NS2 gene have been developed.

The Janus activated kinase (Jak)-Signal Transducer and Activator of Transcription (STAT) pathway

In vitro, RSV replication in epithelial cells strongly induce Type I interferon (IFN) production (65,137,138), a group of anti-viral cytokines that play a central role in mucosal immunity (111). The Type I IFN primarily produced by epithelial cells is IFN-β which is a highly inducible cytokine and works in a paracrine manner to limit viral replication. Type I IFN induces expression of various IFN stimulated genes, including MxA, oligoadenylate synthetase, Protein Kinase R, speckled protein-100, and others that produce an anti-viral state by inhibition of viral translation and replication through largely unknown mechanisms (30). Because of its potent anti-viral effects, many viruses including RSV have adapted specific proteins that serve to antagonize IFN production. For example, using recombinant virus, several groups have shown that RSV nonstructural proteins antagonize the activation of IRF3, one of the major activators of IFN production (8,88,137,138)

The role and elements of IFN-induced signaling pathways are intensively being investigated (see reviews in (27,126,144)). Type I IFNs signal cells by activating receptor (IFNAR)-associated tyrosine kinases, known as the Janus kinases (Jak)-1 and Tyk2 kinases, followed by recruitment of the cytoplasmic STAT -1 and -2 isoforms, and their phosphorylation on critical Tyrosine residues 701 and 689, respectively. This modification produces intermolecular SH2-SH3 domain interactions, which results in STAT homo- and hetero-typic association, forming distinct types of complexes including STAT1, STAT2, and IRF9, termed ISGF3, are transported into the nucleus, where they bind high affinity sequences in target genes, recruiting p300/CBP coactivators, producing chromatin and factor induced acetylation, and inducing gene expression (61). Subsequently, STATs are dephosphorylated and exported from the nucleus (126).

Although the classic view of STAT activation involves kinase activation, the mechanisms by which RSV induces STAT activation appear more complex. In earlier studies, we have shown that RSV replication is a rapid inducer of ROS species, an event associated with accumulation of tyrosine phosphorylated STAT, without detectable changes in Jak/Tyk kinase activity(88).

CHAPTER II: RETINOIC ACID INDUCIBLE GENE-I MEDIATES EARLY ANTI-VIRAL RESPONSE AND TOLL LIKE RECEPTOR 3 EXPRESSION IN RESPIRATORY SYNCYTIAL VIRUS -INFECTED AIRWAY EPITHELIAL CELLS

2.1 INTRODUCTION

The detection of RNA virus by host cells occurs in a cell-type- and pathogen-type-specific manner. The sensors for viral infection primarily involve two kinds of receptors: the cytoplasmic PPRs including 2 DExD/H box RNA helicases, and the pathogen-associated molecular pattern receptors containing 12 Toll-like receptors (TLRs) (59,67,129,130). RIG-I is a highly inducible cytoplasmic RNA helicase that induces antiviral actions after binding double-stranded RNA (dsRNA), a pathway that has been implicated in antiviral responses to Sendai virus, vesicular stomatitis virus, and Newcastle disease virus, as well as the flaviviruses Japanese encephalitis virus, dengue virus 2, and hepatitis C virus (16,70,72). However, the role of RIG-I is cell-type dependent; for example, in fibroblast cells, RIG-I is the major sensor for viral infection, but in plasmacytoid dendritic cells, TLRs play a more important role (70,164). The role of RIG-I in mediating epithelial cell response to RSV infection in airway epithelial cells has not been investigated.

In this study, we examined the roles of RIG-I and TLR3 in RSV-induced gene expression in transformed human alveolar epithelial cells (A549). In a UV-cross-linking experiment, we found that active RIG-I bound RSV transcripts within 12 h of RSV exposure. siRNA-mediated RIG-I silencing inhibited the translocation of both NF-κB and IRF-3, as well as IFN-β, IP-10, CCL-5, and ISG15 expression, at the early phase of RSV infection (9 h p.i.). Surprisingly, siRNA-mediated TLR3 "knockdown" had little influence on the early response of RSV-induced genes but significantly inhibited their late expression. The role of TLR3 is not related to controlling RSV-induced NF-κB DNA binding, but rather is required to mediate the RSV-induced phosphorylation of RelA at serine residue 276. We further found that the TLR3 expression was RSV inducible via a

transcriptional mechanism mediated by two IFN-β -responsive elements, ISRE and STAT, in its proximal promoter. We further found that siRNA-mediated RIG-I silencing inhibited the upregulation of TLR3 and that the paracrine IFN-β secreted from infected cells was necessary and sufficient to induce the expression of TLR3. Together, these data indicate that TLR3 signaling in RSV infection is dependent on early RIG-I signaling and controls NF-κB/RelA subunit phosphorylation.

2.2 MATERIALS AND METHODS

Cell culture. Human A549 pulmonary type II epithelial cells (American Type Culture Collection [ATCC]) were grown in F12K medium (Gibco) with 10% fetal bovine serum (FBS), penicillin (100 U/ml), and streptomycin (100 μg/ml) at 37°C in a 5% CO_2 incubator. African green monkey kidney Vero cells (ATCC) were cultured in Eagle's minimum essential medium with 0.1 mM nonessential amino acids, 1.0 mM sodium pyruvate, and 10% FBS.

Virus preparation and infection. The human RSV A2 strain was grown in HEp-2 cells and purified by centrifugation on discontinuous sucrose gradients (151). The viral titer of purified RSV pools was 8 to 9 log PFU/ml, determined by a methylcellulose plaque assay. Viral pools were aliquoted, quick-frozen on dry ice-ethanol, and stored at − 70°C until they were used. For viral adsorption, cells were transferred into F12K medium containing 2% (vol/vol) FBS and RSV infected at a multiplicity of infection (MOI) of 1 for 18 h prior to harvest and assay.

siRNA-mediated gene silencing. siRNA against human RIG-I (M-012511-00) and TLR3 (M-007745-00) and control siRNA (D-001206-13) were commercially obtained (Dharmacon Research, Inc., Lafayette, CO) and transfected at 100 nM into A549 cells by using a TransIT-siQuest transfection kit (Mirus Bio Corp., Madison, WI) according to the manufacturer's instructions. Forty-eight hours after transfection, cells were RSV infected for the times indicated in the figure legends. The efficiency of siRNA silencing was evaluated using reverse transcriptase PCR (RT-PCR).

Plasmid construction. For the TLR3-Luc reporter, 1.0 kb of the human TLR3 promoter was amplified from A549 cell genomic DNA by PCR using the forward primer

5'-TCAGAGGATCCGGCATGTTCTTAGGCAAACC-3' and reverse prime 5'-TCAGAGATATCCTGTTGGATGACTGCTAGCC-3'. The PCR product was digested with BamHI/SmaI, gel purified, and ligated into the same sites in the pOLUC plasmid. Site-directed mutagenesis was conducted by rolling circle PCR (18 cycles) to mutate the ISRE1 site (forward primer, 5'-CCTCCCTAGGTTTCGCGCTCCTAATTTCTCAAA-3'; reverse primer, 5'-TTTGAGAAATTAGGAGCGCGAAACCTAGGGAGG-3'), the ISRE2 site (forward primer, 5'-AAGCTTTACTTTCACGATCGAGAGTGCCGTCT-3'; reverse primer, 5'-AGACGGCACTCTCGATCGTGAAAGTAAAGCTT-3'), and the STAT site (forward primer, 5'-TTTCTCCCTTTGCCCCCCTTGGAATGCACCAA-3'; reverse primer, 5'-TTGGTGCATTCCAAGGGGGGCAAAGGGAGAAA-3'). The pT1S vector was constructed by removing the cytomegalovirus (CMV) promoter from pCDNA6-V5-HisB (Invitrogen) and replacing it with a fragment containing the cytomegalovirus (CMV) promoter driving the tetracycline transactivator, followed by the simian virus 40 poly(A) signal and a tetracycline-responsive element (TRE). pT1S-RIG-I and pT1S-Mda5 were generated by inserting Flag-tagged RIG-I and Flag-tagged Mda5 into pT1S under the control of the TRE. Plasmids were purified by ion exchange chromatography (QIAGEN, Chatsworth, CA), and mutations were sequenced to verify authenticity. The PRDII luciferase plasmid was a kind gift from Michael Gale.

Helicase RNA UV Cross-linking and immunoprecipitation. The UV-cross-linking assay is modified from the assay described in reference (104). A549 cells were transfected with pT1S vector, pT1S-FLAG-RIG-I, or pT1S-FLAG-Mda5 for 48 h, and the transfectants were then infected with RSV (MOI = 1, 12 h). Cells were washed with prechilled phosphate-buffered saline (PBS) and UV irradiated for 5 min with an 8 W germicidal lamp at a 4-cm distance (GS gene linker; Bio-Rad). Cells were suspended in 500 µl of immunoprecipitation buffer (20 mM Tris-HCl, pH 7.4, 0.15 M NaCl, 5 mM EDTA, 4 µg/ml each leupeptin and pepstatin, and 1 mM phenylmethylsulfonyl fluoride), and lysed by sonication for 20 s. The lysates were treated with 20 U of RNase T_1 and 10 µg of RNase A for 30 min at 37°C to remove unbound RNA. Immunoprecipitation was conducted with anti-FLAG M2 antibody (Ab) for 4 h at 4°C and with protein A-Sepharose for 1 h at 4°C. Total RNA was isolated from half of the immunoprecipitation

16

using proteinase K, and the other half of the immunoprecipitation was fractionated by sodium dodecyl sulfate (SDS)-polyacrylamide gel electrophoresis for Western immunoblotting. Half of the RNA sample was subjected to 35 cycles of RT-PCR with RSV N protein-specific primers and visualized by agarose gel electrophoresis.

        RT-PCR and quantitative real-time PCR (QRT-PCR). Total RNA was extracted using acid guanidium phenol extraction (Tri Reagent; Sigma), and 1 µg of RNA was reverse transcribed using Moloney murine leukemia virus reverse transcriptase (New England Biolabs) in a 20-µl reaction mixture. One µl of cDNA product was diluted 1:2, and 2 µl was amplified in a 25-µl reaction mixture containing 12.5 µl of SYBR green supermix (Bio-Rad) and 0.4 µM each of forward and reverse gene-specific primers (Table 2.1), aliquoted into 96-well, 0.2-mm thin-wall PCR plates, and covered with optical-quality sealing tape. The plates were denatured for 90 s at 95°C and then subjected to 40 cycles of 15 s at 94°C, 60 s at 60°C, and 1 min at 72°C in an ABI 7000 thermocycler. After PCR was performed, PCR products were run on 2% agarose gels to assure a single amplification product. Duplicate cycle threshold (C_T) values were analyzed by using the comparative C_T ($\Delta\Delta C_T$) method (Applied Biosystems). The relative amount of target mRNA($2_T^{-\Delta\Delta C}$)was obtained by normalizing to endogenous GAPDH (glyceraldehyde-3-phosphate dehydrogenase) reference and expressed relative to the amount from uninfected cells. Three measurements were performed for each sample and the experiment was repeated twice.

Gene name	Forward primer (5'-3')	Reverse primer (5'-3')
RIG-I	ATTGCCACCTCAGTTGCTGAT	ACATACTCATAAAGGATGACAAGATTGC
IFN-β	CAACTTGCTTGGATTCCTACAAAG	TGCCACAGGAGCTTCTGACA
CCL5	CATCTGCCTCCCCATATTCCT	GCGGGCAATGTAGGCAAA
IP10	ATTATTCCTGCAAGCCAATTTTG	TCACCCTTCTTTTTCATTGTAGCA
ISG15	GGTGGACAAATGCGACGAA	TGCTGCGGCCCTTGTTAT
RSV N	AAGGGATTTTTGCAGGATTGTTT	TCCCCACCGTAACATCACTTG
GAPDH	GATCATCAGCAATGCCTCCT	TGTGGTCATGAGTCCTTCCA
TLR3	GGTCCCAAGCCTTCAACGA	GGTGAAGGAGAGCTATCCACATTT

Table 2.1 Real-time PCR probes.

Electrophoretic mobility shift assay (EMSA). Nuclear extracts (NE) were prepared as described previously (56). A total of 5 µg NE was incubated in DNA binding buffer (5% glycerol, 12 mM HEPES, 80 mM NaCl, 5 mM dithiothreitol, 5 mM MgCl$_2$, 0.5 mM EDTA) with 1.5 µg of poly(dA-dT) and 0.1 nM IRDye 700/IRDye 800-labeled ds oligonucleotide (Table 2.2) in a total volume of 10 µl. Complexes were fractionated by native polyacrylamide gels in 1x TBE buffer (89 mM Tris, 89 mM boric acid, 2 mM EDTA). For competition, unlabeled ds competitor was added at the time of the binding reaction. Gels were then scanned in an Odyssey infrared scanner (Lincoln, NE).

Gene name	Strand	Sequence (5'-3')
ISRE	Sense	GATCGGAAAGGGAAACCGAAACTGAAGCC
	Antisense	GGCTTCAGTTTCGGTTTCCCTTTCCGATC
ISREm	Sense	GATCGGGCGGGGGCGCCGGCGCTGAAGCC
	Antisense	GGCTTCAGCGCCGGCGCCCCGCCCGATC
κB	Sense	GATGCCATTGGGGATTTCCTCTTTACTG
	Antisense	CAGTAAAGAGGAAATCCCCAATGGCATC
OCT	Sense	GATCCGAGCTTCACCTTATTTGCATAAGCGATTGA
	Antisense	TCAATCGCTTATGCAAATAAGGTGAAGCTCGGATC

Table 2.2 EMSA DNA probes for NFκB and IRF3 binding.

Immunofluorescence microscopy. A549 cells plated on coverslips were mock or RSV infected (MOI = 1) for the times indicated. The cells were fixed with 4% paraformaldehyde in PBS, pH 7.4. The cells were then incubated for 60 min at 37°C with anti-IRF-3 Ab or anti-NF-κB/RelA C20 Ab (Santa Cruz) diluted 1:200 in PBS-T (PBS, 0.1% Tween 20). Cells were washed three times in PBS-T and incubated with secondary fluorescein isothiocyanate-conjugated anti-rabbit Ab in PBS-T for 1 h at 22°C. Nuclei were visualized by staining for 15 min with SYTOX orange (Molecular Probes). Confocal microscopy was performed on a Zeiss LSM510 META system. Images were captured at a magnification of x40. For each condition, 10 pictures were taken and the percentage of cells which showed the nuclear staining for IRF-3 or RelA was counted and expressed as the percentage of total cells examined.

RSV-CM collection and IFN neutralization. RSV-conditioned medium (RSV-CM) was prepared by infecting A549 monolayers with RSV (MOI = 1, 48-h incubation). The supernatant was collected, centrifuged at 3,000 x g, exposed to UV light to inactivate the live virus, quick-frozen, and stored at –70°C until used. For IFN neutralization, 20 µl of RSV-CM was mixed with either 15 µg of rabbit anti-human IFN-ß Ab (Chemicon International) or 15 µg of rabbit immunoglobulin G (IgG) in a total volume of 2 ml of culture medium and incubated for 2 h at 37°C.

Northern blots. Total RNA (30 µg) was fractionated by electrophoresis on a 1% agarose-formaldehyde gel and transferred to a nylon membrane (Zeta Probe GT; Bio-Rad). A TLR3 cDNA probe was made using asymmetric PCR. The membrane was hybridized with 2×10^6 cpm/ml of radiolabeled probe at 60°C overnight in 5% SDS hybridization buffer(167).The membrane was washed with 1x SSC (1x SSC is 0.15 M NaCl plus 0.015 M sodium citrate) with 0.1% SDS for 20 min at 60°C. Internal control hybridization was carried out with ß-actin mRNA. The image was developed and quantified by exposing the membrane to a Molecular Dynamics phosphorimager cassette.

Western immunoblot. Whole-cell extracts were prepared using modified radioimmunoprecipitation assay buffer (50 mM Tris-HCl [pH 7.4], 150 mM NaCl, 1 mM EDTA, 0.25% sodium deoxycholate, 1% Nonidet P-40, 1 mM phenylmethylsulfonyl fluoride, 1 mM NaF, 1 mM Na_3VO_4, and 1 µg each of aprotinin, leupeptin, and pepstatin/ml). One hundred micrograms protein was fractionated by 10% SDS-polyacrylamide gel electrophoresis and transferred to a polyvinylidene difluoride membrane by electroblotting. Membranes were blocked in 5% nonfat dry milk in Tris-buffered saline-0.1% Tween and probed with the primary Ab indicated in the figure legends. Membranes were washed and incubated with IRDye 700-conjugated anti-mouse Ab or IRDye 800-conjugated anti-rabbit Ab (Rockland, Inc.). Finally, the membranes were washed three times with PBS-T and scanned by infrared scanner. RelA C20 Ab (Santa Cruz), anti-phospho-276 RelA Ab (Cell Signaling), anti-phospho-536 RelA Ab (Cell Signaling), and Anti-FLAG M2 Ab (Sigma) were commercially obtained.

2.3 Results

RSV infection activates NF-κB and IRF-3 in airway epithelial cells.

Previous work has shown that RSV infection activates the nuclear factor-κB (NF-κB) and IRF-3 pathways that both are central mediators of antiviral cytokine expression. To test their relative kinetics of activation, A549 cells were RSV infected (MOI = 1); NF-κB activation was measured using an EMSA (Fig. 2.1A), and nuclear IRF-3 activation was measured by Western immunoblotting (Fig. 2.1B). Consistent with our previous work, the NF-κB binding assay in the EMSA showed three distinct complexes (Fig.2.1A) (41,64). The less-mobile complex showed a time-dependent increase in response to RSV infection; previous work has shown that this species represents the heterodimer of the 65-kDa RelA-transactivating subunit and the 50-kDa NF-κB1 DNA binding subunit (41,64). Conversely, the middle complex, representing homodimers of the 50-kDa NF-κB1 DNA subunit, was not affected by RSV treatment. The most-mobile band represents nonspecific DNA binding species. We noted that a significant increase in NF-κB binding was detected 6 h after RSV infection, which suggested the activation of NF-κB in response to RSV infection (Fig.2.1A).
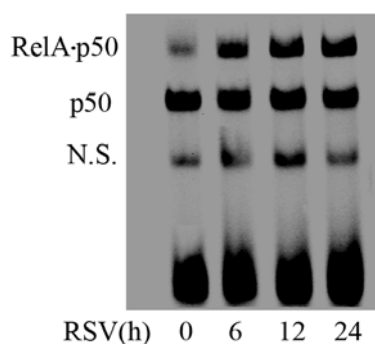

Fig.2.1A EMSA was performed on 5 μg NE using 0.1 nM IRDye 700-labeled DNA probe containing the κB element. The composition of the bound complexes is indicated. NS: none specific binding.

Similarly, IRF-3 pathway activation was rapid, with an increase of nuclear IRF-3 6 h after RSV infection, peaking after 12 h (Fig. 2.1B). The multiple bands detected

20

represented different phosphorylation forms of IRF-3, characteristic of its activation mechanism (14,133). Together, these data indicate that RSV activates both NF-κB and IRF-3 translocation rapidly, within 6 h after RSV infection.
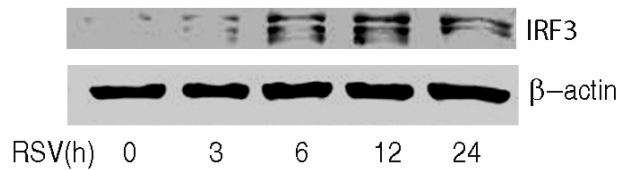

Fig.2.1B Western immunoblot was conducted on 50 μg nuclear extract. Top panel, membrane was stained with anti-IRF-3 Ab. Bottom panel, β-actin was stained as a loading control.

The RIG-I pathway mediates the early phase of RSV-induced gene expression.

RIG-I is a cytoplasmic helicase that activates signaling when it binds RNA. To investigate whether there is a physical interaction between RIG-I and RSV replication products, an RNA helicase UV-cross-linking experiment was performed. In this assay, eukaryotic expression vectors encoding nothing, FLAG-tagged RIG-I, or FLAG-tagged Mda5 were transfected into A549 cells. After 24 h, the transfectants were RSV infected for 12 h and RNA was UV cross-linked to cellular proteins. To determine whether RIG-I or Mda5 bound RSV transcripts, epitope-flagged protein was immunoprecipitated by anti-FLAG Ab, and the released RNA was assayed by RT-PCR. We found that a specific 69-bp band corresponding to the RSV N protein transcript was detected only in immunoprecipitates from RIG-I-transfected cells (Fig. 2.2A).

To further understand the roles of RIG-I and TLR3 in RSV-induced gene expression, A549 cells were transfected with RIG-I, TLR3, or control siRNA and subsequently RSV infected for 0, 9, or 18 h, and QRT-PCR was used to measure the antiviral gene expression. RSV induced RIG-I expression by 30-fold within 9 h of infection, which, significantly, fell to 20-fold after 18 h (Fig.2.2B). Relative to control siRNA-transfected cells, RIG-I siRNA-transfected cells showed significant inhibition of RIG-I expression at 9 h and less inhibition after 18 h of RSV infection (Fig.2.2B). Similarly, RSV induced TLR3 expression 22- and 25-fold at 9 and 18 h, respectively. TLR3 knockdown significantly reduced RSV-induced TLR3 expression at both times.

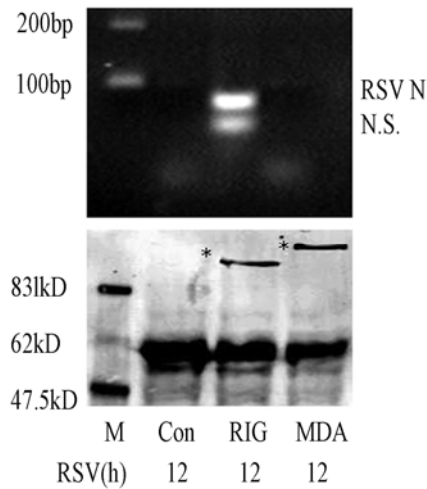These data indicate that RSV induced both RIG and TLR3 expression and that siRNA knockdown was effective.

Fig. 2.2A RNA helicase UV-crosslinking and immunoprecipitation assay. A549 cells were transfected with 2μg pT1S vector, pT1S-FLAG-RIG-I or pT1S-FLAG-Mda5 respectively for 24 h. Thereafter, cells were infected by RSV for 12 h. UV crosslinking and immunoprecipitation experiment were conducted as described in experimental procedure. RT PCR yielded two bands in the sample corresponding to RIG-I immunoprecipitation. The upper band was confirmed as RSV N RNA by sequencing (top panel); the bottom band is a nonspecific product (N.S.). The bottom panel is a Western immunoblot of the immunoprecipitates including RIG-I and Mda5. Specific bands are indicated by *.
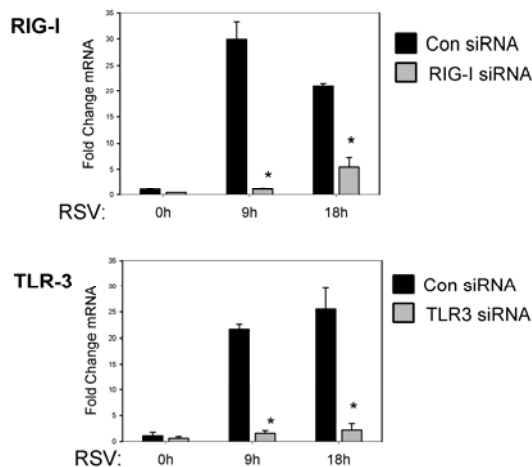

Fig.2.2B A549 cells were transfected with 100 nM of nonspecific siRNA (Con), RIG-I siRNA (RIG-I) or TLR3 siRNA (TLR3) for 48 h.   Cells were infected by RSV for 0-, 9- or 18 h and total RNA was extracted.   Q-RT-PCR was performed to determine changes in RIG-I (top panel) or TLR3 expression (bottom panel) as indicated.   * P< 0.01 compared to control siRNA (Student's t test).
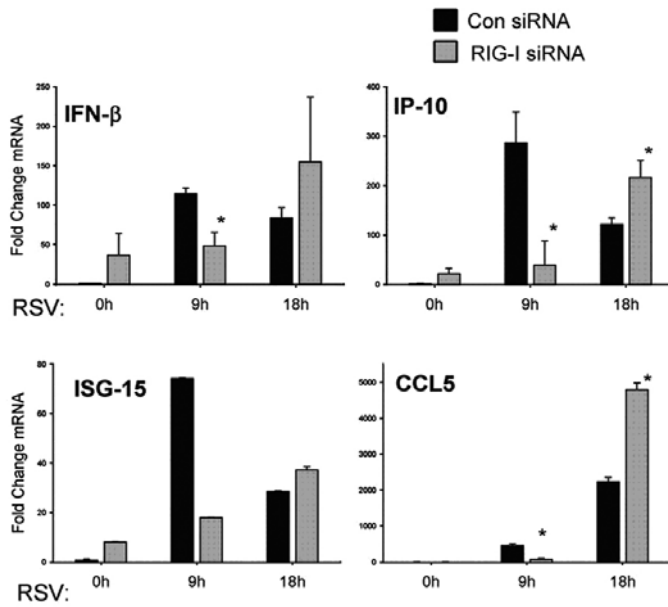
We next examined the effect of RIG-I knockdown on RSV-induced IFN- β, IP-10, ISG15, and CCL-5 expression (Fig.2.2C). RSV strongly induced IFN- β, IP-10, and ISG15 production, at 100-fold, 280-fold, and 75-fold, respectively, after 9 h of infection. By contrast, CCL-5 expression peaked at 2,000-fold 18 h after RSV infection. In the RIG-

I knockdown mutants, basal expression levels of IFN-β and the IFN-responsive IP-10 and ISG15 genes were all increased relative to those of the control siRNA transfectants but were not significantly induced by RSV infection 9 h later (Fig.2.2C). For CCL-5, basal expression was not detectable and, in the RIG-I knockdown, its expression was reduced at 9 h as well. In addition, we noted that after 18 h of RSV infection, levels of IP-10, ISG15, and CCL-5 were enhanced significantly in RIG-I-silenced cells, whereas there was no significant difference in the level of expression of IFN-β between RIG-I-silenced cells and control cells. RSV-induced expression of the same genes was then examined after TLR3 knockdown (Fig.2.2D). In the TLR3 knockdown mutants, the basal expression levels of all investigated genes were increased, and after 9 h of RSV infection, the gene expression levels of IP-10 and CCL-5 were not affected. In contrast to the effects of RIG-I knockdown, expression levels of both IFN-β and ISG15 were increased, rather than inhibited, 9 h after infection. In this group of genes, expression levels were inhibited 18 h after RSV infection (Fig.2.2D). These results suggest that the RIG-I pathway is involved in the early response of host cells to RSV infection. At later phases of RSV infection, other RIG-I-independent pathways are activated that mediate downstream gene expression, including that of TLR3.

The RIG-I pathway mediates early NF-κB/RelA and IRF-3 activation in response to RSV infection.

To determine whether RSV-induced DNA binding of NF-κB or IRF-3 was affected after RIG-I or TLR3 expression was silenced, DNA binding activity was measured in NE by EMSA using either double-stranded NF-κB or ISRE sites. NF-κB-specific DNA binding activity was abolished in RIG-I-silenced cells at 9 h or 18 h after RSV infection compared to that in controls, whereas only a slight decrease in binding occurred in cells after TLR3 silencing (Fig.2.3A, left panel). Conversely, siRNA-mediated RIG-I silencing inhibited specific RSV-inducible IRF-3 binding to its cognate ISRE element 9 h after RSV infection, but a significant increase of IRF-3 binding was observed later (18 h after infection; Fig.2.3B). Similar to its lack of effect on RSV-induced NF-κB DNA binding, siRNA-mediated TLR3 silencing had little detectable effect on inducible IRF-3 binding at any time point (Fig.2.3B). An EMSA experiment using the oligonucleotide containing the
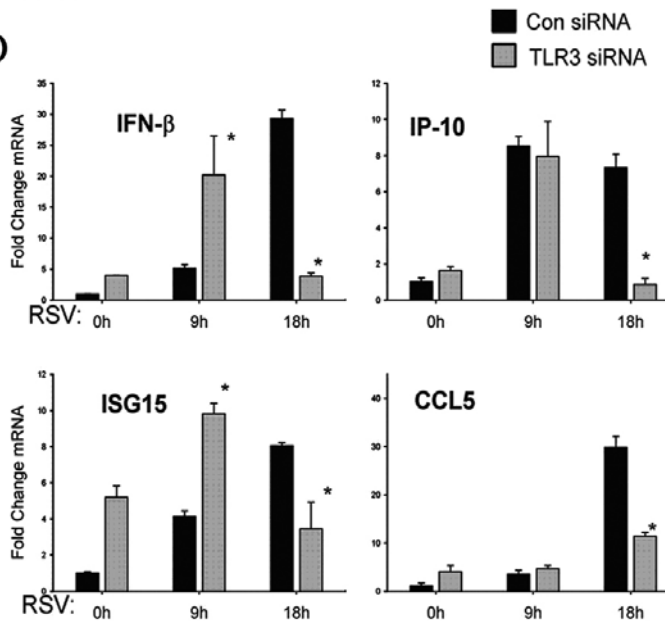
23

C

Fig. 2.2C and 2D A549 cells were transfected with control (Con), RIG-I siRNA (RIG-I) or TLR3 siRNA (TLR3) for 48 h and then RSV infected for 0, 9 or 18 h. CCL-5, IP-10, IFN-β and ISG15 expression were determined by by Q-RT-PCR; shown is fold change relative to unstimulated cells transfected with control siRNA (0 h). *, P<0.05 relative to corresponding group at the same time point (Student's t test). (C) Q-RT-PCR of cells thansfected by RIG-I siRNA and (D) cells transfeceted by TLR3 siRNA.

OCT1 element was conducted, which confirmed equivalent nuclear protein preparation for each extract (Fig. 2.3C). Together, these data indicated that the RIG-I, but not the TLR3 signal, was required for RSV-induced NF-κB and IRF-3 DNA binding.

24

The RIG-I pathway mediates early NF-κB/RelA and IRF-3 activation in response to RSV infection.

To determine whether RSV-induced DNA binding of NF-κB or IRF-3 was affected after RIG-I or TLR3 expression was silenced, DNA binding activity was measured in NE by EMSA using either double-stranded NF-κB or ISRE sites. NF-κB-specific DNA binding activity was abolished in RIG-I-silenced cells at 9 h or 18 h after RSV infection compared to that in controls, whereas only a slight decrease in binding occurred in cells after TLR3 silencing (Fig.2.3A, left panel). Conversely, siRNA-mediated RIG-I silencing inhibited specific RSV-inducible IRF-3 binding to its cognate ISRE element 9 h after RSV infection, but a significant increase of IRF-3 binding was observed later (18 h after infection; Fig.2.3B). Similar to its lack of effect on RSV-induced NF-κB DNA binding, siRNA-mediated TLR3 silencing had little detectable effect on inducible IRF-3 binding at any time point (Fig.2.3B). An EMSA experiment using the oligonucleotide containing the OCT1 element was conducted, which confirmed equivalent nuclear protein preparation for each extract (Fig. 2.3C). Together, these data indicated that the RIG-I, but not the TLR3 signal, was required for RSV-induced NF-κB and IRF-3 DNA binding.

To determine whether RIG-I was required for cytoplasmic-nuclear translocation, we next examined the subcellular distributions of NF-κB and IRF-3 using confocal microscopy in RSV-infected cells transfected with control siRNA or RIG-I siRNA. In control siRNA-transfected cells, 32% of cells showed nuclear RelA accumulation 9 h after RSV infection; this number increased to 63% 18 h after infection. By contrast, in RIG-I-silenced cells, nuclear RelA translocation was significantly inhibited, with only 13% of cells after 9 h and 22% of cells after 18 h showing nuclear RelA signals (Fig.2.3D and F). In the case of IRF-3 activation, in control siRNA-transfected cells, 21% (9 h) and 38% of cells (18 h) showed IRF-3 nuclear translocation after RSV infection, whereas in RIG-I-silenced cells, 8% and 29% of cells showed nuclear IRF-3 accumulation 9 and 18 h after infection, respectively (Fig.2.3E and F). These data indicated that RIG-I expression was necessary for nuclear translocation of both RelA and IRF-3 at early times after
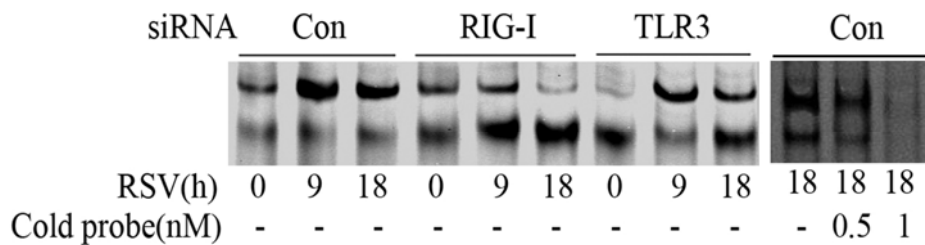
Fig.2.3A A549 cells were transfected with 100 nM of nonspecific siRNA (Con), RIG-I siRNA (RIG-I) or TLR3 siRNA (TLR3) for 48 h followed by RSV infection for 9- or 18 h. Nuclear extract (NE) from each siRNA treatment were prepared and assayed by EMSA.   Shown are bound complexes on the IRDye 700-labeled κB oligonucleotides visualized by infrared scanning (left panel).   A competition experiment was performed using the sample from control siRNA treated group infected by RSV for 18 h, incubated with 0, 0.5- or 1 nM unlabeled DNA probe oligonucleotides (right panel).
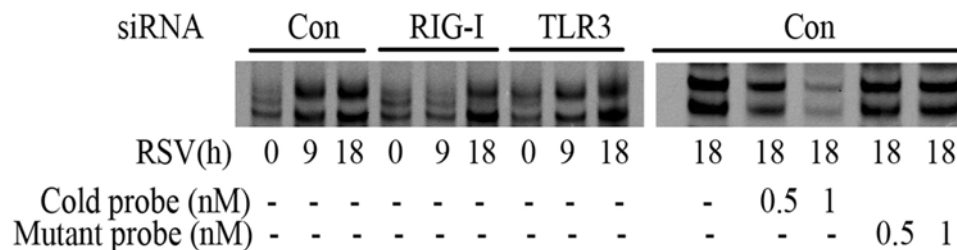

Fig.2.3B IRF-3 binding at different times of RSV infection.   EMSA was performed on NE using 0.1nM IRDye 700-labeled ISRE binding site (left panel). A competition experiment with unlabelled probe and mutant probe were conducted (right panel).
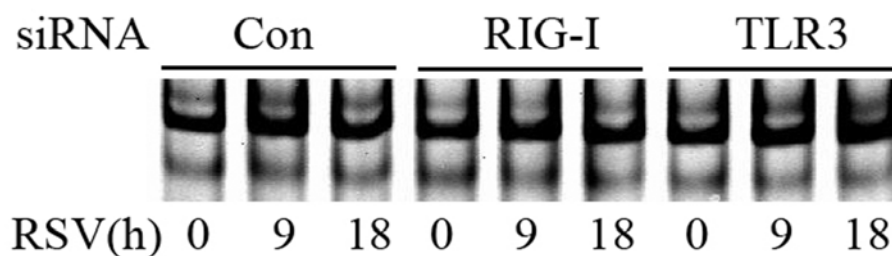

Fig.2.3C   OCT-1 binding.   EMSA was performed using the same NE as in fig 2.3A and 2.3B binding 0.1 nM IRDye 800-labeled OCT-1 binding site.

RSV infection (9 h). In addition, we noted that there was no statistically significant difference between the RIG-I siRNA group and control groups for IRF-3

26

nuclear translocation 18 h after RSV infection, and this later increase in IRF-3 binding was consistent with the preserved RSV-induced IRF-3 DNA binding detected by EMSA (Fig.2.3B), suggesting that, in the absence of RIG-I, other redundant pathways may mediate IRF-3 activation later during the infection.
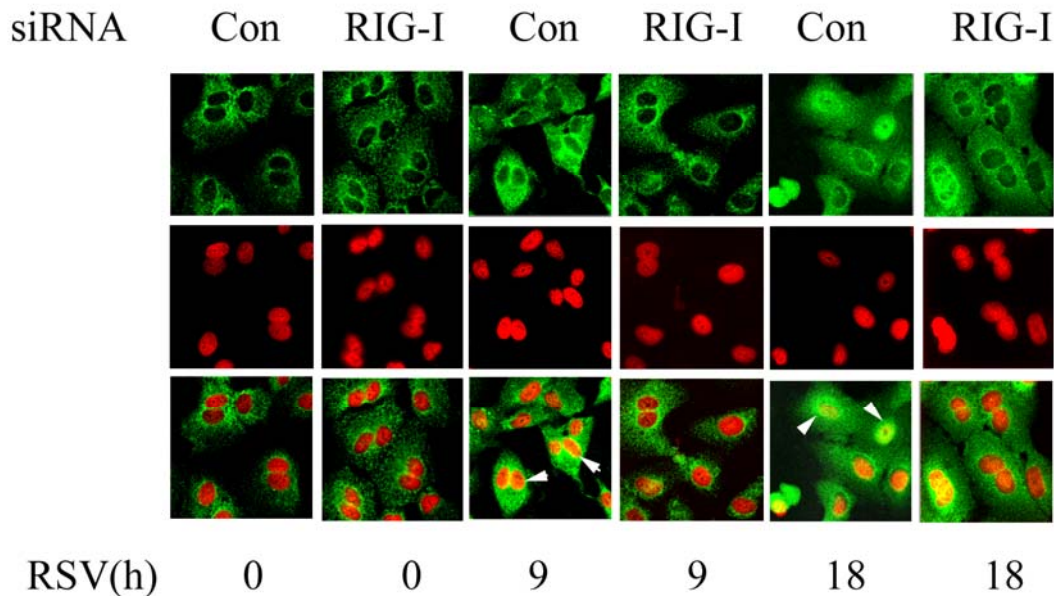

Fig.2.3D   A549 cells were transfected with either control (Con) or RIG-I siRNA (RIG-I) for 48 h and then RSV infected for 0, 9- or 18h.   The cells were fixed, incubated with rabbit anti-RelA Ab, and then stained with FITC conjugated anti-rabbit secondary Ab (green color).   The nuclei were stained with Sytox Orange (red).   The slides were imaged using confocal microscopy, and the colors were merged on the bottom panel. Co-localization of RelA and nuclei are showed by yellow color. White arrows indicated the cells which had RelA nuclear translocation.

The TLR3 pathway regulates the phosphorylation of NF-κB/RelA at serine 276.
        Our findings suggested that the TLR3 pathway was not required for inducing NF-κB/RelA or IRF-3 DNA binding activity in response to RSV infection (Fig. 2. 3A and B), yet it significantly inhibited the expression of genes which we have found to be NF-κB dependent, including the CCL-5 and IP-10 genes (149). To examine whether TLR3 signaling affected NF-κB/RelA transcriptional activity, we tested RSV-inducible NF-κB
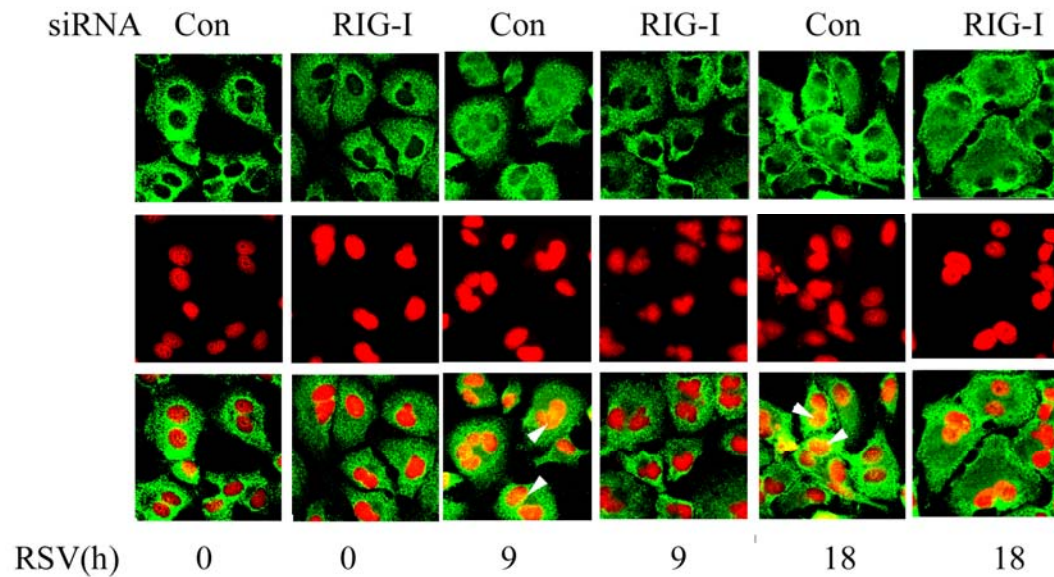
27

Fig.2.3E A549 cells were treated as in (D) except for using rabbit anti-IRF-3 Ab. Co-localization of IRF-3 and nuclei are showed by yellow color and indicated by white arrows.
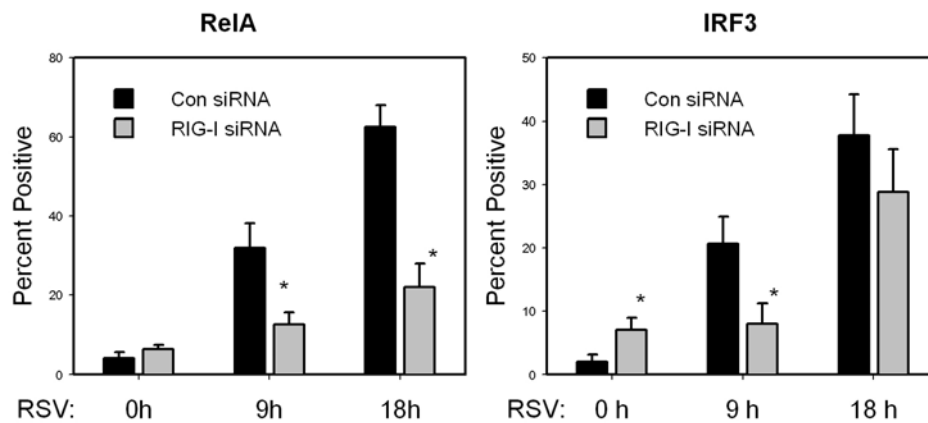

Fig.2.3F The percentage of cells with nuclei positive for RelA or IRF-3 at each time point and for each treatment was calculated based on 5 randomly photographed fields from two independent experiments (the photos were taken double blindly by a technician from the core facility). The indicated (*) value means a significant difference between siRNA groups at the same time point of RSV infection ($P<0.05$, student's test).

activity using a luciferase reporter plasmid containing the IFN-β PRDII domain in control or TLR3 siRNA-transfected cells. Reporter gene expression levels increased four- and eightfold after 9 and 18 h of RSV infection in the cells transfected with control siRNA, whereas NF-κB-dependent reporter gene expression was significantly inhibited in TLR3-silenced cells (Fig.2. 4A). This suggested that the TLR3 pathway controls NF-κB transcriptional activation.
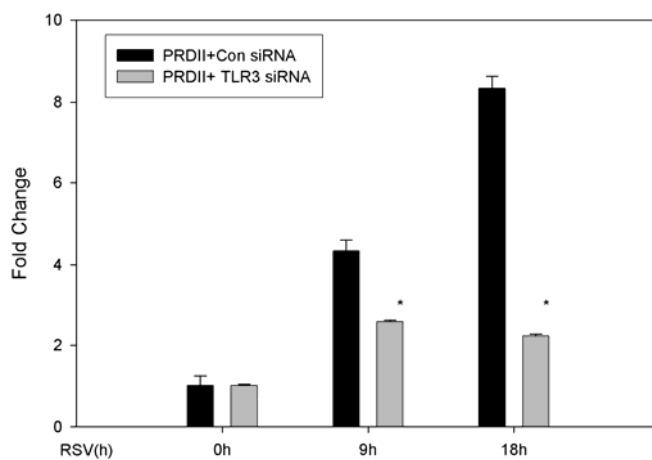

Fig.2. 4A A549 cells were transfected with control siRNA (Con) or TLR3 siRNA (TLR3) and a luciferase reporter plasmid containing PRDII domain was co-transfected for 48 h. Cells were infected by RSV for 0, 9- or 18h before cell lysis. Shown is normalized luciferase activity expressed as fold change relative to uninfected cells. The experiment represents one of the three experiments. * $P<0.05$, n=3, student's test.

NF-κB is known to be a nuclear phosphoprotein with activating sites at serine residues 276 (154,171) and 536 (18,122). We therefore investigated whether RSV induced RelA phosphorylation and, if so, whether it was inhibited by TLR3 silencing. In control siRNA-transfected cells, RelA phosphorylation on serine 276 and 536 sites increased 9 and 18 h after RSV infection. By contrast, in TLR3 siRNA transfectants, serine 276 phosphorylation was significantly inhibited 18 h after RSV infection (Fig.2.4B).

Together, these data suggested that the activation of the TLR3 pathway in airway epithelial cells controls the phosphorylation of RelA at serine 276 as its mechanism for regulating RSV-induced NF-κB-dependent gene expression at the late phase of infection.

The RIG-I pathway mediates RSV-induced TLR3 upregulation by increasing paracrine IFN-β secretion.

Previous studies (52,118,119) and ours (Fig.2.2B) have shown that TLR3 expression is induced by RSV infection. To further investigate the interaction between the RIG-I pathway and the TLR3 pathway, we next explored the effect of RIG-I knockdown on TLR3 transcription and expression. QRT-PCR was conducted to measure endogenous TLR3 mRNA levels after RIG-I expression was silenced. In the control siRNA group, the TLR3 mRNA levels were increased 6- and 18-fold after 9 or 18 h of RSV infection.
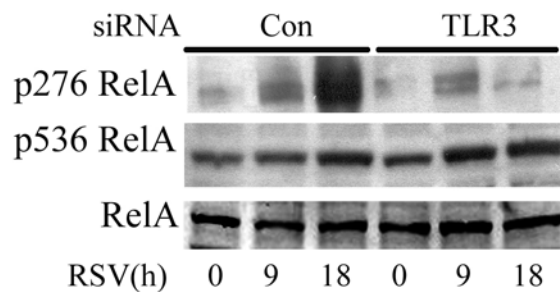

Fig.2.4B A549 cells were transfected with control siRNA (Con) or TLR3 siRNA (TLR3) and then RSV infected for 0, 9- or 18 h. Western immunoblot was performed to detect changes in phospho-Ser276 RelA (top panel), phospho-Ser536 RelA (middle panel) and Rel A (bottom panel) using 100 μg whole cell extract.

siRNA-mediated RIG-I silencing abolished the RSV-induced TLR3 induction. These data suggested that the activation of the epithelial RIG-I pathway is required for RSV-induced TLR3 upregulation (Fig.2.5A).
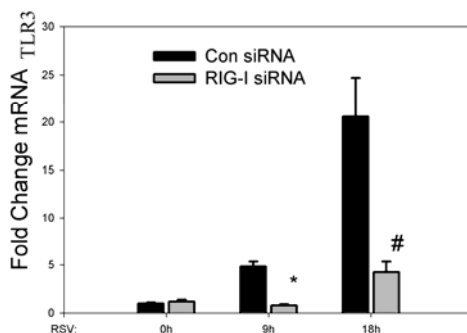

Fig.2.5A A549 cells were transfected with control siRNA (Con) and RIG-I siRNA for 48 h and infected with RSV for 0, 9- or 18h. QRT-PCR was performed using TLR3 probe. #, P<0.01; *,P<0.05 relative to control siRNA at the same time point. The result shown here are representative of two independent experiments.

To initially localize the regulatory regions in the TLR3 gene, a computational analysis of the human TLR3 promoter was conducted using position weight matrices

(TRANSFAC)(155). In this analysis, we predicted two interferon response elements (ISRE1 and ISRE2) and one STAT site. A 1.0-kb fragment of the human TLR3 promoter containing these regulatory regions was cloned and inserted into a luciferase reporter plasmid, generating hTLR3/LUC. To determine their relative contributions, each ISRE and STAT site was individually mutated to non-DNA binding sequences in the context of the 1-kb hTLR3/LUC (Fig.2.5B).


```
                        ISRE1
-901 ACCTCCCTAGGTTTCGTTTTCCTAATTT......
                        CGC
            STAT
-151 CTTCTTGGAATGCACCAAACATAAAAG......
        CC

        ISRE2
-101 CACTTTCGAGAGTGCCGTCTATTTGCCA......
        GA
```

Fig.2.5B   Noncontiguous genomic sequence of hTLR3 promoter.   Location relative to major transcription start site is shown at left.   Underlines, two predicted ISRE sites (ISRE-1 and -2) and one STAT site.   Bold font, site directed mutagenesis of each individual regulatory element was performed by rolling circle PCR.

The wild-type hTLR3/LUC and its respective site mutants were then transfected into A549 cells and luciferase reporter activity was measured in the absence or presence of RSV infection. We found that hTLR3/LUC was induced sixfold by RSV relative to activity in the uninfected control (Fig.2.5C). In addition, mutation of the ISRE1 site did not affect RSV-induced reporter gene expression, but mutation of either the ISRE2 or STAT site significantly decreased RSV-induced reporter gene activity (Fig.2.5C).
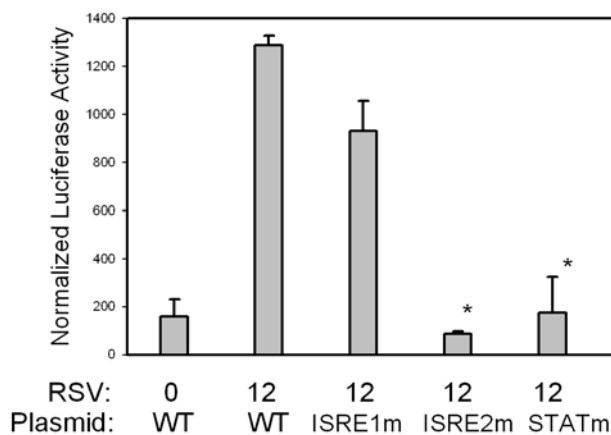

Fig.2.5C   A549 cells were transfected with either wild type hTLR3/LUC reporter gene or differing site mutants.   Twenty-four h later, cells were RSV-infected and normalized luciferase activity measured 12 h thereafter. *, $P<0.001$ relative to wild type hTLR3/LUC activity at 12 h.

31

Because RSV is known to induce IFN-β secretion by airway epithelial cells (65,137,138) and others have reported that type I IFNs enhance TLR3 expression (150), we next investigated whether RSV-induced TLR3 expression is controlled in a paracrine manner by IFN-β secretion.Conditioned medium (CM) from RSV-infected A549 cells (24 h after infection) was collected, and naïve A549 cells were incubated with 2.5% (vol/vol) of UV-inactivated RSV-CM (UV-RSV-CM). Six and twelve hours after exposure, RNA was extracted and Northern blotting was conducted to measure TLR3 expression. We found that UV-RSV-CM induced TLR3 expression in naïve A549 cells, indicating that paracrine activators of TLR3 expression were present in infected A549 cell culture supernatants. To determine whether the paracrine mediator in the RSV-CM was IFN- β, two other plates were treated with UV-RSV-CM neutralized with either rabbit IgG or neutralizing anti-IFN-β Ab. The UV-RSV-CM induction of TLR3 was significantly and selectively inhibited in the medium after IFN-β was neutralized (Fig.2.5D).
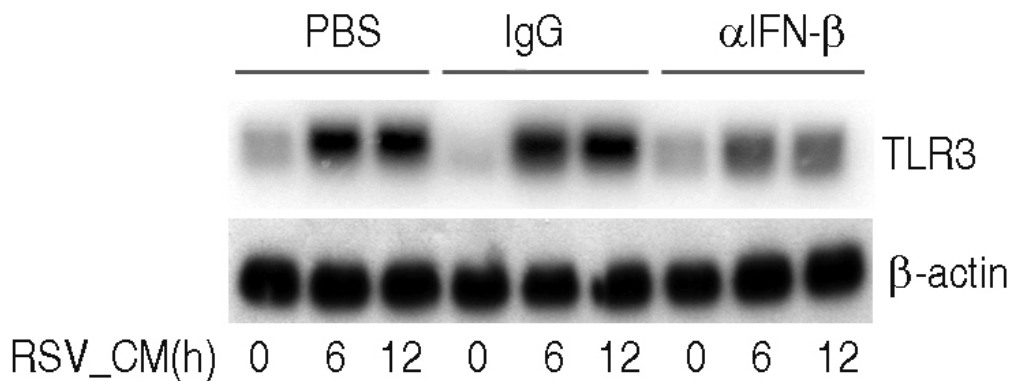

Fig.2.5D Naïve A549 cells were treated with 20 % (vol/vol) UV-RSV-CM taken from RSV-infected cells for the indicated times (in h).   Prior to addition to A549 cells, UV-RSV-CM was preincubated with either phosphate buffered saline (PBS), rabbit IgG (IgG) or neutralizing anti-IFN-β Ab for 2 h.   Autoradiogram from Northern Blot hybridization is shown.

These data suggested that IFN-β acts in a paracrine manner to up-regulate TLR3 expression. To further establish that paracrine IFN-β secretion is necessary for RSV-

induced TLR3 expression, RSV-induced TLR3 expression was measured in Vero cells, cells deficient in IFN-β expression but capable of productive RSV replication (140,166). Although RSV infection increased TLR3 expression in A549 cells, it did not induce TLR3 in Vero cells. Importantly, adding UV-RSV-CM to Vero cells induced TLR3 gene expression (Fig.2.5E). These data indicate that IFN-β is necessary and sufficient for TLR3 upregulation.
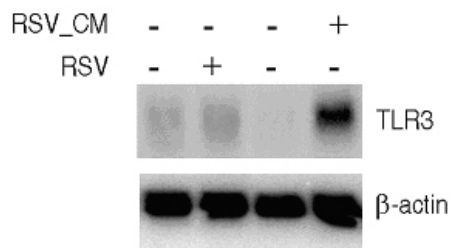

Fig.2.5E IFN-β deficient Vero cells were infected with RSV (RSV) for 12 h or were treated with 20 % (vol/vol) UV treated conditioned medium (RSV_CM) for 12 h. The condition medium was collected from A549 cells 24 h after RSV infection. Top panel, 20 μg total RNA was isolated and Northern Blot hybridization conducted using TLR3 cDNA probe. Bottom panel, β-actin hybridization.

2.4 DISCUSSION

RSV is the major etiologic agent of epidemic wheezing and bronchiolitis in children, leading causes of hospitalization in children (127). In natural infections, airway epithelial cells are the primary sites for RSV invasion and these represent the cell type where productive replication takes place (3). Previous studies have shown that host cells primarily use two different classes of "sensors" for viral detection. One is a group of pattern recognition receptors localized in the cytoplasm that includes the DExD/H box-containing RNA helicases, RIG-I, and the melanoma differentiation-associated gene 5 (Mda5), and the second is a group of membrane-bound pathogen-associated molecular pattern receptors known as the TLRs (59). In this study, we found that the expression of both RIG-I and TLR3 is rapidly induced by RSV infection in alveolar-like A549 cells. Which of these two mechanisms is used by airway epithelial cells to detect RSV infection and their interrelationships are not understood.

In this study, we are the first to demonstrate that RIG-I mediates RSV-induced early signaling events leading to the nuclear translocation of NF-κB and IRF-3, two key transcription factors controlling inflammatory cytokine and chemokine expression in

33

airway epithelial cells (59). We have shown that RIG-I, but not the related Mda5 molecule, specifically binds RSV RNA. In addition, siRNA-mediated RIG-I knockdown significantly inhibits the activation of NF-κB and IRF-3, especially at the early phase of RSV infection (9 h p.i.). The mechanisms by which RIG-I couples to transcription factor activation are partially understood. After RNA virus infection, transcription and replication of the virus yields RNA intermediates which are bound by the helicase domain of RIG-I. This event activates the two amino-terminal caspase-recruiting domains (CARD), which in turn, are required for binding another CARD-containing molecule, known as mitochondrion antiviral signaling (MAVS). Although we have not investigated its role here, MAVS has been identified as the only downstream adaptor for RIG-I. The CARD-mediated association between RIG-I and MAVS then leads to the activation of NF-κB and IRF-3. IRF-3 activation appears to be mediated by activation of the atypical IKKs, TBK1/IKKε, that phosphorylate IRF-3, resulting in its dimerization and nuclear translocation.

By contrast, the mechanism for NF-κB activation is not fully understood. Our previous work has shown that RSV controls NF-κB nuclear translocation by its effects on IκBα proteolysis(64); interpreted together with our studies demonstrating that RIG-I is required for NF-κB nuclear translocation, these data suggest that RIG-I is upstream of the canonical NF-κB pathway. We note that a recent publication showed that TNF receptor-associated factor 3 (TRAF3) was involved in the activation of the IKK complex through the RIG-I-MAVS pathway (120). In this regard, it will be of interest to examine whether TRAF3 is involved in RSV-induced NF-κB activation. Finally, our immunohistochemistry experiments indicate that the NF-κB translocation response, as well as the IRF-3 response, occurs only in a subpopulation (~30%) of RSV-infected cells. These findings are consistent with other recent studies, which used an even higher multiplicity of infection (138). These findings indicate that there is significant heterogeneity in the RSV-induced antiviral cell-signaling response.

The activation of both RIG-I-dependent and RIG-I-independent pathways by West Nile virus has also been reported recently (39). Using RIG-I-null embryonic fibroblasts, it was found that West Nile virus activated IRF-3 through the RIG-I pathway at the early

phase of viral infection. However, at late times of infection, West Nile virus was still able to activate IRF-3 through a RIG-I-independent pathway whose mechanism is unknown (39). These data are consistent with our findings (Fig.2.3B). We suspect that the activation of the RIG-I-independent pathway may have a higher threshold, signaling only under conditions of higher levels of viral replication. It will be of interest to identify the mediators of this RIG-I-independent pathway; these could include protein kinase R, TLR, or other cytoplasmic RNA helicases not yet identified.

In our data and the work published by others (118), TLR3 pathway inhibition affects the expression of some antiviral genes, such as CCL-5 and IP-10. However, the exact mechanism underlying this observation was not known previously. We show here that the TLR3 pathway does not contribute to the DNA binding activity of NF-κB following RSV infection (Fig.2.3A and B). Rather, it regulates the transcription of these genes by modulating the phosphorylation of RelA at serine residue 276 (Fig.2.4B). Serine 276 phosphorylation is controlled by several protein kinases, including the catalytic subunit of PKA and the mitogen- and stress-activated protein kinase-1 (154,171). Serine 276 phosphorylation is required to induce intermolecular interaction between RelA and the p300 coactivator, thereby resulting in transcriptional activation (154,172). It is not presently known which kinase mediates RelA serine 276 phosphorylation in response to RSV, and we will investigate this in future studies.

The results of our study indicate that compared to RIG-I signaling, the TLR3 pathway functions only later during the evolution of RSV infection. The subcellular localization of TLR3 in uninfected cells may determine its kinetics and role in antiviral response. In particular, some studies have indicated that TLR3 is localized, at least partially, in an endosomal compartment in unstimulated cells (28,94). Because RSV is a paramyxovirus which enters the cell directly by pH-independent fusion with the plasma membrane (57), TLR3 would likely encounter its dsRNA ligand only later in the viral life cycle. The implication here is that other viruses that enter via the endosomal pathway may be able to activate the TLR3 pathway as a primary event. Although TLR3 is partially endosomal in unstimulated cells, in response to stimulation, newly synthesized TLR3 distributes to the plasma membrane (52). The translocation of TLR3 might allow RSV-

infected cells to respond to extracellular dsRNA. Alternatively, dsRNA released during late RSV infection might be taken up by cells and transported to the endosomal compartments where it can be recognized by TLR3. Differentiating the mechanisms will require further study.

Recently, two groups have reported the interaction between RSV and TLR3 (52,118,119). The identical phenomenon that they observed was that the expression of TLR3 was induced by RSV infection. However, the mechanism of this induction is not clearly understood. In this study, we found that IFN-β secreted from RSV-infected epithelial cells is necessary and sufficient to activate TLR3 expression. Importantly, induction of TLR3 is not directly the result of cytoplasmic RSV replication, because TLR3 expression was not induced by RSV infection in Vero cells. Vero cells are capable of high levels of RSV replication (140,166), but are deficient in IFN-β expression (35). The induction of TLR3 in response to RSV infection was absent in Vero cells, but when Vero cells were treated with RSV-conditioned media, rich in IFN- β, TLR3 was induced. These observations suggest that TLR3 activation is a secondary paracrine response mediated by local IFN-β secreted by RSV-infected epithelial cells. The induction of TLR3 expression in epithelial cells by measles virus and type I interferon has also been reported recently (143,150). Like RSV, measles virus is a negative-sense single-stranded paramyxovirus. Measles virus infection increased the expression of TLR3 through a transcriptional mechanism involving the ISRE2 binding sites in the hTLR3 promoter (150). Consistent with this finding, we also found that the ISRE2 site was essential for TLR3 induction in response to the IFN-β present in UV-RSV-CM. However, we found that a proximal STAT site is also required for hTLR3 promoter expression. Here, IFN-β binds to its IFNAR1 receptor, inducing the activation of receptor-associated Jak/Tyk tyrosine kinases and phosphorylation of receptor-associated STATs. This process induces the formation of IFN-stimulated gene factor 3, including STAT1 and STAT2 and IRF-9 (1). Because the hTLR3 promoter contains a functionally important ISRE and a STAT site, it is uniquely poised to integrate signals from the RSV-IRF and IFN-STAT pathways into enhanced transcriptional activation. Since IFN-β played an essential role for inducing TLR3 expression in response to RSV infection, it was reasonable to find that RIG-I was

involved in this process. siRNA-mediated RIG-I silencing abolished the endogenous TLR3 induction in response to RSV. This result suggests that RIG-I is a primary sensor for RSV detection in airway epithelial cells and that TLR3 expression is secondary to RIG-I-signaling action.

In summary, we found that the RIG-I pathway mediates the early response of airway epithelial cells to RSV infection, which initiates the innate immune response. The TLR3 pathway only affects the late-time gene expression, which regulates the phosphorylation of RelA at serine 276. TLR3 expression is induced by RSV in a paracrine manner that depends on RIG-I-induced IFN-β secretion.

CHAPTER III: RSV-INDUCES REL A RELEASE FROM CYTOPLASMIC 100 KDA NF-KB2 COMPLEXES VIA A NOVEL RIG-I_NIK SIGNALING PATHWAY

3.1 INTRODUCTION

Previous studies have showed that RSV activates the NF-κB transcription factor (64,88), a pathway controlling the inducible expression of 13 cytokines and chemokines (168). Five members of the NF-κB family have been reported, including three subunits with transactivating function, RelA, RelB, c-Rel, and two DNA binding subunits, NF-κB1 (p50) and NF-κB2 (p52) (135). The NF-κB molecules are sequestered in the cytoplasm by interacting with a group of inhibitory proteins including IκBα, IκBβ, IκBε, p100 and p105 (6). It has been reported that NF-κB activation can be controlled by two separate pathways, the canonical and noncanonical pathways, activated by distinct stimuli and under control of distinct IκB kinase (IKK) complexes.   We found that RSV was able to activate NIK kinase activity and increase p52 formation (19), however, the mechanism by which RSV activates the NIK·IKKα complex is unknown.

In this study, we discover RIG-I silencing by use of siRNA inhibits basal and RSV-inducible p52 formation. Further investigation revealed that the COOH terminus of NIK associates with the RIG-I·MAVS complex. We further discovered RSV induced RelA activation in IKKγ$^{-/-}$ mouse embryonic fibroblasts (MEFs), cells lacking a functional canonical NF-κB pathway.   In nondenaturing co-immunoprecipitation experiments, we demonstrated that the NIK·IKKα complex induced RelA release from cytoplasmic p100 complexes.   Together, these findings indicate RIG-I controls RelA activation by two distinct downstream signaling modules, one mediated by canonical pathway activation and the second involving a novel cross-talk pathway involving complex formation with NIK-IKKα whose activation liberates RelA from p100 sequestration.   Targeted disruption of this pathway may have significant effects in modulating the inflammatory response to RSV without affecting the innate immune response.

3.2 MATERIALS AND METHODS

Cell cultures. Humna A549 pulmonary type II epithelial cells (American Type Culture Collection [ATCC]) were grown as in chapter II. Wild type, NIK$^{-/-}$ (162), IKK$\alpha^{-/-}$ (31) and IKK$\gamma^{-/-}$ (160) MEFs were cultured in Eagle's minimum essential medium (Gibco) with 0.1 mM nonessential amino acids, 1.0 mM sodium pyruvate, and 10% FBS. HEK293 cells were cultured in Eagle's minimum essential medium (Gibco) with 0.1 mM nonessential amino acids, 1.0 mM sodium pyruvate, and 10% FBS.

Virus preparation and infection. The human RSV A2 strain was grown in Hep-2 cells and prepared as described in chapter II.

Plasmid construction- Expression. vectors encoding full-length and a series of deletion mutants of NIK were produced by PCR and cloned as Bam H1/Xba I sequences into the pEGFP-Myc plasmid (InVitrogen). The sequences of the primers are shown in Table 3.2.   A Flag- tagged full length NIK expression vector (FLAG_EGFP_NIK) was constructed as a COOH terminal fusion in pEGFP plasmid.   Expression vectors encoding Flag epitope-tagged RIG-I and its deletion mutants were under the control of tetracycline response element (TRE) in a modified pT1S plasmid as describe before (87). Expression vectors encoding Myc epitope- tagged MAVS and different deletion mutants were produced by PCR and cloned into modified pcDNA3_strawberry plasmid; the primers used are listed in Table 3.3

Name	Span (aa)	Sense	Antisense
NIK-FL	8-947	GAATGAGGATCCTGCCCAGGTGCCCCTGGC	GAGGTCTAGATTAGGGCCTGTTCTCCAGCTGGCC
NIK-C1	380-947	AACCGGATCCGTCCTGCTCACTGAGAAACTCAAGC	GAGGTCTAGATTAGGGCCTGTTCTCCAGCTGGCC
NIK-C2	661-947	GAGGCGGATCCCTGAAGAGCCCTTGGAGGGGAG	GAGGTCTAGATTAGGGCCTGTTCTCCAGCTGGCC
NIK-C3	796-947	GAGGCGGATCCCTCTCGTGCCTCAGCATCGAC	GAGGTCTAGATTAGGGCCTGTTCTCCAGCTGGCC
NIK-N1	8-660	GAATGAGGATCCTGCCCAGGTGCCCCTGGC	AACGATCTAGATTAACCTCCCACTTGCTGTAGTGCCCGGTTCACC
NIK-N2	8-387	GAATGAGGATCCTGCCCAGGTGCCCCTGGC	AACGATCTAGATTACTTGAGTTTCTCAGTGAGCAGGACACCCCTGTTG
NIK-N3	8-233	GAATGAGGATCCTGCCCAGGTGCCCCTGGC	CGATCTAGATTAATCGAGGCAGAGCCGGCCGTAGGCCCTCGCCAAGC

Table 3.2 Primers for constructing NIK deletion mutations.

Name	Sense	Anti-sense
MAVS	AAGTATAAGCTTATGCCGTTTG CTGAAGAC	TTCATATCTAGACTAGTGCAG ACGCCGCCGG
MAVS_dN	ATAACTAAGCTTTACCAGCCTC GGACCTCG	TTCATATCTAGACTAGTGCAG ACGCCGCCGG
MAVS_dC	AAGTATAAGCTTATGCCGTTTG CTGAAGAC	ATACATTCTAGATGAGGGCCT GTGGCATGGC

Table 3.3 Primers for constructing MAVS deletin mutations.

siRNA-mediated gene silencing. siRNA against human RIG-I (M-012511-00), mouse RelB (M-040784-01), mouse RelA (M-040776-00) and control siRNA (D-001206-13) were commercially obtained Dharmacon Research, Inc.(Lafayette, CO). The siRNA targeting RIG-I and control siRNA were transfected at 100 nM into A549 cells by using a TransIT-siQuest transfection kit (Mirus Bio Corp., Madison, WI) according to the manufacturer's instructions. The control siRNA and the siRNA targeting RelA and RelB were transfected at 50 nM into MEF cells using reverse transfection according to manufacturer's protocol. Forty-eight hours after transfection, cells were RSV infected as indicated time. The silencing efficiency of siRNA was evaluated using reverse transcriptase PCR (RT-PCR) for RIG-I as well as Western immunoblot for RelB and RelB.

RT-PCR and quantitative real-time PCR (QRT-PCR). Total RNA was extracted using acid guanidium phenol extraction (Tri Reagent; Sigma). One microgram of RNA was reversely transcribed using Super Script III in a 20 μl reaction mixture. One μl of cDNA product was diluted 1:2, and 2 μL was amplified in a 25 μL reaction mixture containing 12.5 μL of SYBR green supermix (Bio-Rad) and 0.4 μM each of forward and reverse gene-specific primers (Table 3.1), aliquoted into 96-well, 0.2-mm thin-wall PCR plates, and covered with optical-quality sealing tape. The plates were denatured for 90 s at 95°C and then subjected to 40 cycles of 15 s at 94°C, 60 s at 60°C, and 1 min at 72°C in iCycler (BioRAD). After PCR was performed, PCR products were run on 2% agarose gels to assure a single amplification product. Static analysis of gene expression was described before (87).

Gene name	Forward sequence	Reverse sequence
Groβ	CACTCTCAAGGGCGGTCAA	TGGTTCTTCCGTTGAGGGAC
IP10	CGATGACGGGCCAGTGA	CGCAGGGATGATTTCAAGCT
Rantes	TCCAATCTTGCAGTCGTGTTTG	TCTGGGTTGGCACACACTT
GAPDH	CATGGCCTTCCGTGTTCCTA	GCGGCACGTCAGATCCA

Table 3.1 Probes for real-time PCR

Electrophoretic mobility shift assay (EMSA). A total of 35 μg whole cell extracts (WCEs) were incubated in DNA-binding buffer containing 5% glycerol, 12 mM HEPES, 80 mM NaCl, 5 mM DTT, 5 mM $MgCl_2$, 0.5 mM EDTA, 1 μg of poly (dA-dT), and 100,000 cpm of ^{32}P-labeled double-stranded oligonucleotide containing NF-κB binding sites in a total volume of 25 μL as describe before (149). Gels were dried and exposed to BioMax film (Kodak) for autoradiography.

Co-immunoprecipitation and Western immunoblot. WCEs were prepared using modified radioimmunoprecipitation assay (RIPA) buffer (50 mM Tris-HCl [pH 7.4], 150 mM NaCl, 1 mM EDTA, 0.25% sodium deoxycholate, 1% IGEPAL CA-630, 1 mM PMSF, 1 mM NaF, 1 mM Na_3VO_4, and 1 μg/ml each of aprotinin, leupeptin, and pepstatin). WCEs were pre-cleared with protein A-Sepharose 4B (Sigma) for 10 min at 4 °C and immunoprecipitation was conducted for 2 hours at 4 °C with primary Ab. Immune complexes were then precipitated by adding 50 μL of protein A-Sepharose beads (50% slurry) and incubated for 1 h at 4°C. Beads were washed three times with cold TB buffer (150 mM NaCl, 5 mM EDTA, 50 mM Tris-HCl [pH 7.4], 0.05% IGEPAL CA-630), and immune complexes were fractionated by 10% SDS-polyacrylamide gel electrophoresis and transferred to a polyvinylidene difluoride membrane by electroblotting. Membranes were blocked in 5% nonfat dry milk in Tris-buffered saline–0.1% Tween and probed with the primary Ab indicated in the figure legends. Membranes were washed and incubated with IRDye 700-conjugated anti-mouse Ab or IRDye 800-conjugated anti-rabbit Ab (Rockland, Inc.). Finally, the membranes were washed three times with TBS-T and scanned by an Odyssey infrared scanner. Sources of primary Ab were: anti-Flag M2 mAb (Stratagene), rabbit anti-RelA C20 polyclonal Ab (Santa Cruz), and anti-p52 polyclonal Ab (Upstate,Charlottesville, VA).

Electroporation. Two million freshly isolated MEFs were suspended in 100 μl MEF2 nucleofactor solution (Amaxa), and transfected (program A023) with 5 μg plasmid DNA. After transfection, cells were immediately transferred to DMEM and cultured for at least 48 h before treatment.

3.3 RESULTS

RSV-induced p52 formation is RIG-I, NIK and IKKα dependent.

Recently, we have reported that RSV infection activated the noncanonical pathway (19). To illustrate, we stimulated A549 cells with the LTβ agonist, LT-related inducible ligand that competes for glycoprotein D binding to herpesvirus entry mediator on T cells (LIGHT), a noncanonical pathway activator (76), and compared p52 formation with that induced by RSV infection (Fig.3.1A). LIGHT rapidly and strongly induced p52 formation within 30 min after treatment, which persisted for more than 6 h. In addition, we noted p100 expression was upregulated, a consequence of p100 being downstream of the NF-κB pathway (148). Similarly, RSV infection induced p52 formation detectable 12 h after RSV adsorption and persisted for 24 h (Fig.3.1A). Although p100 was also induced at the 12 h point, its level fell at 24h, and this was probably due to the transient activation of the noncanonical pathway in RSV infection (19).
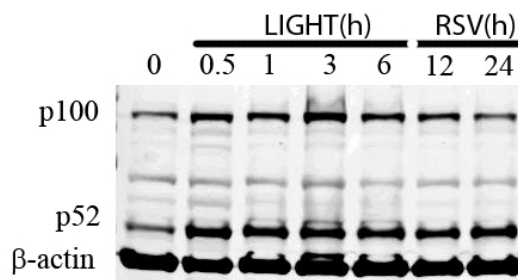

Fig.3.1A A549 cells were treated with LIGHT for 0, 0.5 h, 1 h, 3 h and 6 h, as well as infected with RSV (M.O.I. 1) at 12 h and 24 h. Whole cell extracts were collected and Western immunoblot was conducted to detect the expression of p100 and its proteolytic product p52.

We next examined whether RIG-I mediated RSV-induced p52 formation.   For this, we used siRNA mediated transfection to silence RIG-I expression.   In comparison with control siRNA transfected cells, where RIG-I mRNA was not detectable in uninfected cells and its expression was strongly upregulated 24 h after RSV infection, accumulation of RIG-I mRNA was significantly reduced in transfectants with RIG-I

specific siRNA (Fig.3.1B, top).   Importantly, after RSV infection, the basal and RSV induced p52 was significantly decreased in RIG-I silenced cells (Fig.3.1B, bottom).
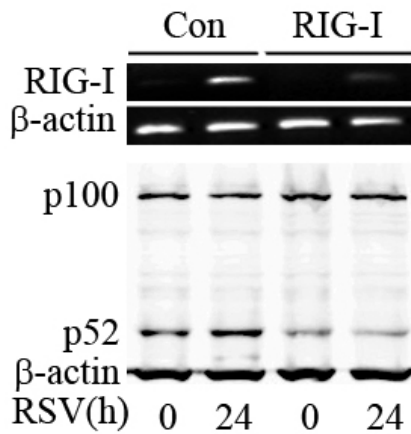

Fig.3.1B A549 cells transfected with control (Con) siRNA and RIG-I siRNA for 48 h were then RSV infected for 0 and 24 h. Total RNA was extracted and assayed by RT-PCR to measure the expression of RIG-I (upper panel).   B-Actin is a control.   Shown is an ethidium bromide stained agarose gel. Whole cell lysates were prepared from the same cell treatment and p100 and p52 by Western immunoblot using NH$_2$ terminal anti-NF-κB2 Ab (lower panel).   The blot was probed with β-Actin as a loading control.

To confirm the NIK and IKKα dependence in noncanonical pathway activation, p52 formation was determined in wild type (WT), NIK deficient (NIK$^{-/-}$), IKK$\alpha^{-/-}$ and IKK$\gamma^{-/-}$ MEFs (mouse embryonic fibroblasts).   Here, p52 formation was observed in WT and IKK$\gamma^{-/-}$ MEFs 24 h after RSV infection, but was completely abolished in NIK$^{-/-}$ and IKK$\alpha^{-/-}$ cells (Fig.3.1C).   These data suggested that RSV-induced p52 formation was RIG-I dependent, involving the known NIK and IKKα kinases.
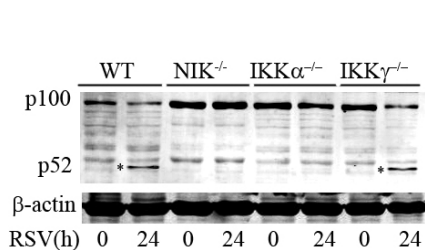

Fig.3.1C   WT, NIK$^{-/-}$, IKK$\alpha^{-/-}$ and IKK$\gamma^{-/-}$ MEFs were infected by RSV (M.O.I. 1) for 0 and 24 h. Whole cell lysates were assayed by Western immunoblot to detect p100 expression and p52 formation (indicated by asterisk). β-Actin was a loading control.   p52 was detected only in RSV infected WT and IKK$\gamma^{-/-}$ cells.
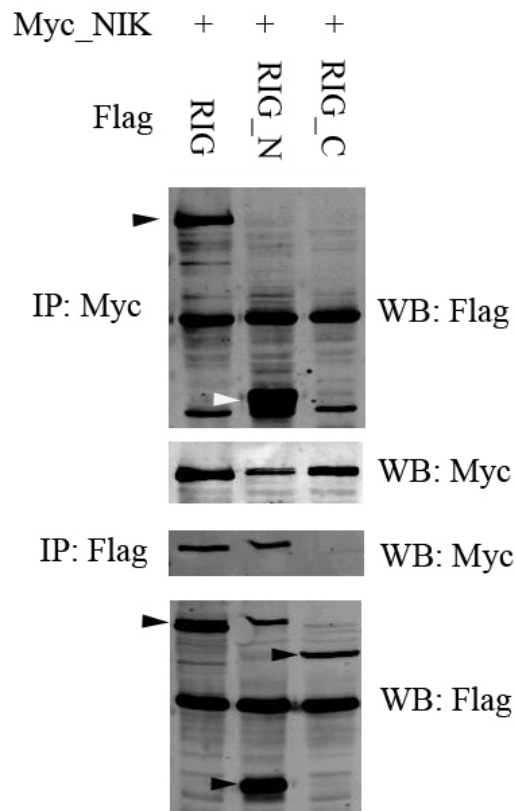
RIG-I and MAVS associate with NIK and IKKα.
        To further investigate the novel functional interaction between RIG-I and NIK, and determine the domains involved, co-immunoprecipitation experiments were conducted. First, full length Myc_NIK and different Flag_RIG-I constructs were co-

43

transfected into HEK293 cells. The RIG-I constructs included full length RIG-I, the RIG-I NH$_2$ terminus containing the two CARD domains (RIG_N), and the RIG-I COOH terminus containing the helicase domain (RIG_C). NIK was precipitated using the anti-Myc Ab, and RIG-I association detected by anti-Flag Western immunoblot (Fig.3.2A, the first panel from top). These results indicated that NIK bound to full length RIG-I and RIG_N, but not RIG_C, suggesting that the two CARD domains of RIG-I are required for RIG-I·NIK complex formation.To confirm this finding, the reverse experiment was performed using the anti-Flag Ab to precipitate RIG-I and the NIK association determined using anti-Myc Ab in the Western immunoblot. The same result was observed in this experiment (Fig.3.2A the third panel from top).

 We next investigated whether the downstream RIG-I adapter, MAVS, complexed with NIK. Co-immunoprecipitation experiments were performed using full length Flag- and GFP- tagged NIK and different deletion mutations of MAVS. For this experiment, 4 forms of Myc and Strawberry tagged MAVS plasmids were used including wild type MAVS (MAVS), MAVS deleted in its NH$_2$-terminal CARD domain (MAVS_dN), MAVS deleted in its COOH-terminal trans-membrane (Tm) domain (MAVS_dC) and MAVS without both its CARD and Tm domains (MAVS_Dou). First, full length NIK was precipitated using anti-Flag Ab and MAVS association deteced by anti-Myc Ab in Western immunoblot (Fig.3.2B, the first panel from top). The converse experiment was conducted to precipitate MAVS using anti Myc Ab, and NIK detected using anti-Flag in Western blot (Fig.3.2B, the third panel from top). Both experiments produced the same result - only the full length MAVS associated with NIK.

 To identify which NIK domains were required for MAVS complex formation, co-immunoprecipitation experiments were conducted using different NIK deletion mutants. A series of expression vectors encoding NH$_2$ and COOH terminal domain deletions were tested (Fig.3.2C). Our results suggested that the N-terminal deletion mutants of NIK (C1, C2 and C3) associate with MAVS, but the C-terminal deletions (N1, N2 and N3) did not (Fig.3.2D).This result suggested that the COOH terminus containing aa 660-947 were required for binding MAVS.

Myc_NIK + + +

Flag RIG RIG_N RIG_C

IP: Myc WB: Flag

WB: Myc

IP: Flag WB: Myc

WB: Flag

Fig.3.2A   HEK293 cells were transfected with eukaryotic expression vectors encoding Myc-tagged NIK (Myc_NIK) and different deletion mutants of Flag epitope-tagged RIG-I, including full length RIG-I (RIG), the NH$_2$ terminal CARD domains (RIG_N) and the COOH terminus (RIG_C). 36 h after transfection, whole cell lyses were prepared and Myc_NIK immunoprecipitated (IP) using anti-Myc Ab. RIG-I association of were detected by Western immunoblot (WB) probing with anti-Flag Ab. Black arrow-head shows the location of full length of RIG-I; white arrow head indicates RIG_N (the first panel from top). To monitor IP recovery, the presence of Myc_NIK in immunoprecipitate was measured by probing the same membrane with anti-Myc Ab (the second panel from top). Conversely, Flag_RIG and its deletion mutants were IPed using anti-Flag Ab, and Western immunoblot was performed using anti-Myc Ab (third panel from top). Note that Myc-NIK is only seen in the IPs from RIG and R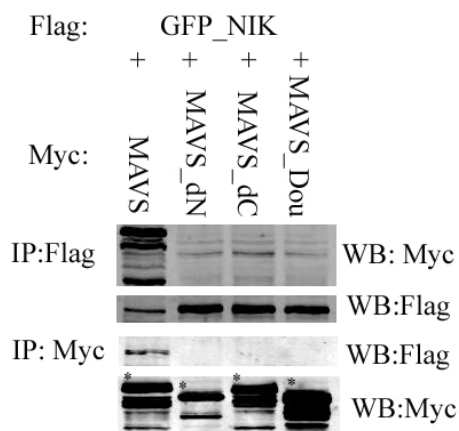IG_N co-transfected cells.   To monitor IP recovery, the presence of RIG-I measured by anti-Flag Ab; each isoform is indicated by black arrow-heads (bottom panel).

Flag: GFP_NIK

+ + + +

Myc: MAVS MAVS_dN MAVS_dC +MAVS_Dou

IP:Flag WB: Myc

WB:Flag

IP: Myc WB:Flag

WB:Myc

Fig.3.2B   HEK 293 cells were transfected with Flag_GFP_NIK and different forms of Myc_MAVS.   IP was conducted using anti-Flag and MAVS detected by anti-Myc Ab in Western (top panel).   IP of Flag_GFP_NIK was confirmed by WB (second panel). Conversely, the MAVS was IPed using anti-Myc Ab, and the presence of NIK determined in WB using anti-Flag Ab (third panel).   IP of Myc-MAVS was confirmed by reprobing the membrane with anti-Myc (bottom panel). Note that only full length MAVS associates with NIK.
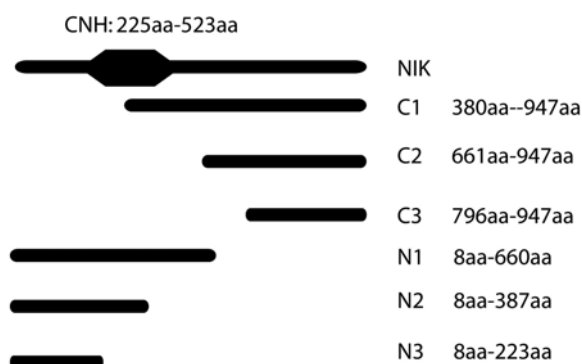
45

Fig.3.2C Schematic diagram of NIK and deletion mutants. The Ser-Thre kinase domain is indicated by black octagon. N-terminal deletion mutants C1, C2 and C3, and C-terminal deletion mutants N1, N2 and N3. At right is span (in amino acids) of the various deletions.
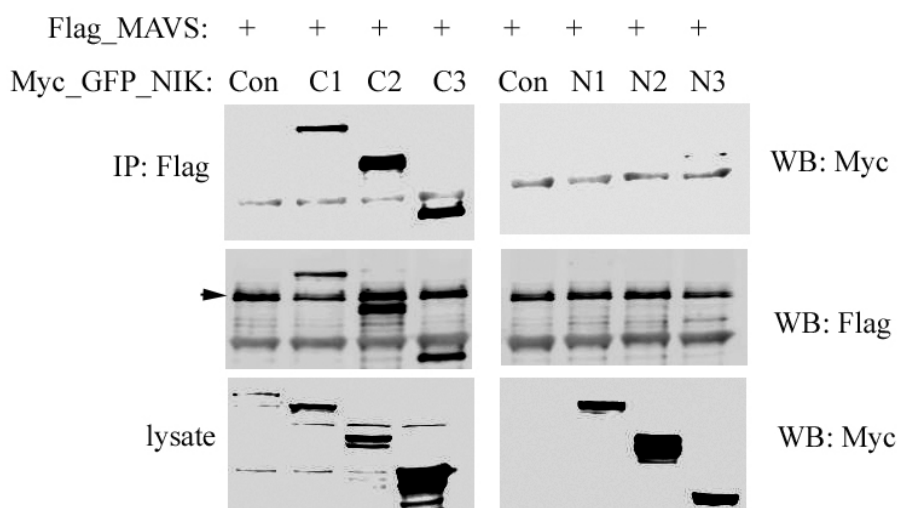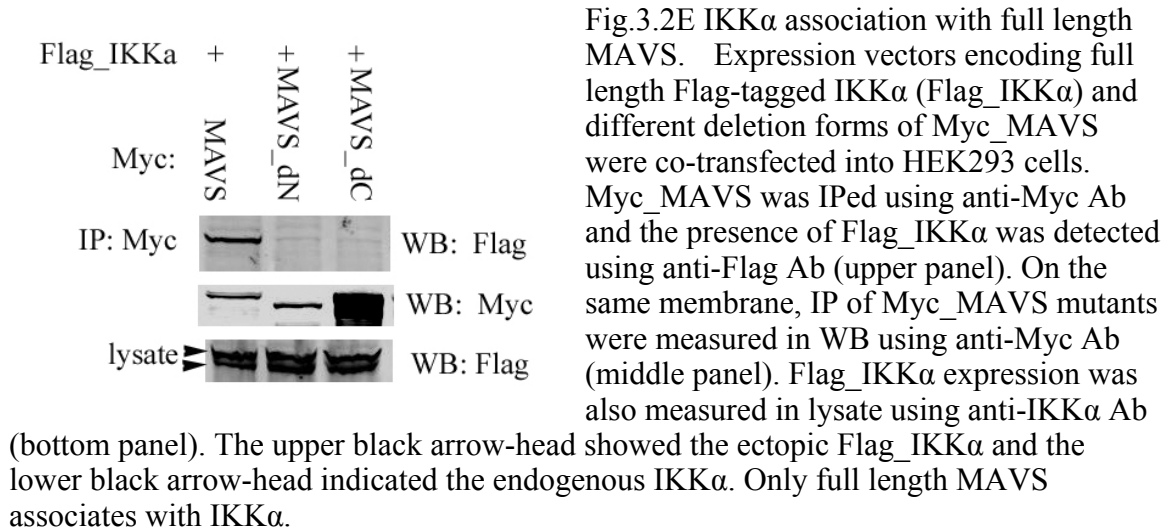
Fig.3.2D Full length Flag-MAVS was transfected in the absence (Con) or presence of different deletion forms of NIK into HEK293 cells. Whole cell extracts were prepared and subjected to co-IP experiment using anti-Flag Ab. Association with NIK C1, C2, C3, N1, N2 and N3 deletions was detected in WB using anti-Myc Ab (upper panel). The presence of Flag_MAVS in the IP was detected by WB. Its location is indicated by black arrow-head (middle panel). The expression levels of different deletion forms of NIK were measured in WB in the lysates used for IP (Lower panel). Note that only the COOH terminal fragments (C1, C2, C3) bind MAVS.

Full length IKKα was co-expressed with full length or deletion mutants of

MAVS. The complex was precipitated using anti-Myc Ab and IKKα association

46

detected using anti-Flag Ab in the Western immunoblot. Our result suggested that only full length of MAVS binds IKKα (Fig.3.2E).

Fig.3.2E IKKα association with full length MAVS. Expression vectors encoding full length Flag-tagged IKKα (Flag_IKKα) and different deletion forms of Myc_MAVS were co-transfected into HEK293 cells. Myc_MAVS was IPed using anti-Myc Ab and the presence of Flag_IKKα was detected using anti-Flag Ab (upper panel). On the same membrane, IP of Myc_MAVS mutants were measured in WB using anti-Myc Ab (middle panel). Flag_IKKα expression was also measured in lysate using anti-IKKα Ab (bottom panel). The upper black arrow-head showed the ectopic Flag_IKKα and the lower black arrow-head indicated the endogenous IKKα. Only full length MAVS associates with IKKα.

RSV activates RelA translocation in IKKγ-/- MEFs.

To further understand the function of NIK·IKKα complex in RSV induced signaling, we RSV infected WT, IKKγ$^{-/-}$, NIK$^{-/-}$ and IKKα$^{-/-}$ MEFs and assayed for canonical NF-κB DNA binding activity using a RelA/NF-κB1-selective probe (149). In WT cells, RSV induces the presence of the RelA·NF-κB1 DNA binding complex 12 and 24 h after viral adsorption Surprisingly, in IKKγ$^{-/-}$ cells, the DNA binding activity of RelA was abolished at 12 h of RSV infection, but was strongly induced 24 h of infection(Fig.3.3A, left panel). To identify which member of NFκB family that forms this DNA protein complex, proteins from RSV infected IKKγ$^{-/-}$ cells which were incubated with anti-RelA Ab, anti-RelB Ab, and anti-p52 Ab. Supershift was conducted and only the sample incubated with RelA produced a migrated band, which suggested the increase of RelA and DNA binding in RSV infected IKKγ$^{-/-}$ cells.

To further demonstrate that RelA translocated into the nucleus in IKKγ$^{-/-}$ cells, WT and IKKγ$^{-/-}$ MEFs were RSV infected, and sucrose cushion purified nuclear extracts were assayed for RelA abundance by Western immunoblot. Here, RSV infection

strongly induced RelA signal. Importantly, RSV infection also increased the nuclear accumulation of RelA in IKKγ$^{-/-}$ MEFs (Fig.3.3B).
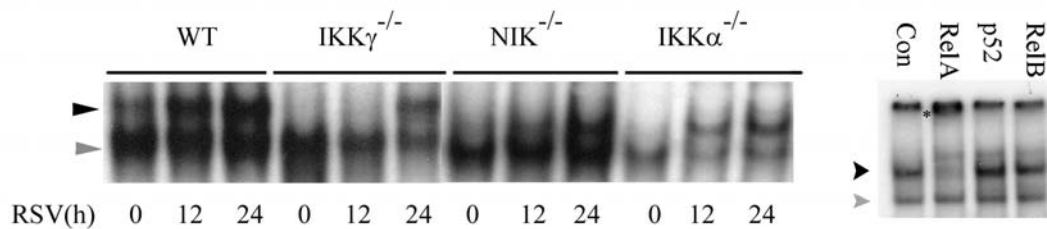

Fig.3.3A WT, IKKγ$^{-/-}$, NIK$^{-/-}$ and IKKα$^{-/-}$ MEFs were infected by RSV (M.O.I.=1) for time indicates, and whole cell lysates assayed by EMSA using a DNA probe specifically targeting RelA (Left panel). The location of the inducible RelA·NF-κB1 complex are shown by black arrowhead; the NF-κB1 homodimer is indicated by gray arrow-head. Proteins from RSV-infected IKKγ$^{-/-}$ cells were incubated with anti-RelA, anti-RelB and anti-p52 Abs for 1 h and supershift experiment was conducted. The asterisk indicates the supershifted band in the RelA complex; note the significant attenuation of inducible complex binding in the extracts incubated with anti-RelA Ab (Right panel).

To determine whether that RelA was transcriptionally competent, a NF-κB luciferase reporter gene (the IFN-β PRD II domain (44)) was transfected into IKKγ$^{-/-}$ MEFs and exposed to the absence or presence of RSV. A 3-fold increase in normalized luciferase activity was observed in the RSV-infected cells (Fig.3.3C).
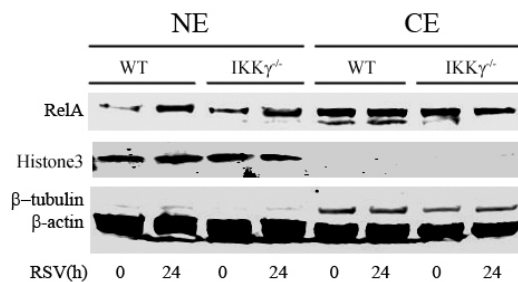

Fig.3.3B WT and IKKγ$^{-/-}$ MEFs were infected with RSV for 0 h or 24 h. Nuclear extracts were collected and Western immunoblot performed using anti-RelA Ab (Upper panel). Histone 3 was used as a nuclear protein marker and β-tubulin was used as a cytoplasmic protein marker. β-actin was used as a loading control. Note the increase in RelA in response to RSV infection in the NE
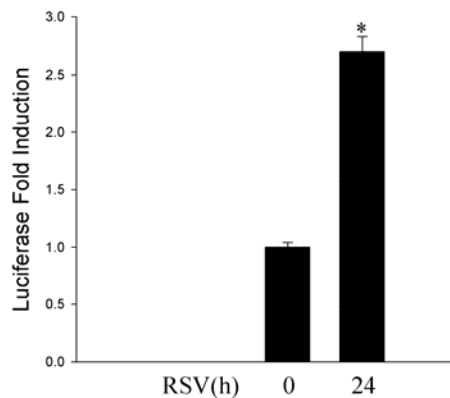
48

Fig.3.3C IKKγ-/- MEFs were transfected with an NF-κB-dependent PRD II reporter gene, subsequently RSV infected for 24 h. Luciferase reporter assay was measured.   Show is fold change in normalized luciferase reporter activity. Asterisk indicates a significant increase of reporter gene expression at 24 h of RSV infection compared to 0 h of infection (P<0.05, t test)

We further investigated the RSV induced endogenous gene expression in IKKγ-/- cells after RelA or RelB was silenced by siRNA. The efficiency of siRNA knockdown was evaluated using Western immunoblot to detect RelA and RelB expression (Fig.3.3D). After IKKγ-/- cells were transfected by siRNA for 48 h, cells were RSV infected for another 24 h.   The expression of IP10, Rantes and Groβ were tested by real-time PCR. In cells transfected with control siRNA, IP10, Rantes and Groβ increase about 8-fold, 15-fold and 7-fold respectively. A similar level of induction was observed in the cells transfected with siRNA targeting RelB, whereas the expression of all the genes decreased after RelA was silenced in IKKγ-/- cells (Fig.3.3D). These data suggested the existence of an IKKγ-independent signaling pathway that activates RelA translocation and transcriptional activity.

An IKKγ-independent component of RelA activation involves liberation from p100 complexes.

To determine canonical pathway activation, WCEs were prepared from RSV-infected WT, NIK^{-/-}, IKKα^{-/-} and IKKγ^{-/-} MEFs, and Western immunoblot performed using anti-IκBα Ab.   RSV-induced IκBα proteolysis was observed in WT, NIK^{-/-} and IKKα^{-/-} cells; however, no detectable IκBα degradation was observed in IKKγ^{-/-} MEFs (Fig.3.4A). This data not only demonstrated that RSV was able to activate canonical NF-κB pathway, but also indicated that RSV-induced RelA activation in IKKγ^{-/-} cells was

independent of IκBα proteolysis.
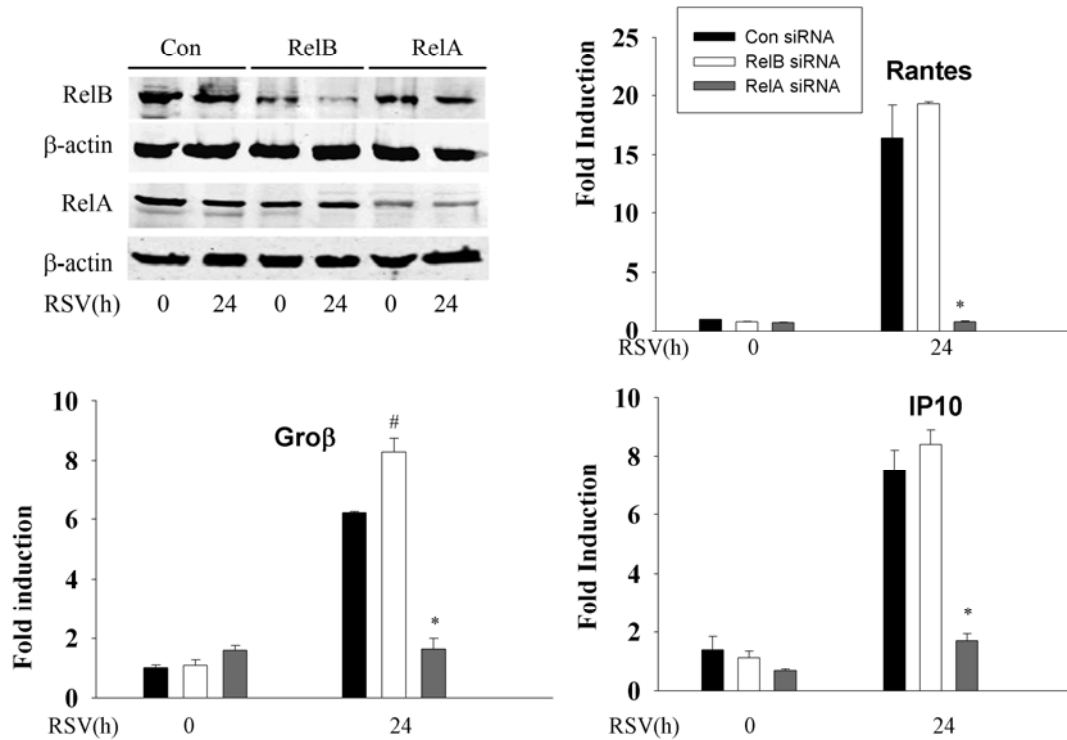

Fig.3.3D siRNA mediated knockdown of RelA/RelB. IKKγ$^{-/-}$ MEFs were transfected with control-, RelB-specific, and RelA-specific siRNA as indicated for 48 h. Cells were either uninfected or RSV infected for 24 h as indicated. Western immunoblot was performed to evaluate silencing efficiency. Top left panel, anti-RelB, third panel anti-RelA. Each blot was reprobed with anti-β-actin as loading controls. IKKγ$^{-/-}$ were transfected by control-, RelA and RelB- specific siRNA. 48 h after transfection, cells were infected by RSV for another 24 h. RNAs were extracted and Q-RT-PCR was conducted using probes detecting IP10, Rantes and Groβ. Shown is fold induction of mRNA. Note that RSV inducible gene expression is significantly inhibited only in the RelA silenced cells. * indicates a significant decrease of gene expression in RSV infected cells transfected by RelA siRNA compared to RSV infected cells transfected by RelB siRNA or Control siRNA (*P*< 0.001, t test). # indicates a significant increase of Groβ expression in RSV infected cells transfected by RelB siRNA compared to RSV infected cells transfected by Control siRNA (*P*<0.05, t test).
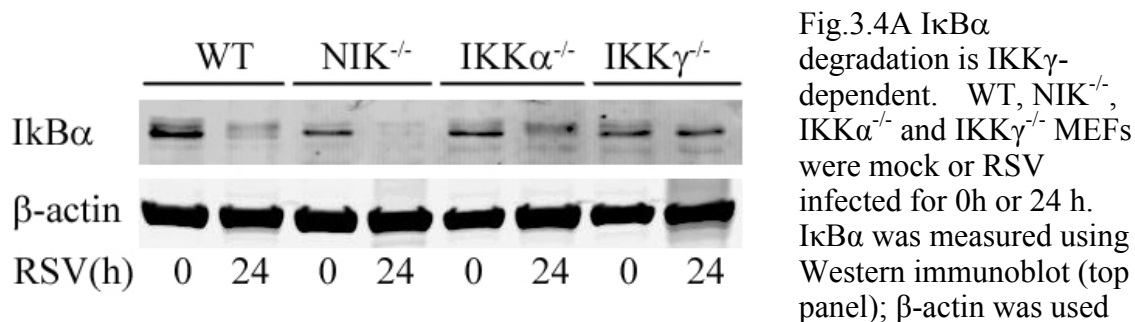
WT   NIK⁻ᐟ⁻   IKKα⁻ᐟ⁻   IKKγ⁻ᐟ⁻

IkBα

β-actin

RSV(h)   0   24   0   24   0   24   0   24

Fig.3.4A IκBα degradation is IKKγ-dependent. WT, NIK$^{-/-}$, IKKα$^{-/-}$ and IKKγ$^{-/-}$ MEFs were mock or RSV infected for 0h or 24 h. IκBα was measured using Western immunoblot (top panel); β-actin was used as an internal control (bottom panel). Note that IkB is degraded in WT, NIK$^{-/-}$, and IKKα$^{-/-}$ MEFs, but not significantly in IKKγ$^{-/-}$ MEFs.

Previous studies have reported that p100 forms a heterodimer with RelA and acted as an inhibitor to sequester RelA in the cytoplasm (69,141). However, the pathways controlling RelA release from p100 are not known. Since our findings showed that p52 formation was IKKγ-independent (Fig.3.1C), we investigated whether RSV induced RelA release from p100 associated complexes in WT and IKKγ$^{-/-}$ MEFs. To quantitate the p100-RelA complex, nondenaturing co-immunoprecipitation was performed. Here, p100 was precipitated in cytoplasmic extracts from RSV-infected WT and IKKγ$^{-/-}$ MEFs and Western immunoblot was performed using anti-NF-κB2 and anti-RelA Abs. In uninfected WT MEFs, p100 was strongly associated with RelA; 24 h after RSV adsorption, p100-associated RelA was significantly decreased. Importantly, the same phenomenon occurred in the IKKγ$^{-/-}$ MEFs (Fig. 3.4B). These data suggested that RSV-induced RelA translocation is, in part, mediated by an IKKγ-independent proteolysis of p100.

RSV replication was increased in IKKγ$^{-/-}$, but not in NIK$^{-/-}$ and IKKα$^{-/-}$ MEFs.

To determine the role of the canonical and noncanonical/crosstalk pathways in anti-viral response, WT, NIK$^{-/-}$, IKKα$^{-/-}$ and IKKγ$^{-/-}$ MEFs were RSV infected. Expression of viral proteins was then determined using Western immunoblot using anti-RSV P, N and M protein Ab. Although the level of viral protein expression was similar in WT, NIK$^{-/-}$, and IKKα$^{-/-}$ MEFS, a significant increase in viral protein expression was observed in the IKKγ$^{-/-}$ MEFs (Fig.3.5A).
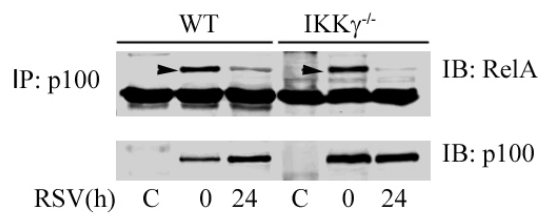
Fig. 3.4B   p100 sequesters RelA in the cytoplasma and RSV induces RelA releasing from p100 complexes.   WT and IKKγ-/- MEFs were infected by RSV for 0 h and 24 h. p100 was subjected to nondenaturing co-IP using anti-p100 Ab; nonimmune rabbit IgG was used as nonspecific binding control.   RelA association was detected by Western immunoblot using anti-RelA Ab (top).   Specific RelA staining is indicated by black arrow-head.   To monitor p100 recovery, the membrane was re-probed with anti-NF-κB2 Ab (bottom).   Note that RelA associates with p100 in uninfected cells, but this binding is lost in response to RSV infection.
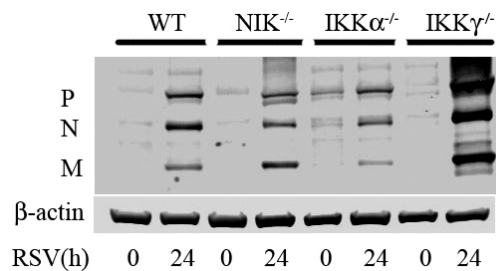

Fig.3.5A   WT, NIK$^{-/-}$, IKKα$^{-/-}$ and IKKγ$^{-/-}$ MEFs were RSV infected for 24 h. Whole cell extracts were prepared and the expression of RSV P, N and M proteins detected by Western blot (Upper panel). β-actin was used as a loading control (Lower panel).   The expression of RSV proteins are significantly increased in IKKγ-/- cells.
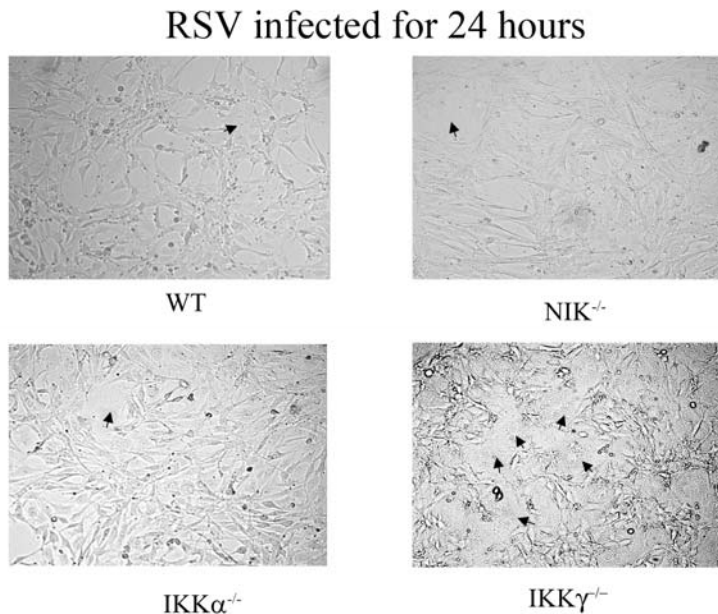
RSV infected for 24 hours

Fig.3.5B Cytopathic effect and cell fusion in response to RSV. WT, NIK$^{-/-}$, IKKα$^{-/-}$ and IKKγ$^{-/-}$ MEFs were cultured on cover slips and RSV infected for 24 h. Shown is a representative field from light microscopy (10x magnification). Note multinucleated and fused cells in IKKγ$^{-/-}$ MEFs (black arrow-heads).

52

3.4 DISCUSSION

RIG-I is a major initial intracellular sensor that detects RSV infection and activates the downstream NF-κB and IRF3 pathways by complexing with the MAVS adapter (87). In this study, we focused on the mechanistic details for how RSV induces NF-κB pathways.   Currently it is thought that NF-κB is regulated by two separate mechanisms, termed the canonical and noncanonical pathways.   The canonical NF-κB pathway is IKKγ-dependent and liberates RelA from cytoplasmic IκBα complexes.   By contrast, the noncanonical pathway is both NIK- and IKKα-dependent and results in RelB release from cytoplasmic p100 complexes. Although most stimuli activate either the canonical pathway (TNF/IL-1) or the noncanonical pathway (LIGHT/LTβ), RSV efficiently activates both (19,42,64). The mechanism for how RIG-I couples to the canonical pathway is largely understood, but the mechanism how RSV activates the noncanonical pathways via the NIK·IKKα kinase complex is unclear.   Here we make the surprising findings that RIG-I activates RelA translocation from p100 complexes by the noncanonical NIK·IKKα subunits in IKKγ$^{-/-}$ cells.   These data indicate the existence of an additional RSV-inducible "cross-talk" pathway that mediates translocation of the potent transcriptional RelA transactivator.

To our knowledge, this data is the first to demonstrate that NIK associates with the RIG-I-MAVS signaling complex.   NIK is a serine-threonine kinase of the mitogen activated MAP kinase family known to associate with the TNF receptor associated factors (TRAFs)-2, and 3, the TRAF-and NIK-associated factor (TNAP) and the IKKα kinase (62,85,90,91,156).   TRAF association allows NIK to couple with activated receptors in the TNF superfamily.   Additionally, previous work shows that that NIK serves as a scaffolding molecule, binding IKKα, an event that permits IKKα to complex with p100 in order to phosphorylate and initiate p52 formation (29).   These multiprotein interactions have been partially mapped to the NIK molecule.   The NH$_2$ terminus of NIK has binds TRAF3 and TNAP (62,85), whereas the COOH terminus is known to interact with TRAF2 (aa 624-947 of NIK) and IKKα (aa 735-947 of NIK) (90,91,156).   Our

deletion experiments indicate that the NIK COOH terminus (aa 660-947) is also required for MAVS interaction.   Because of the number of protein interactions, it is highly likely that a macromolecular complex is being formed between NIK, IKKα, RIG-I and MAVS to produce a functional signaling complex.   More detailed work will be required to identify which proteins directly interact.

MAVS is an essential signal transducer for mediating activated RIG-I signaling. MAVS does not have known enzymatic activity and apparently serves as a site for signaling complex assembly.   In this regard, the RIG-I·MAVS complex has been shown to be uniquely localized to the surface of mitochondria via a short COOH terminal transmembrane domain on the MAVS protein (132). Although devoid of enzymatic activity MAVS itself is apparently subject to multiple post-translational modifications and alternative translation initiation, a phenomenon indicated by the multiple sizes of MAVS in Western blots [Fig. 2B, and ref (132)].   Previous work has shown that in the absence of MAVS, cells are unable to activate the canonical NF-κB- or the IRF3 signaling pathways in response to dsRNA or viral infections (72,79,100,109,132). Interestingly, in the absence of mitochondrial targeting, MAVS is unable to associate with RIG-I or mediate its signaling.   Our data indicate that mitochondrial localization is required for NIK interaction, because NIK being unable to bind to the COOH terminally deleted MAVS which aberrantly targets to the cytoplasm (Fig. 2B and ref (132)).   A similar finding is made for the IKKα-MAVS interaction (Fig. 2E).   The explanation for a mitochondrial requirement for signaling is currently unknown.   Our data is the first to demonstrate that NIK association with the RIG-I-MAVS complex mediates a third signaling pathway, a cross-talk pathway involved in RelA release from p100 complexes.

RelA is sequestered in the cytoplasm through association with discrete IκB like proteins, including IκBα, IκBβ, IκBε, BCL-3, and p100 which serve to function as reservoirs for NF-κB (69,98,105,125,141).   The canonical pathway primarily involves stimulus-induced RelA liberation from IκBα, IκBβ and IκBε-sequestered complexes.   In this study, we find that RSV induces the degradation of IκBα in WT, NIK$^{-/-}$ and IKKα$^{-/-}$ MEFs, but not in IKKγ$^{-/-}$ MEFs. This result suggests that RSV-induced IκBα proteolysis

is IKKγ dependent. However, surprisingly, RSV is still able to activate RelA translocation and transcriptional activation in IKKγ$^{-/-}$ MEFs. We note that Lin et al. also reported a similar 3-fold increase of NF-κB dependent reporter gene expression finding that in IKKγ$^{-/-}$ MEFs in response to VSV. Although the identity of the transactivator was not investigated, they did note that reporter gene activity was inhibited by dominant negative IκBα, suggesting RelA involvement (169). Our study provides a mechanistic link for the viral inducible activation of RelA via forming a complex with RIG-I-MAVS and the noncanonical NIK-IKKα kinases.

RelA liberated as a result of p100 processing appears to be under separate stimulus-specific control than the canonical pathway. For example, this cross-talk pathway was recently described as being downstream of LTβ, a TNF superfamily ligand that also induces IκBα independent RelA release from cytoplasmic p100 complexes (7). Our studies indicate that RNA viral infection also activates RelA release from sequestered p100.   Moreover, since LTβ signaling is independent of RIG-I-MAVS, we conclude that several signaling cascades can converge on the cytoplasmic p100-RelA complexes including those activated by TNF superfamily of receptors and cytoplasmic RIG-I like helicases.   Finally, we emphasize that although the existence of this cross-talk pathway was initially indicated by the ability of RSV to induce RelA activation in IKKγ$^{-/-}$ MEFs, this pathway is activated in wild type MEFs and A549 epithelial cells.   In both cell types, cytoplasmic RelA is associated with p100, and that p100 processing is induced (as exemplified by p52 processing) in response to RSV infection.

Our study indicates that the activation of the noncanonical NIK·IKKα complexes induces the release of p100-associated RelA as well as the noncanonical RelB·NF-κB2 (p52) complex (Fig. 6). The prototypical NF-κB DNA binding complex is composed of a heterodimer of a transactivating subunit (RelA, RelB) with a DNA binding subunit (NF-κB1, NF-κB2). Currently we understand the canonical RelA·NF-κB1 heterodimer is the predominant DNA binding complex in A549 cells detected in gel binding studies, and responsible for most of the transcriptional activating properties (64,149). Discussed earlier, RSV induced RelA is coming from two separate cytoplasmic pools, IκBα/IκBβ

and p100. Although p100 processing releases both RelA and RelB in IKKγ^{-/-} MEFs, we find here by side-by-side siRNA knockdown that RelA, and not RelB, is the major mediator of RSV-induced RANTES, IP-10 and Gro-β expression.

The exact role of the noncanonical RelB·NF-κB2 (p52) complex in epithelial cells is less clear. Previous work using siRNA mediated knockdown of p52 indicates that p52 complexes only contribute to a minor degree RSV-inducible cytokine expression (19). In lymphocytes, the RelB·NF-κB2 complex activates a distinct spectrum of genes, including BAFF, SDF and BLC-3 (29). Because these genes are not expressed by epithelial cells the role of the noncanonical pathway is presently unclear. Presently the only suggestive data is that the RelB·NF-κB2 complex modifies the rate of canonical pathway activation in RSV infection (19).

Previously our group showed that inhibition of canonical NF-κB pathway using a peptide that disrupted IKKγ-IKKβ interaction (the NEMO binding peptide) significantly down-regulated the inflammatory reaction in RSV infected mice, despite robust, increased, RSV replication (55). Recently, IKKγ was also shown to mediate viral induced activation of IRF3 pathway downstream of the MAVS complex; inhibition of IKKγ was permissive for increased viral replication (169). Together, these findings indicate that inhibiting of IKKγ function will affect both the NF-κB-dependent inflammatory response as well as the IRF-3 mediated anti-viral response. In our study of the cross-talk pathway, we have made the intriguing finding that a portion of RSV-induced inflammatory cytokine production is mediated by the noncanonical NIK·IKKα complex. Inhibiting NIK and IKKα signaling does not result in increased RSV replication. These characteristics of the NIK·IKKα mediated cross-talk pathway makes NIK and IKKα potential targets for therapeutics targeting acute broncholitis caused by RSV infection.

CHAPTER IV: DIFFERENTIAL FUNCTION OF IKKγ AND IKKγΔ IN IRF3 SIGNALING

4.1 INTRODUCTION

The initiation of host cell anti-viral signaling depends on an intact of RIG-I-MAVS pathway. (70-72,79,100,109). RIG-I detects the invasion of RNA viruses and recruits its downstream adaptor, MAVS, leading to the activation of two transcriptional factors, NFκB and IRF3.The activation of NFκB pathway requires the IκB kinase (IKK) complex, also known as the "signalsome". This signal complex contains two closely related kinase subunits, (IKKα and IKKβ) and a regulatory subunit IKKγ, also know as NFκB essential modulator (NEMO) (165). The activation of IKK complex induces the phosphorylation, ubiquitination and degradation of inhibitor of NFκB (IκB), as well as the nuclear translocation and DNA binding of NFκB. For the activation of IRF3, two IKK-related kinases, TANK-binding kinase 1 (TBK1) and IKKε, play an essential role (60). TRAF family member-associated NF-κB activator (TANK) links TBK1and IKKε to the upstream TRAF molecules (54). Recently, the interaction between TANK and IKKγ has been reported and the "branching point" between NFκB and IRF3 downstream of RIG-I·MAVS signaling was located on IKKγ. In IKKγ deficient cells, the activations of both NFκB and IRF3 were abolished in response to different RNA viruses (169).

In previous work, my lab has identified a 43-kDa protein IKKγΔ, which is an alternative splicing variant of IKKγ excluding exon 5. Here we demonstrated that in contrast to IKKγ, IKKγΔ was unable to associate with TANK and IKKε. In response to Sendai virus and RSV infection, IKKγΔ failed to activate IRF3 and induce type I interferon. However, IKKγΔ was still able to bind IKKα and IKKβ, and activate NFκB pathway in response to TNFα. Together, these data suggest that by affecting inflammatory reaction without affecting the anti-viral response, IKKγΔ can activate the NFκB pathway but not the IRF3 pathway.

4.2 MATERIALS AND METHODS

Cell cultures. Human A549 pulmonary type II epithelial cells (American Type Culture Collection [ATCC]) were grown in F12K medium (Gibco) with 10% fetal bovine serum (FBS), penicillin (100 U/ml), and streptomycin (100 g/ml) at 37°C in a 5% CO2 incubator. Wild type and IKKγ-/- (160) MEFs were cultured in Eagle's minimum essential medium (Gibco) with 0.1 mM nonessential amino acids, 1.0 mM sodium pyruvate, and 10% FBS. IKKγ and IKKγΔ reconstituated stable MEFs were described previously(56). HEK293 cells were cultured in Eagle's minimum essential medium (Gibco) with 0.1 mM nonessential amino acids, 1.0 mM sodium pyruvate, and 10% FBS.

Virus preparation and infection. The human RSV A2 strain was prepared as in Chapter II . Sendai virus was purchased from Charles River Laboratory. MEF cells were infected with 100 hemagglutinin units/ml and harvested at the time indicated (38).

Plasmid construction. Expression vectors encoding Flag epitope-tagged RIG-I NH2 terminus and Flag eiptope-tagged MAVS were described before (37). Expression vectors encoding Flag epitope- tagged MAVS were described in (132). PEF6-Flag-IKKα and PEF6-Flag-IKKβ were described in (56). Myc-IKKγ and Myc-IKKγΔ were cloned into HindIII/XbaI sites of pcDNA 3 using an upstream primer: 5'-ATCAAT<u>GGATCC</u> ATGGAACAGAAGTTGATTTC CGAAGAAGAG CTCGGATCCATGAATTAGGCA CC T-3' and downstream primer: 5'-AGTATC<u>AAGCTT</u>CTACTC AATGCACTCC ATGACAT-3'.

RT-PCR and quantitative real-time PCR (QRT-PCR). Total RNA was extracted using acid guanidium phenol extraction (Tri Reagent; Sigma). One microgram of RNA was reversely transcribed using Super Script III in a 20 μl reaction mixture. One μl of cDNA product was diluted 1:2, and 2 μL was amplified in a 25 μL reaction mixture containing 12.5 μL of SYBR green supermix (Bio-Rad) and 0.4 μM each of forward and reverse gene-specific primers (Table 4. 1), aliquoted into 96-well, 0.2-mm thin-wall PCR plates, and covered with optical-quality sealing tape. The plates were denatured for 90 s at 95°C and then subjected to 40 cycles of 15 s at 94°C, 60 s at 60°C, and 1 min at 72°C in iCycler (BioRAD). After PCR was performed, PCR products were run on 2% agarose

gels to assure a single amplification product. Static analysis of gene expression was described before (87).

Gene name	Forward sequence	Reverse sequence
IRF7	AAATGCTGGGCTCCAAACC	GAGGTCCCCGGCATCACT
IFN-α1	ACCTCCACCAGCAGCTCAA	CCCCACCTGCTGCATCAG
IFN-α4	TTGTCTGCTACTTGGAATGCAA	TGAGCTGCTGATGGAGGTCATC
IFN-β	CGGACTTCAAGATCCCTATGGA	TGGCAAAGGCAGTGTAACTCTTC
IP10	CGATGACGGGCCAGTGA	CGCAGGGATGATTTCAAGCT
Rantes	TCCAATCTTGCAGTCGTGTTTG	TCTGGGTTGGCACACACTT
GAPDH	CATGGCCTTCCGTGTTCCTA	GCGGCACGTCAGATCCA

Table 4.1 Probes for real-time PCR.

Electrophoretic mobility shift assay (EMSA). A total of 35 µg whole cell extracts (WCEs) were incubated in DNA-binding buffer containing 5% glycerol, 12 mM HEPES, 80 mM NaCl, 5 mM DTT, 5 mM $MgCl_2$, 0.5 mM EDTA, 1 µg of poly (dA-dT), and 100,000 cpm of ^{32}P-labeled double-stranded oligonucleotide containing NF-κB binding sites (149) and IRF3 binding site (87) in a total volume of 25 µL as describe before. Gels were dried and exposed to BioMax film (Kodak) for autoradiography.

Native PAGE for Separation of IRF-3 Dimers from Monomers. 7% native gel without stacking gel was made as describe in (84). The gel was prerun in 1× native running buffer (10× native running buffer: 30 g Tris base, 144 g glycine. Add ddH$_2$O to 1 liter, and store at 4°C) freshly supplemented with 1% sodium deoxycholate (DOC,Sigma) at 40 mA for 30 min. Mix 50 µg protein with native PAGE buffer (4× native PAGE buffer (10 mL): Mix 5 mL 0.5 M Tris-HCl, pH 6.8, 4 mL glycerol, 0.4 g sodium DOC, 0.5 mg bromophenol blue. Add ddH$_2$O to 10 mL, and store in aliquots at −20°C) and run at a constant current (25 mA) for 120 min.

Co-immunoprecipitation and Western immunoblot. Who cell extracts (WCEs) were prepared using modified radioimmunoprecipitation assay (RIPA) buffer (50 mM Tris-HCl [pH 7.4], 150 mM NaCl, 1 mM EDTA, 0.25% sodium deoxycholate, 1% IGEPAL CA-630, 1 mM PMSF, 1 mM NaF, 1 mM Na$_3$VO$_4$, and 1 µg/ml each of

aprotinin, leupeptin, and pepstatin). WCEs were pre-cleared with protein A-Sepharose 4B (Sigma) for 10 min at 4 °C and immunoprecipitation was conducted for 2 hours at 4 °C with primary Ab. Immune complexes were then precipitated by adding 50 μL of protein A-Sepharose beads (50% slurry) and incubated for 1 h at 4°C. Beads were washed three times with cold TB buffer (150 mM NaCl, 5 mM EDTA, 50 mM Tris-HCl [pH 7.4], 0.05% IGEPAL CA-630), and immune complexes were fractionated by 10% SDS-polyacrylamide gel electrophoresis and transferred to a polyvinylidene difluoride membrane by electroblotting. Membranes were blocked in 5% nonfat dry milk in Tris-buffered saline–0.1% Tween and probed with the primary Ab indicated in the figure legends. Membranes were washed and incubated with IRDye 700-conjugated anti-mouse Ab or IRDye 800-conjugated anti-rabbit Ab (Rockland, Inc.). Finally, the membranes were washed three times with TBS-T and scanned by an Odyssey infrared scanner. Sources of primary Ab were: anti-Flag M2 mAb (Stratagene), rabbit anti-IRF3 polyclonal Ab (Santa Cruz), anti-Myc mAb (Santa Cruz), anti-STAT1 polyclonal Ab(Santa Cruz) and anti-phospho-STAT1 (Cell Signaling).

Electroporation. Two million freshly isolated MEFs were suspended in 100 μl MEF2 nucleofactor solution (Amaxa), and transfected (program A023) with certain amount plasmid DNA as described. After transfection, cells were immediately transferred to DMEM and cultured for at least 48 h before treatment.

4.3 RESULTS

The replication of RNA viruses is increased in IKKγΔ reconstituted MEF cells.

To compare the function of IKKγ and IKKγΔ in response to RNA viruses, IKK$^{-/-}$ MEF cells were reconstituted with IKKγ or IKKγΔ, and the level of expression was investigated using Western immunoblot (Fig.4.1A, middle panel). Ectopic IKKγΔ has a higher expression level compared to the expression of ectopic IKKγ. IKKγ$^{-/-}$ cells, IKKγ reconstituted and IKKγΔ reconstituted MEFs were infected by Sendai virus as the time indicated, and the expression of viral proteins was studied by Western immunoblot. In IKK$^{-/-}$ and IKKγΔ reconstituted MEFs, there were a significant increase of Sendai viral proteins at 12 h and 24 h of infection relative to that in IKKγ$^{+/+}$ (Fig.4.1A, top panel).

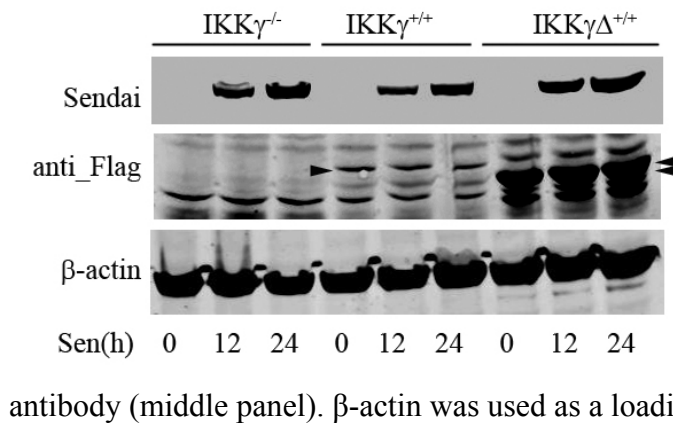Fig.4.1A IKKγ-/-, IKKγ reconstituted and IKKγΔ reconstituted MEFs were infected by Sendai virus at 0, 12 h and 24 h. 100 μg WCEs were used for Western immunoblot and the viral protein was detected by anti-Sendai virus antibody (upper panel). The expression of ectopic IKKγ and IKKγΔ was tested by anti-Flag antibody (middle panel). β-actin was used as a loading control (bottom panel).

We also investigated the replication of RSV in wild type, IKKγ reconstituted, IKKγ$^{-/-}$ and IKKγΔ reconstituted MEFs. 24 h after RSV infection, a significant increase of RSV P, N and M protein was observed in IKKγ$^{-/-}$ MEFs and IKKγΔ reconstituted MEFs, as compared to WT or IKKγ$^{+/+}$, there is no obvious difference in RSV protein expression (Fig.4.1B).
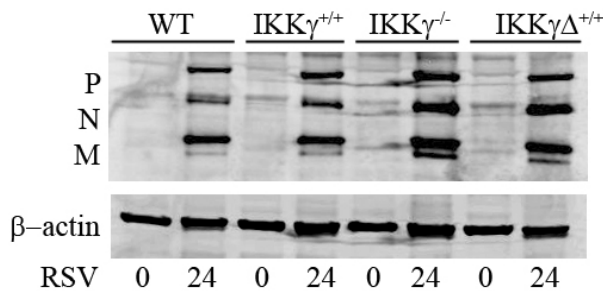
Fig.4.1B Wild type, IKKγ reconstituted, IKKγ$^{-/-}$ and IKKγΔ reconstituted MEFs were infected by RSV (M.O.I.=1) for 24 h. RSV viral protein P, N and M were detected by anti-RSV antibody (upper panel) and β-actin was used as a loading control (bottom panel).

Since RSV induces cellular fusion *in vitro,* we also counted the numbers of multinucleated cells in wild type, IKKγ$^{-/-}$, IKKγ and IKKγΔ reconstituted IKKγ$^{-/-}$ MEFs at 24 h of RSV infection. In IKK$^{-/-}$ and IKKγΔ reconstituted MEFs, about 13 and 15 fusion cells/high power field were detected respectively, while in wild type and IKKγ reconstituted MEFs, only 1 and 2 fusion cells were observed (Fig.4.1C). All these data suggested that RNA viruses had a higher level of replication in IKKγ$^{-/-}$ and IKKγΔ reconstituted MEFs than in wild type and IKKγ reconstituted MEFs.
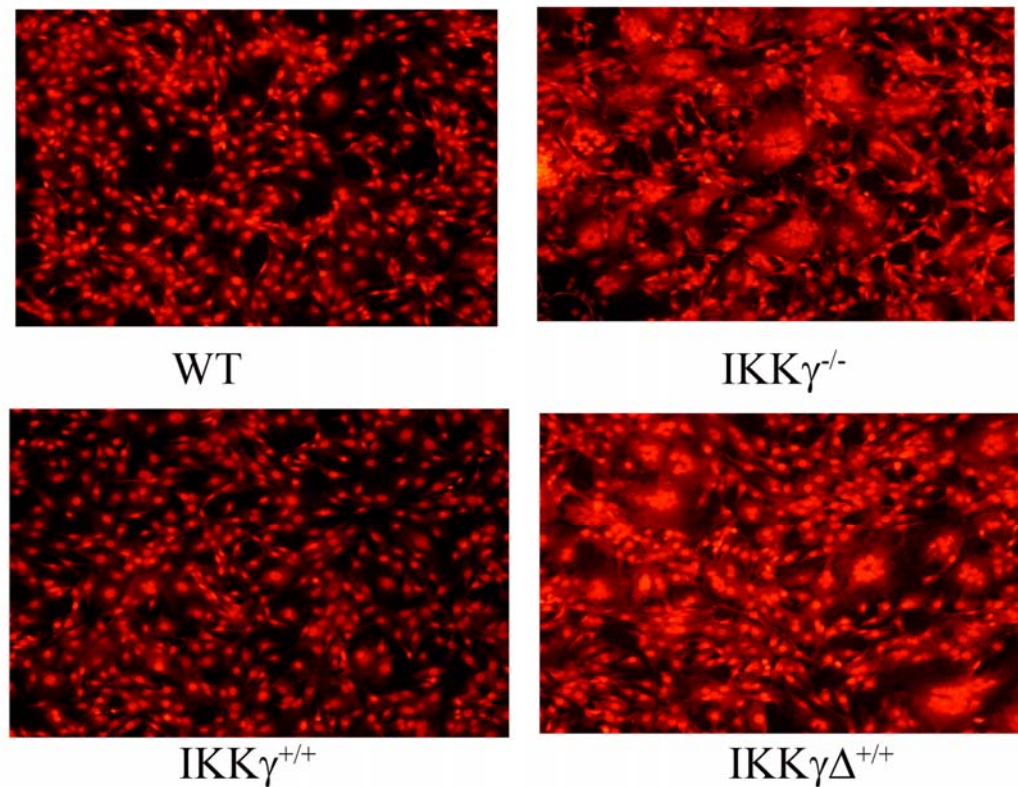
61

Fig.4.1C Wild type, IKKγ$^{-/-}$, IKKγ and IKKγΔ reconstituted IKKγ$^{-/-}$ MEFs were RSV infected for 24 h. Cells were fixed with 4% paraformaldehyde in PBS and stained with SYTOX orange (Molecular Probes). Fluorescence microscopy was performed on a Zeiss LSM510 META system. Images were captured at a magnification of x10.

RNA viruses induce less anti-viral gene expression in the cells transfected with IKKγΔ than the cells transfected with IKKγ.

To understand the mechanism under the difference of viral replication rate in these MEFs, wild type, IKKγ reconstituted and IKKγΔ reconstituted MEFs were infected by Sendai virus for 16 h. The induction of IRF7, IFN-α4, IFN-β, IP10 and Rantes were investigated by QRT-PCR. Sendai virus induced a significant increase in these genes in wild type and IKKγ reconstituted cells, but the expression of these genes was greatly attenuated in the IKKγΔ reconstituted MEFs (Fig.4.2A). A similar result was observed in RSV infected wild type, IKKγ reconstituted and IKKγΔ reconstituted MEFs. The expression of IRF7, IFN-α4, IFN-α1 and IFN-β was attenuated in the IKKγΔ reconstituted MEFs (Fig.4.2B)

62

Since IFN subsequently activated the Jak-STAT pathway, the phosphorylation of STAT1 and the expression of STAT1 in response to RNA viruses were also investigated by Western immunoblot.in IKKγ$^{-/-}$ MEFs, IKKγ reconstituted and IKKγΔ reconstituted cells infected by Sendai virus or RSV at 12 h and 24 h. The phosphorylation of STAT1 and a strong induction of STAT1 were only observed in IKKγ reconstituted cells (Fig.4.2C and Fig.4.2D).

Since IKKγΔ has a higher expression level in reconstituted IKKγ$^{-/-}$ MEFs, which may affect the downstream gene expression, a transient transfection expression was conducted, while equivalent levels of IKKγΔ or IKKγ could be achieved. IKKγ$^{-/-}$MEFs were transfected with either IKKγΔ or IKKγ as well as the CARD domains of RIG-I or MAVS using electroporation. 36 h after transfection, the expression of STAT1 was investigated by Western immunoblot. RIG_N and MAVS strongly induced STAT1 expression in IKKγ transfected cells, whereas they induced only a small increase of
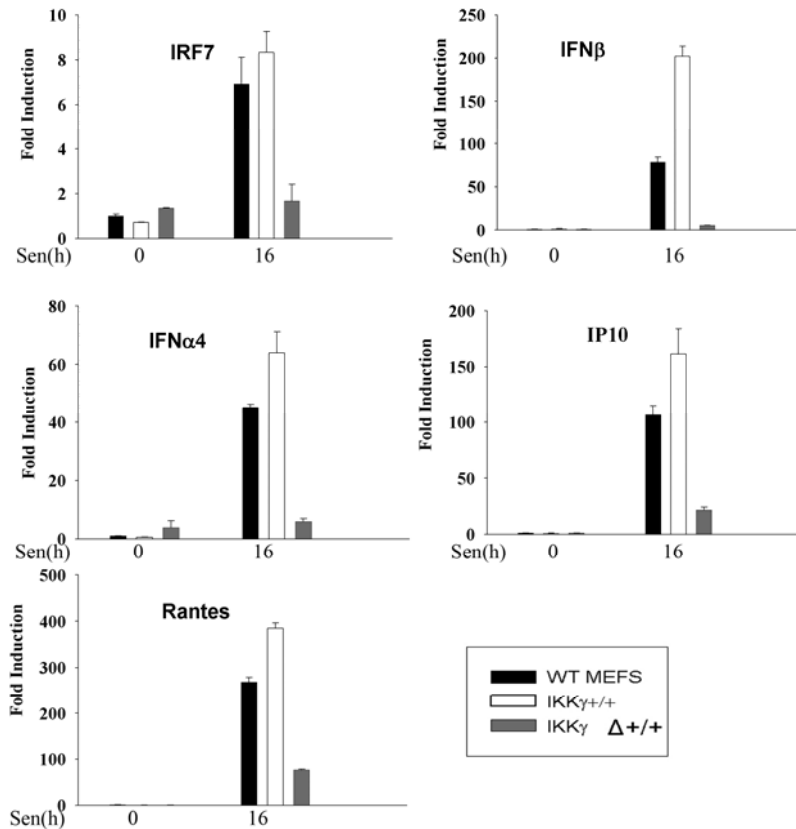

Fig.4.2A Wild type, IKKγ reconstituted and IKKγΔ reconstituted MEFs were infected by Sendai virus for 16h. Total RNAs were extracted and QRT-PCR was conducted using probes for IRF7, IFN-α4, IFN-β, IP10 and Rantes.

63

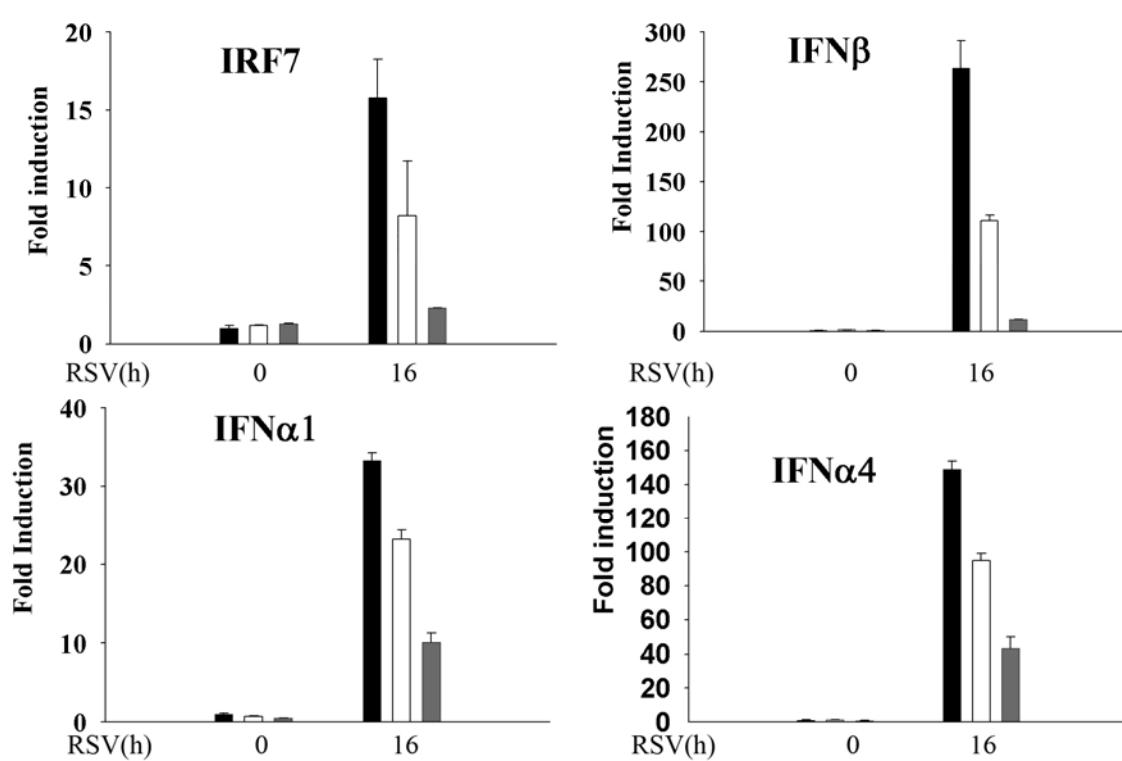Fig.4.2B   Wild type, IKKγ reconstituted and IKKγΔ reconstituted MEFs were RSV infected for 16 h. Total RNAs were extracted and QRT-PCR was conducted using probes for IRF7, IFN-α1, IFN-α4, and IFN-β.
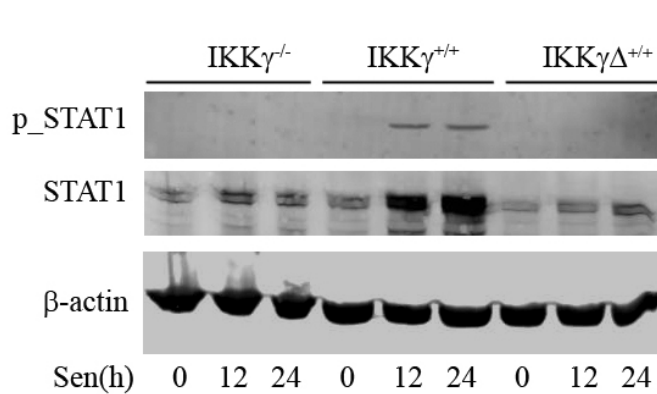

Fig.4.2C   IKKγ$^{-/-}$, IKKγ reconstituted and IKKγΔ reconstituted   MEF cells were infected by Sendai virus at 0 h, 12h and 24 h. The phosphorylation of STAT1 was detected by anti-phospho-STAT1 antibody (top panel). The expression of STAT1 was showed in the middle panel and β-actin was used as a loading control (bottom panel).
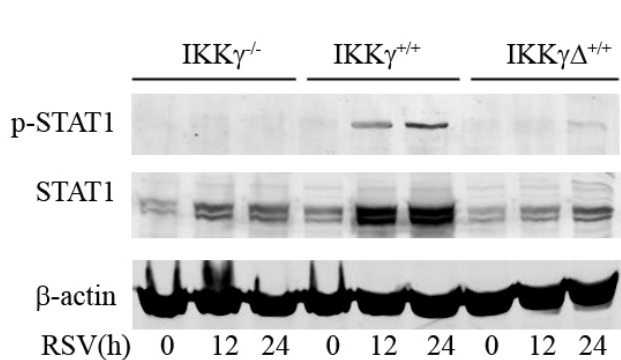
Fig.4.2D IKKγ$^{-/-}$ MEFs, IKKγ reconstituted and IKKγΔ reconstituted cells were RSV infected at 0 h, 12h and 24 h. The phosphorylation of STAT1 was demonstrated in the top panel. The expression of STAT1 was showed in the middle panel and β-actin was used as a loading control (bottom panel).

STAT1 expression in IKKγΔ transfected cells (Fig.4.2E). All these data suggest that IKKγ and IKKγΔ differently couple to the IRF-IFN pathway downstream of RIG-I and MAVS in response to RNA viruses.
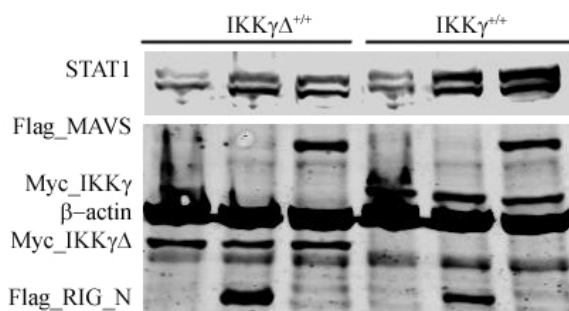

Fig.4.2E IKKγ-/-MEFs were transfected by IKKγΔ (left three lanes) or IKKγ (right three lanes) and with RIG-I_N (the second lane and the 5th lane) or MAVS (the third lane and the 6th lane) using electroporation. 36h after transfection, 100 µg WCEs was investigated by Western immunoblot (top panel), and the expression of Myc_IKKγ, Myc_IKKγΔ, Flag_MAVS and Flag_RIG_N were also detected by anti-Myc or anti-Flag Ab (bottom panel).

IKKγΔ failed to activate the IRF3 pathway, but was still able to activate NFκB pathway.

Previous study has demonstrated that downstream of RIG-I_MAVS, IKKγ is an essential regulatory factor for both NF-κB and IRF3 activation (169). We therefore tested whether there were differences between IKKγ and IKKγΔ in activating NF-κB and IRF3. IKKγ and IKKγΔ were co-transfected in the obsence or presence of activated RIG-I (RIG-N) or MAVS into IKKγ$^{-/-}$MEFs. The expression of Flag_MAVS, Flag_RIG-N, Myc_ IKKγ and Myc_IKKγΔ were confirmed by Western immunoblot (Fig.4.3A).

Translational activation of these constructed proteins was tested on NF-κB selected (PRDII) or IRF3 selected PRDIII reporter gene. RIG_N failed to induce luciferase activity in IKKγ$^{-/-}$MEFs, whereas a 3-4 fold induction of PRDII and PRDIII luciferase activity were observed in IKKγ transfected cells (Fig.4.3B). In the cells transfected with IKKγΔ, RIG_N was able to activate the NF-κB driven PRDII but not the IRF3-driven PRDIII reporter gene. A similar result was found in the cells transfected with MAVS. MAVS only induced PRDII luciferase activity but not PRDIII reporter activation when co-transfected with IKKγΔ. This result suggested that IKKγ activated both NFκB and IRF3 pathway, whereas IKKγΔ only activates NF-κB activation.

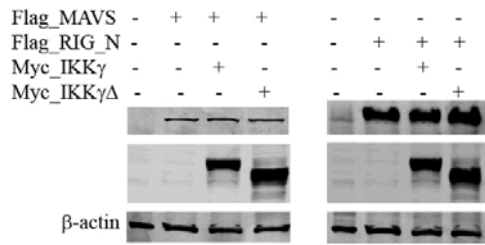

Fig.4.3A 6 μg IKKγ or IKKγΔ were transfected into IKKγ$^{-/-}$MEFs, and 2 μg NH2 terminus of RIG-I (RIG-N) or 2 μg MAVS were co-transfected using electroporation. 48 h after transfection, the expression of Flag_MAVS (top left panel), Flag_RIG-N (top right panel), Myc_ IKKγ (middle panel) and Myc_IKKγΔ (middle panel) were investigated by Western immunoblot.

To prove this hypothesis, IKKγ reconstituted and IKKγΔ reconstituted MEFs were infected by Sendai virus at the indicated time and the nuclear proteins were extracted.   EMSA was conducted and a probe containing ISRE site from the promoter of ISG15 was labeled by P^{32} and the formation of DNA-IRF3 complex was observed in IKKγ reconstituted MEFs at 12 h and 24 h of Sendai virus infection (Fig.4.3C)

Also, the nuclear accumulation of IRF3 was tested by Western immunoblot, an increase of nuclear IRF3 was observed at 12h and 24h of infection (Fig.4.3D).

To further confirm this finding, IKKγ$^{-/-}$, IKKγ reconstituted and IKKγΔ reconstituted MEFs were infected by either Sendai virus or RSV, and the formation of IRF3 dimer was studied by native gel electrophresis and Western immunoblot.   Only in IKKγ reconstituted MEFs, IRF3 formed dimers after 12 h of either Sendai virus or RSV infection (Fig.4.3E and 4.3F).
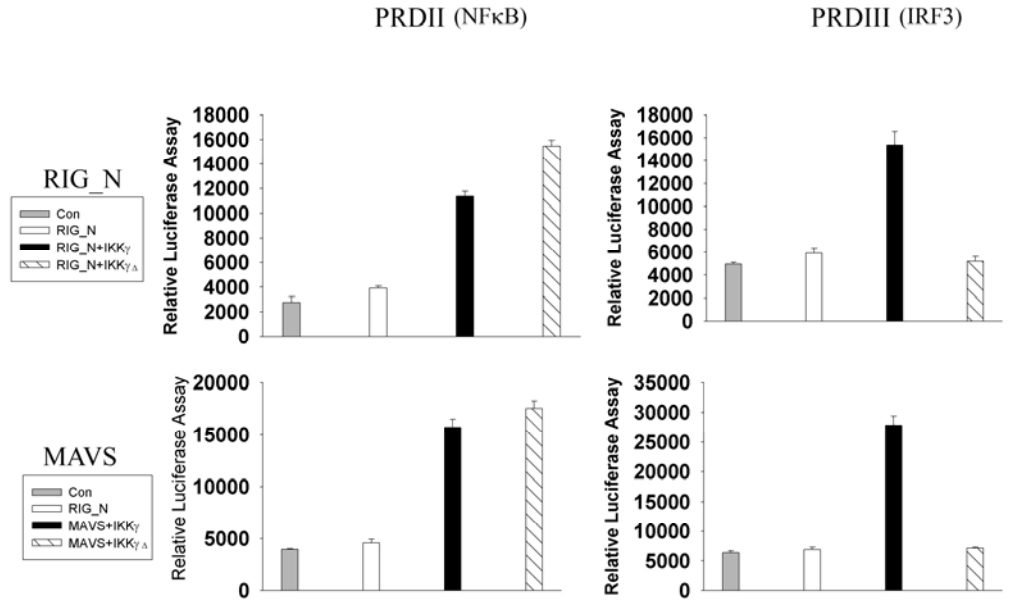
66

Fig.4.3B Two luciferase reporter genes encoded by PRDII (2μg) and PRDIII (1μg) of IFN-β were co-transfected with RIG_N, MAVS, IKKγ and IKKγΔ as in Fig.4.3A. 36 h after transfection, reporter assay was conducted.

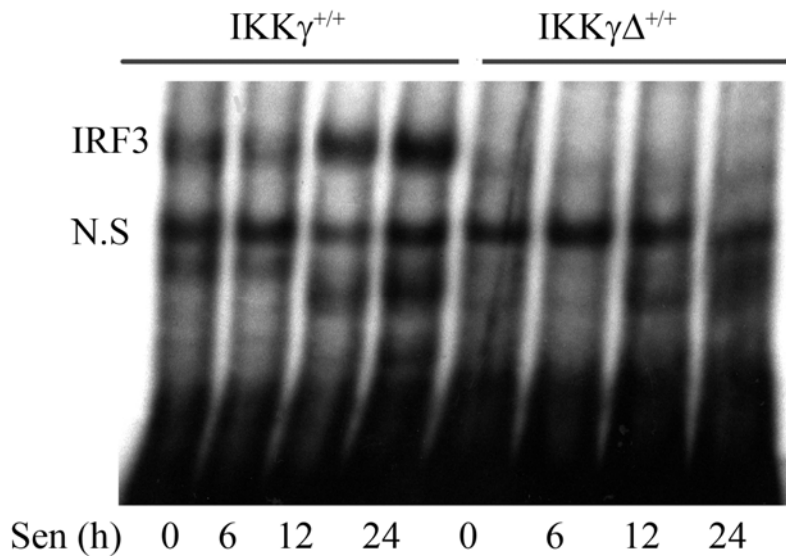Fig.4.3C   IKKγ reconstituted and IKKγΔ reconstituted MEFs were infected by Sendai virus at 0 h, 6 h, 12 h and 24 h and the nuclear proteins were extracted.   EMSA was conducted using a probe containing ISRE site from the promoter of ISG15.
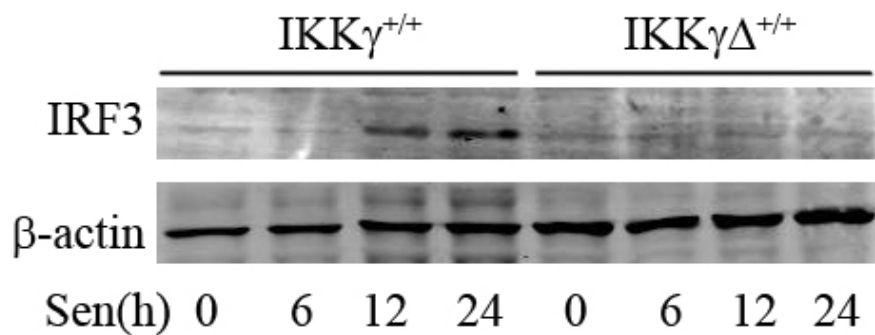
Fig.4.3D   IKKγ reconstituted and IKKγΔ reconstituted MEFs were infected by Sendai virus at 0 h, 6 h, 12 h and 24 h and the nuclear IRF3 was detected by Western immunoblot (top panel).
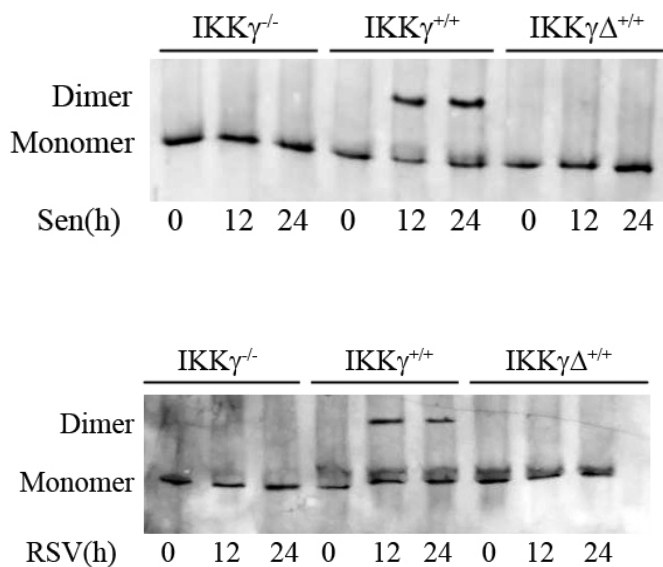
Fig.4.3E and 4.3F   IKKγ-/- , IKKγ reconstituted and IKKγΔ reconstituted MEFs were infected by Sendai virus (4.3E)or RSV (4.3F) for 0 h, 12 h and 24 h. 50 μg WCEs were fractionated in a native gel and Western immunoblot was conducted using anti-IRF3 antibody to show the formation of IRF3 dimer.

We next investigated whether there is difference between IKKγ and IKKγΔ in activating the NF-κB pathway, IKKγ$^{-/-}$ MEFs were transfected with either IKKγ or IKKγΔ using electroporation. 96 h after transfection, cells were treated with TNFα at the time indicated and EMSA was conducted to test the DNA binding. An increased DNA binding activity was observed 15 min after TNFα treatment in IKKγ transfected cells,

whereas in IKKγΔ transfected cells it took 30 min to see the increase of DNA binding (Fig.4.3G).

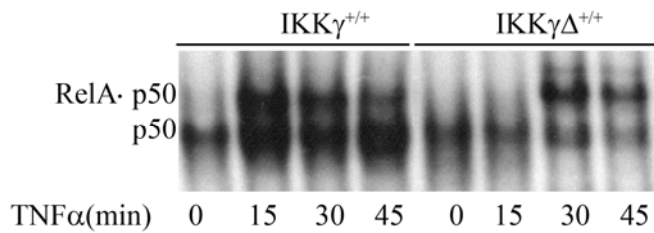Fig.4.3G   IKKγ-/- MEFs were transfected with either IKKγ (6μg) or IKKγΔ (6μg) using electroporation. 96 h after transfection, cells were treated with TNFα at 0, 15, 30 and 45 min and EMSA was conducted to test the DNA binding

activity of NFκB.

The degradation of IκBα was also tested in the same samples. In the cells transfected with IKKγ, IκBα was degraded 15 min after TNFα treatment, whereas in IKKγΔ transfected cells, a slight increase of IκBα was detected at 0 min before TNFα treatment and IκBα was degraded 30 min in response to TNFα treatment (Fig.4.3H). These data indicate IKKγΔ is able to couple to NF-κB activation.
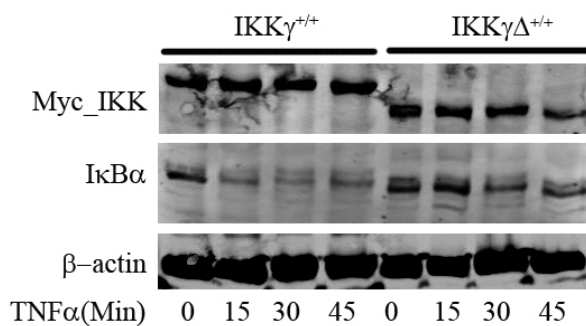
Fig.4.3H IKKγ-/- MEFs were transfected with either IKKγ (6 μg) or IKKγΔ (6 μg) using electroporation. The expression of IKKγ and IKKγΔ were investigated by Western immunoblot (top panel). 96 h after transfection, cells were treated with TNFα at 0, 15, 30 and 45 min and IκBα was detected by Western immunoblot (middle panel). β-actin was used as an internal loading control (bottom panel)

TNFα activates NFκB in HelaS3 cells.

Previous work in my lab demonstrated that IKKγΔ was universally expressed at variant ratios with IKKγ in different tissue types and cell types. Here, I tested the expression of IKKγ and IKKγΔ using Western immunoblot in 7 different cell types

including IKKγ$^{-/-}$ MEFs as a control. I found both IKKγ and IKKγΔ were expressed in wild type MEF cells, 293 cells, A549 cells, HepG2 cells and Hela cells, whereas in HelaS3 cells, IKKγΔ was the predominant form of IKKγ (Fig. 4.4A).
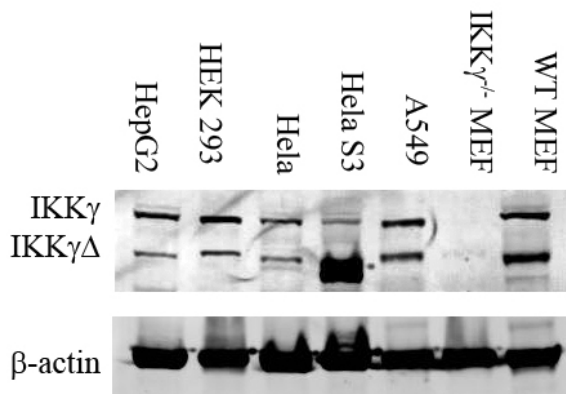
Fig. 4.4A   100 μg whole cell extracts from HepG2, HEK293, Hela, HelaS3, A549, IKKγ$^{-/-}$ MEFs and wild type MEFs were fractionated by SDS-PAGE and Western immunoblot was conducted using anti-IKKγ antibody (top panel). β-actin was used as an internal loading control (bottom panel).

To investigate whether IKKγΔ was able to activate the NF-κB pathway, HelaS3 cells were treated with TNFα at different time points and EMSA was conducted using a NF-κB specific probe. A significant increase of DNA binding appeared at 5 min and reached its peak at 15 min after TNFα treatment (Fig.4.4B).

Fig.4.4B   HelaS3 cells were treated with TNFα at 0, 5, 15, 30, 45, and 60 min. EMSA was conducted using 30 μg WCEs to detect the binding of NF-κB probe.

The degradation of IκBα was also observed 5 min after TNFα treatment and the resynthesis of IκBα occured at 30 min after TNFα treatment (Fig.4.4C). This data suggested that IKKγΔ is able to activate NF-κB in response to TNFα signaling.

IKKγ binds TANK, but not IKKγΔ.

Previous study demonstrated that the interaction between TANK and IKKγ directed the RIG-I·MAVS signaling to IRF3 (169). Our data showed that IKKγΔ failed to activate IRF3. To understand the mechanism of this phenomenon, we first tested whether IKKγΔ was associated with MAVS. For this purpose Myc_ IKKγ or Myc_ IKKγΔ was co-transfected with Flag_MAVS into HEK293 cells, and IKKγ or IKKγΔ was pulled
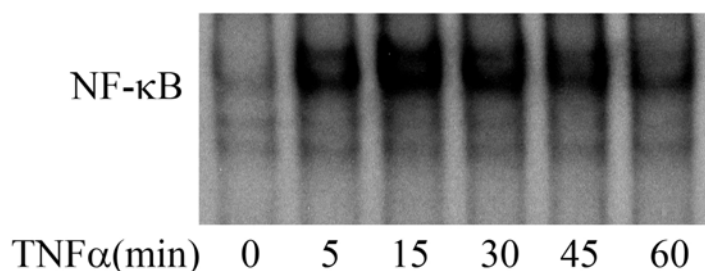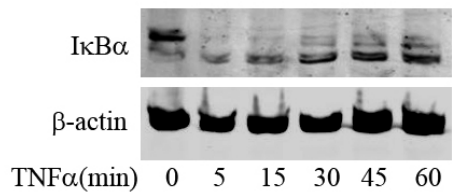
Fig.4.4C HelaS3 cells were treated with TNFα at 0, 5, 15, 30, 45, and 60 min. 100 μg WCEs were fractionated by SDS-PAGE and Western immunoblot was used to detect IκBα (top panel).

down using anti-Myc Ab. The association of MAVS was detected by anti-Flag antibody, and both IKKγ and IKKγΔ were able to bind MAVS (Fig.4.5A).
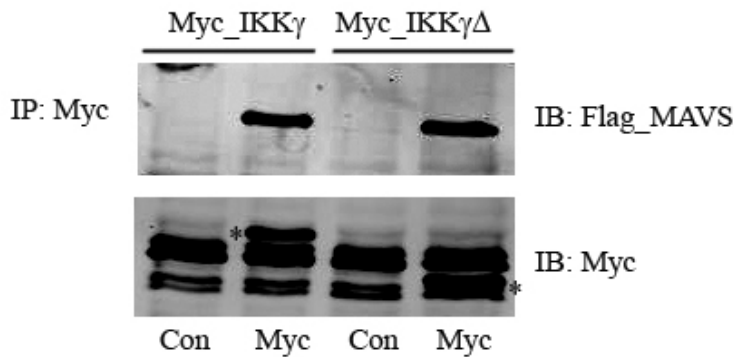
Fig.4.5A. Myc_ IKKγ or Myc_ IKKγΔ was co-transfected with Flag_MAVS into HEK293 cells. 48 h after transfection, 500 μg WCEs were collected and incubated with a control mous antibody (the first lane and the third lane) or anti-Myc Ab (the second lane and the fourth lane). The proteins were pulled down and the association of MAVS was detected by Western immunoblot with anti-Flag antibody (top panel). The presence of Myc_ IKKγ and Myc_ IKKγΔ was also detected by anti-Myc antibody and demonstrated using asterisks (bottom panel).

Since TANK is an essential molecule to link IKKγ to TBK1·IKKε, we next investigated whether IKKγΔ was able to bind TANK. In this experiment, Myc_ IKKγ or Myc_ IKKγΔ was co-transfected with TANK-V5, and co-immunoprecipitation

71

experiment was conducted to pull down Myc_ IKKγ or Myc_ IKKγΔ. The association of TANK was detected by anti-V5 Ab in Western immunoblot and we found that only IKKγ was associated with TANK, but not IKKγΔ (Fig.4.5B).
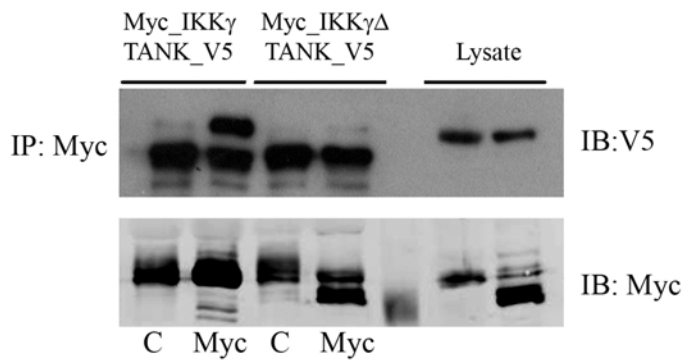
Fig.4.5B Myc_ IKKγ or Myc_ IKKγΔ was transfected into HEK293 cells with TANK-V5. 48 h after transfection, WCEs were incubated with a control mouse antibody and anti-Myc antibody. Myc_ IKKγ or Myc_ IKKγΔ was pulled down and the association of TANK was detected by anti-V5 antibody (left side of top panel). 100 μg WCEs were also fractionated by SDS-PAGE and Western immunoblot was conducted to check the expression of TANK_V5 (right side of top panel). The presence of Myc_ IKKγ or Myc_ IKKγΔ in precipitates and WCEs were investigated by Western immunoblot (bottom panel).

TANK is an external adaptor that mediates the recruitment of the atypical IKKε to IKKγ. Because IKKγΔ is unable to bind TANK, we investigated whether IKKε could bind IKKγΔ. For this purpose, Flag_IKKα, Flag_IKKβ or Flag_IKKε was co-transfected with Myc_ IKKγ or Myc_ IKKγΔ, along with or without TANK_V5. IKKγ or IKKγΔ was precipitated by anti-Myc Ab, and the association of IKK molecules was detected by anti-Flag Ab. Although both IKKγ and IKKγΔ were able to recruit IKKα and IKKβ, only IKKγ bound IKKε when TANK was present (Fig. 4.5C). Together these data demonstrated that IKKγΔ was unable to recruit TANK and IKKε.

4.4 DISCUSSION

IKKγ is an essential regulatory subunit of the canonical IKK complex. IKKγ deficient cells were unable to activate NF-κB in response to many stimuli including TNFα and IL-1 (117). Recently, IKKγ has also been reported to mediate the activation of TBK1 and IKKε, two key kinases that induce IRF3 activation. TANK is a critical factor

to link TBK1 and IKKε to IKKγ (17,54). A recent study just reported that in response to RNA viruses, RIG-I and MAVS signaling bridges to IRF3 and NF-κB pathway at the level of IKKγ. In IKKγ$^{-/-}$ cells, the replication of RNA viruses was increased, the production of type I interferon was down-regulated, and the activation of both IRF3 and NF-κB pathways was inhibited (169).
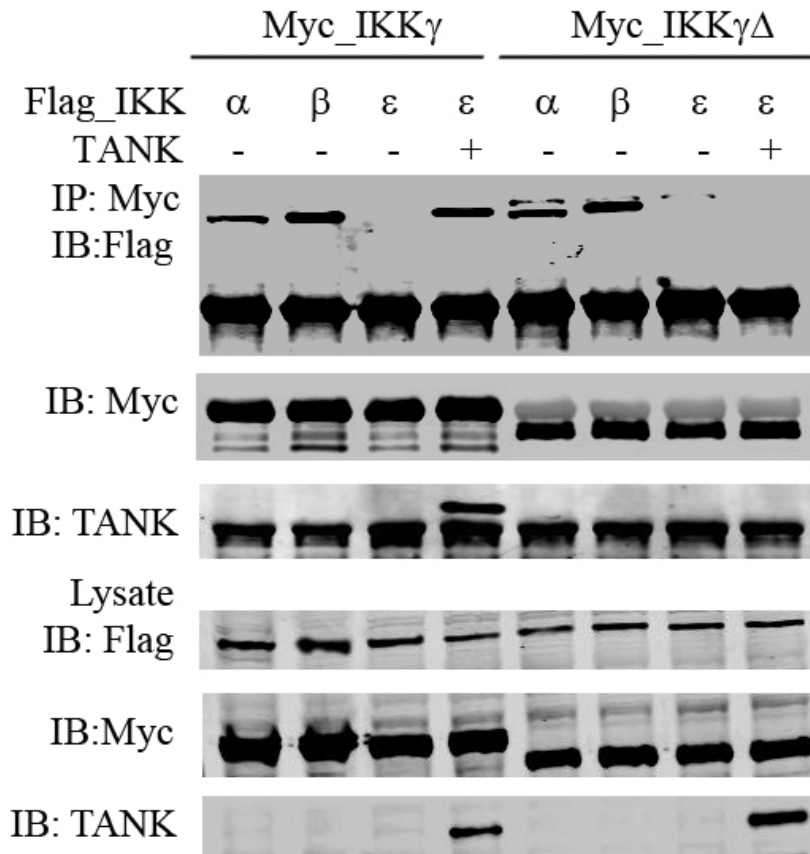
Fig. 4.5C   Flag_IKKα, Flag_IKKβ or Flag_IKKε was co-transfected with Myc_ IKKγ or Myc_ IKKγΔ, along with or without TANK_V5 into HEK293 cells. 48 h after transfection, WCEs were collected and Myc_ IKKγ or Myc_ IKKγΔ was pulled down using anti-Myc Ab. The association of Flag tagged proteins were detected by anti-Flag antibody (The first panel from top). The presence of Myc_ IKKγ, Myc_ IKKγΔ and TANK_V5 in precipitates were also tested by Western immunoblot (the second and third panel from top). The expression of these ectopic proteins in WCEs were also investigated by Western immunoblot (the three panels on the bottom).

The IKKγ gene is encoded by the 10-exon-containing gene located at chromosome Xq28 (66). Mutations in the IKKγ gene including different truncations of the IKKγ protein have been linked to the syndromes of incontinentia pigmenti and anhidrotic ectodermal dysplasia associated with immunodeficiency in human (26). Although human IKKγ transcripts containing an alternatively spliced first exon have been reported and deposited in GenBank (AI24572, AF091453), these alternatively spliced transcripts encode wild type IKKγ (66). Previous work from my lab first demonstrated the existence of a IKKγ exon 5 deletion transcript. Using a specific reverse transcription-PCR assay, we found that IKKγΔ is widely expressed in cultured human cells and normal human tissues. We also repeated this finding and investigated the expression of IKKγΔ in 7 cultured cell lines using Western immunoblot. Consistent with our previous finding, both IKKγ and IKKγΔ were expressed in A549 cells, HepG2 cells, 293 cells, Hela cells and wild type MEFs. In HelaS3 cells, IKKγΔ is the predominant form.

IKKγ contains 419 amino acids is glutamine-rich protein. Programs for secondary-structure prediction demonstrated three key structures including two extended coiled-coil motifs (93-196aa and 246-302aa) and a leucine zipper (302-365aa). Such motifs are likely to be involved in protein–protein interactions (117). The region deleted by exon 5 occlusion encodes amino acids 174 to 224aa which include part of the first coiled-coil domain (56). As an adaptor protein, IKKγ is known to associate with many proteins in the IRF3 and NF-κB activation, including upstream kinases like IKKα, IKKβ, TBK1 and IKKε, and also is the target for direct IKK activators like RIG I and MAVS. Our co-immunoprecipitation experiment demonstrated that same as IKKγ, IKKγΔ was still associated with MAVS (Fig. 5A), suggesting there may be no difference between IKKγ and IKKγΔ for their recruitment to upstream activator in response to RNA viruses. Mapping studies have also shown that IKKγ binds to the IKKα and β subunits through a region in its NH$_2$-terminal 119 aa, a region unaffected in the IKKγΔ splice variant (96,99,161). Consistent with this finding, our co-immunoprecipitation experiments demonstrated that IKKγΔ binds both IKKα and IKKβ which may explain why IKKγΔ is

still able to activate NF-κB pathway. A recent study also mapped 150-250aa of IKKγ as the TANK binding domain (17). Another study also showed a deletion mutant of IKKγ without 196-250aa can not bind TANK (169). Our study demonstrated that IKKγΔ, which lacks 174-224aa, was unable to bind TANK. TANK, as an adaptor protein, has been reported to link the interaction between IKKγ and TBK1·IKKε, and pass the upstream signal from RIG I·MAVS to IRF3 pathway (169). Consistent with these findings, our result suggested that IKKγΔ can not activate IRF3 pathway and fails to induce type I interferon production.

In this study, we also found that in response to TNFα, IκBα was degraded and the DNA binding activity of NF-κB was increased in HelaS3 cells in which IKKγΔ is a predominant form (Fig.4B and 4C). Interestingly, in HelaS3 cells without any treatment, the molecular weight of IκBα was slight bigger than the new synthesized IκBα and similar as the phosphorylated IκBα (Fig. 4C, 0 min and 30 min after TNFα treatment), suggesting that in HelaS3 cells, IκBα may be phosphorylated by IKKγΔ containing IKKs without any treatment. Our previous findings also indicated that IKKγΔ has stronger self-association properties than the wild-type protein, and it has an enhanced ability to activate NF-κB pathway (56). Related to this study, IKKγΔ was unable to associate with TANK and failed to activate IRF3. As a "pure" NF-κB adaptor, greater signaling from RIG-I·MAVS may pass to NF-κB through IKKγΔ.

CHAPTER V: SUMMARY AND FUTURE DIRECTION

5.1 CHARACTERIZING RIG-I SIGNALING

What did we already know about RIG-I signaling?

RIG-I is an essential intracellular sensor to detect infection by most of the single-stranded RNA (ssRNA) viruses like Sendai virus, influenza virus and Japanese encephalitis etc. (60,70,71). Mitochondrial antiviral signaling (MAVS) has been identified as the only downstream adaptor for RIG-I which leads to the activation of canonical NF-κB pathway and IRF3 pathway (72,79,100,109). MAVS contains three protein domains including a N-terminal CARD domain, a Proline-rich domain and a C-terminal transmembrane domain (Tm) (72,79,100,109). CARD domain of MAVS is an essential motif to interact with CARD domains in RIG-I. The Tm domain of MAVS is a critical motif to localize MAVS on the surface of mitochondria. The deletion mutant of either CARD or Tm was unable to initiate NF-κB and IRF3 signaling, which suggests that both of these two motifs are necessary for MAVS function (79). Three TRAF-interaction domains (TIM) have been identified in MAVS sequence which played a very important role to link MAVS to downstream signaling. One TRAF2 and one TRAF6 binding site were identified in the praline-rich domain of MAVS, and another TRAF6 domain was localized just in front of TM domain. It has been demonstrated that TRAF6 interacting domain is a critical motif to activate NF-κB pathway (159). Since the TIM sequence of TRAF2 overlap with TIM sequence of TRAF3, a study showed recently that TRAF3 interacting domain is a critical domain for IFN production (120).

Although previous data suggested that different TIMs in MAVS may be the key point to bifurcate NF-κB and IRF3 signaling, a recent study has localize the branching point at IKKγ(169). In IKKγ$^{-/-}$ cells, RNA viruses failed to activate both NF-κB and IRF3 pathway, was unable to induce IFN production and had a higher viral replication level compared to wild type cells. IKKγ has been known as the regulatory subunit of classic IKK complex (IKKα, IKKβ and IKKγ) to activate canonical NF-κB pathway. The

interaction between IKKγ and two key kinases, TBK1 and IKKε which activate IRF3 signaling, has just been discovered. Another adaptor protein, TANK, plays a critical role to recruit TBK1 and IKKε to IKKγ (17,54,169).

In summary, two key points about RIG-I·MAVS signaling have been known by previous studies and illustrated in Fig.5.1A.

In response to RNA viruses, host cells activate RIG-I·MAVS signaling, leading the activation of both NF-κB and IRF3 pathway.

IKKγ is the branching point downstream of RIG-I·MAVS signaling.

New lights from my research concerning RIG-I signaling?
1.   Identify RIG-I as an intracellular receptor to detect RSV infection and induce anti-viral signaling.

Infected host cells detect and respond to RNA viruses using different mechanisms in a cell-type-specific manner, including retinoic acid-inducible gene I (RIG-I)-dependent and Toll-like receptor (TLR)-dependent pathways. Because the relative contributions of these two pathways in the recognition of RSV infection are unknown, I examined their roles in my study. We found that RIG-I helicase binds RSV transcripts within 12 h of infection. Short interfering RNA (siRNA)-mediated RIG-I "knockdown" significantly inhibited early nuclear factor-kappaB (NF-κB) and interferon response factor 3 (IRF3) activation 9 h postinfection (p.i.). Consistent with this finding, RSV-induced beta interferon (IFN- β), interferon-inducible protein 10 (IP-10), chemokine ligand 5 (CCL-5), and IFN-stimulated gene 15 (ISG15) expression levels were decreased in RIG-I-silenced cells during the early phase of infection but not at later times (18 h p.i.). In contrast, siRNA-mediated TLR3 knockdown did not affect RSV-induced NF--κB binding but did inhibit IFN- β, IP-10, CCL-5, and ISG15 expression at late times of infection. Further studies revealed that TLR3 knockdown significantly reduced NF-κB/RelA transcription by its ability to block the activating phosphorylation of NF-κB/RelA at serine residue 276. I further found that TLR3 induction following RSV infection was regulated by RIG-I-dependent IFN- β secreted from infected airway epithelial cells and was mediated by both IFN response-stimulated element (ISRE) and signal transducer and activator of
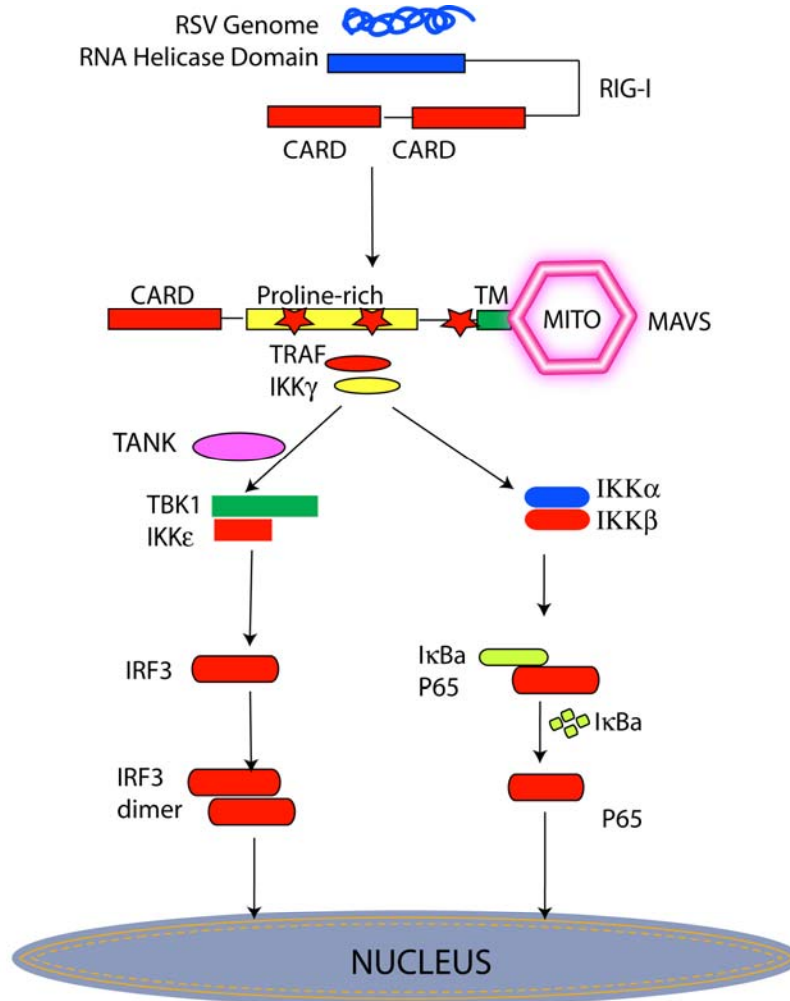
Fig 5.1 Old map of RIG-I·MAVS signaling. Shown is a schematic model that shows the signaling cascade downstream of RIG-I that diverges to activate the canonical NFκB, and IRF3 pathway. The presence of RSV dsRNA is sensed by the cytosolic RIG-I helicase, that associates with the mitochondrial bound MAVS via heterotypic CARD domain interactions. This complex mediates activation of the typical IKK complex (IKKα, IKKβ and IKKγ) resulting in RelA release from IκBα -sequestered complexes. In addition, RIG-I·MAVS complex also activates two IKK-like kinases, TBK1 and IKKε, leading the phosphorylation, dimeration and nuclear translocation of IRF3. Abbreviations: CARD, caspase recruitment domain; Mito, mitochondria; p65, RelA.

transcription (STAT) sites in its proximal promoter. Together these findings indicate distinct temporal roles of RIG-I and TLR3 in mediating RSV-induced innate immune responses, which are coupled to distinct pathways controlling NF-κB activation.

2. Identify RSV induced NIK·IKKα activation is mediated by RIG·MAVS signaling.

Our group first demonstrated that RSV was able to activate non-canonical NF-κB pathway characterized by the activation of NIK and IKKα, as well as the formation of p52 from the proteolysis of p100. I also demonstrated that retinoic acid inducible gene I (RIG-I) was one of the major intracellular RSV sensors and a key regulator in airwayepithelial cells to initiate anti-viral signaling. In the next study, I also demonstrated RIG-I was involved in the activation of NIK·IKKα complex. Our co-immunoprecipitation experiments not only demonstrated that NIK associated with either RIG-I or its downstream adaptor, mitochondrial antiviral signaling (MAVS), but also showed the association between IKKα and MAVS. To further understand the role of NIK· IKKα complex, we compared RSV-induced NF-κB activation using wild type, IKKγ deficient, NIK deficent and IKKα deficient MEF cells. Interestingly, we found that in IKKγ deficient cells, RelA, whose activation is IKKγ dependent, was still activated. We proved that part of RelA was associated with an IκBα-like inhibitor p100. The RSV-induced proteolysis of p100 not only produced p52, but also released RelA and increased its nuclear translocation. This finding suggested that part of the RelA activation in response to RSV infection was induced by NIK·IKKα complex.

3. Identify IKKγΔ only activates NF-κB signaling downstream of RIG·MAVS

We have reported the existence of a splicing variant of IKKγ missing its exon 5, and named this natural variant as IKKγΔ. In my next study, I compared the function of IKKγ and IKKγΔ in response to ssRNA virus. We found a significant increase of viral replication IKKγΔ reconstituted MEF cells, but not in the cells reconstituted by IKKγ. We demonstrated that IKKγΔ failed to activate IRF3 in response to either Sendai virus or respiratory syncytial virus (RSV) and was unable to induce the anti-viral gene expression such as IRF7, IFN-α4 and IFN-β. Our study also showed that TNFα successfully induces

the degradation of IκBα and DNA binding of RelA in IKKγ deficient cells transfected by ectopic IKKγΔ.   Further study proved that IKKγΔ was able to bind IKKα and IKKβ, but not TANK and IKKε. These data suggested that the exon 5 domain of IKKγ is an essential domain to bind TANK, and IKKγΔ who misses this exon was only involved in the activation of NF-κB, but not IRF3.

My new discovery of RIG-I·MAVS signaling is illustrated in Fig.5.1B.

5.2 FUTURE DIRECTION

My research revealed two new signaling pathways downstream of RIG-I·MAVS. The first discovery is the RIG-I·MAVS mediated activation of NIK·IKKα in response to RSV infection, leading the proteolysis of p100 and releasing RelA. Inhibition of NIK or IKKα down-regulates NF-κB pathway but didn't affect viral replication. This character of NIK·IKKα cross-talk pathway makes it a potential target for RSV treatment. The inhibitors for NF-κB pathway have been extensively studied. There are over 150 agents that have been shown to inhibit activation of NF-κB at the IKK step (48). Three types of chemical IKKα/β inhibitors have been reported including ATP analogs (β-carboline and SC-839)(110), the synthetic compound (BMS-345541 (11)and several thiol-reactive compounds. One study on the gene-based inhibitors reported that overexpression of dominant-negative IKKα or NIK, but not a dominant-negative IKKβ blocks caspase-induced NF-κB activation (134), and another study showed that adenoviral-mediated delivery of an IKKβ dominant-negative kinase may have therapeutic potential for airway inflammatory diseases such as asthma (9,15). Using kinase inhibitor including NIK inhibitor, IKKα inhibitor and IKKβ inhibitor to treat RSV infection may be a interesting topic for future study.

My second discovery is the activation of IKKγΔ downstream of RIG-I·MAVS. As a natural splicing variant of IKKγ, IKKγΔ competes with wild type IKKγ and only directs RIG-I·MAVS signaling to NF-κB. With the increase expression level of IKKγΔ, IKKγ initiated IRF3 pathway will be inhibited and the production of type I interferon will be down-regulated. However, the mechanism under the processing of IKKγ to IKKγΔ is

unknown. Future study to understand the regulation of IKKγ splicing will favor the

management of IRF3 and NF-κB. Increasing IRF3 signaling and down-regulating NF-κB
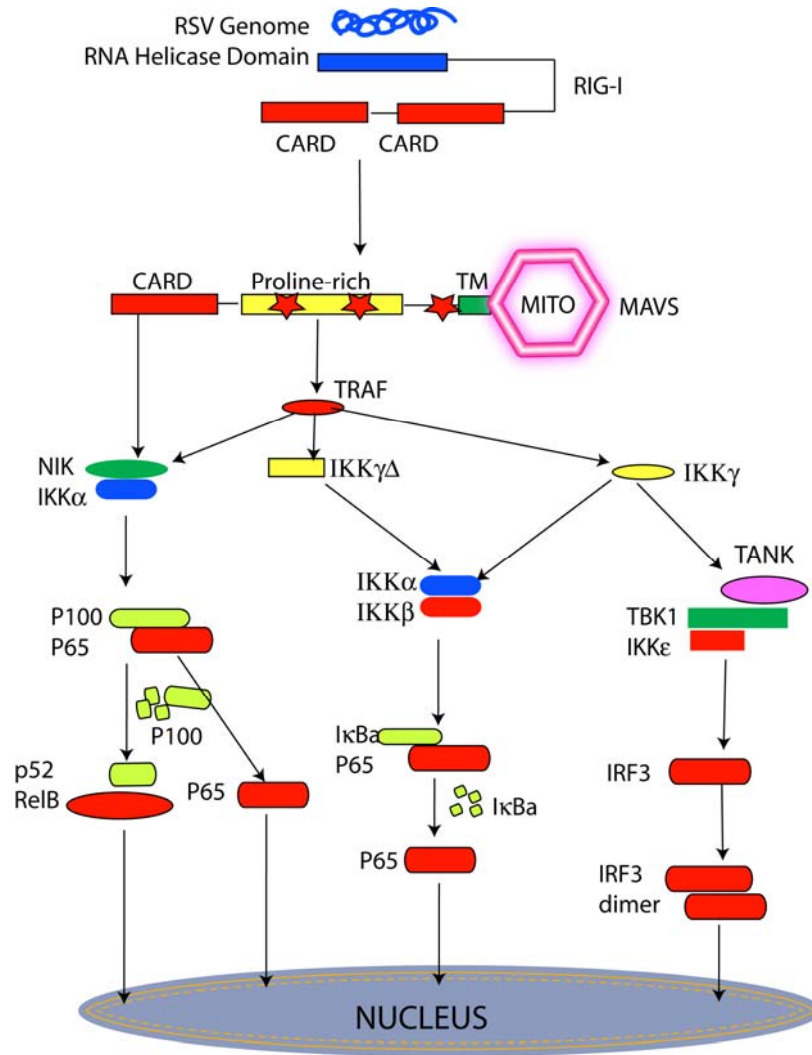
Fig 5.2 The update of RIG-I·MAVS signaling. Shown is a new schematic model that demonstrates the signaling cascade downstream of RIG-I. Compared to Fig 5.1, my dissertation research revealed two new signaling pathways including the cross-talk NFκB pathways and the IKKγΔ pathway. The NIK·IKKα complex is activated by RIG-I·MAVS, resulting in activation of the cross-talk pathway by stimulating 100 kDa NF-κB2 proteolysis and releasing RelA. IKKγΔ, a splicing variant of IKKγ, is able to activate canonical NFκB, but fails to activate the IRF3 pathway downstream of RIG-I·MAVS.

will inhibit the inflammatory reaction, and at the same time improve the clearance of RSV. In addition, IKKγ also served as a target for IKK complex inhibition. Introduction of a cell-permeable 10 amino-acid peptide named as NEMO-binding domain of IKKβ can block the binding of IKKγ to IKKβ and inhibit canonical NF-κB pathway induced by NFα (96). Moreover, this peptide has also shown efficacy in mouse models of inflammation by both topical and systemic administration (55,83,96). Similarly, introduction of peptides corresponding to the region of IKKγ including the coiled-coil-2 and leucine zipper, which are required for oligomerization of IKKγ, can also block NF-κB activation (2). Further studies of these IKKγ inhibitors on the activation of IRF3 pathway may be an interesting topic.

Reference List

1. **Aaronson, D. S. and C. M. Horvath**. 2002. A road map for those who don't know JAK-STAT. Science **296**:1653-1655.

2. **Agou, F., F. Ye, S. Goffinont, G. Courtois, S. Yamaoka, A. Israel, and M. Veron**. 2002. NEMO trimerizes through its coiled-coil C-terminal domain. J.Biol.Chem. **277**:17464-17475.

3. **Aherne, W. T., T. Bird, S. D. B. Court, P. S. Gardner, and J. McQuillin**. 1970. Pathological changes in virus infections of the lower respiratory tract in children. J.Clin.Path. **23**:7-18.

4. **Alexopoulou, L., A. C. Holt, R. Medzhitov, and R. A. Flavell**. 2001. Recognition of double-stranded RNA and activation of NF-[kappa]B by Toll-like receptor 3. Nature **413**:732-738.

5. **Atreya, P. L., M. Peeples, and P. L. Collins**. 1998. The NS1 protein of human respiratory syncytial virus is a potent inhibitor of minigenome transcription and RNA replication. J Virol **72**:1452-1461.

6. **Baldwin, A. S. J.** 1996. The NF-kappa B and I kappa B proteins: new discoveries and insights. Annu Rev Immunol **14**:649-683.

7. **Basak, S., H. Kim, J. D. Kearns, V. Tergaonkar, E. O'Dea, S. L. Werner, C. A. Benedict, C. F. Ware, G. Ghosh, I. M. Verma, and A. Hoffmann**. 2007. A fourth IkappaB protein within the NF-kappaB signaling module. Cell **128**:369-381.

8. **Bossert, B., S. Marozin, and K. K. Conzelmann**. 2003. Nonstructural Proteins NS1 and NS2 of Bovine Respiratory Syncytial Virus Block Activation of Interferon Regulatory Factor 3. J.Virol. **77**:8661-8668.

9. **Broide, D. H., T. Lawrence, T. Doherty, J. Y. Cho, M. Miller, K. McElwain, S. McElwain, and M. Karin**. 2005. Allergen-induced peribronchial fibrosis and mucus production mediated by IkappaB kinase beta-dependent genes in airway epithelium. Proc.Natl.Acad.Sci.U.S.A **102**:17723-17728.

10. **Buckingham, S. C., H. S. Jafri, A. J. Bush, C. M. Carubelli, P. Sheeran, R. D. Hardy, M. G. Ottolini, O. Ramilo, and J. P. DeVincenzo**. 2002. A randomized, double-blind, placebo-controlled trial of dexamethasone in severe respiratory

83

syncytial virus (RSV) infection: effects on RSV quantity and clinical outcome. J Infect Dis **185**:1222-1228.

11. **Burke, J. R., M. A. Pattoli, K. R. Gregor, P. J. Brassil, J. F. MacMaster, K. W. McIntyre, X. Yang, V. S. Iotzova, W. Clarke, J. Strnad, Y. Qiu, and F. C. Zusi**. 2003. BMS-345541 is a highly selective inhibitor of I kappa B kinase that binds at an allosteric site of the enzyme and blocks NF-kappa B-dependent transcription in mice. J.Biol.Chem. **278**:1450-1456.

12. **Cade, A., K. G. Brownlee, S. P. Conway, D. Haigh, A. Short, J. Brown, D. Dassu, S. A. Mason, A. Phillips, R. Eglin, M. Graham, A. Chetcuti, M. Chatrath, N. Hudson, A. Thomas, and P. A. Chetcuti**. 2000. Randomised placebo controlled trial of nebulised corticosteroids in acute respiratory syncytial viral bronchiolitis. Arch.Dis Child **82**:126-130.

13. **Carrat, F., M. Leruez-Ville, M. Tonnellier, J. L. Baudel, J. Deshayes, P. Meyer, E. Maury, J. Galimand, C. Rouzioux, and G. Offenstadt**. 2006. A virologic survey of patients admitted to a critical care unit for acute cardiorespiratory failure. Intensive Care Med **32**:156-159.

14. **Casola, A., N. Burger, T. Liu, M. Jamaluddin, A. R. Brasier, and R. P. Garofalo**. 2001. Oxidant tone regulates RANTES gene expression in airway epithelial cells infected with respiratory syncytial virus. Role in viral-induced interferon regulatory factor activation. J Biol Chem **276**:19715-19722.

15. **Catley, M. C., J. E. Chivers, N. S. Holden, P. J. Barnes, and R. Newton**. 2005. Validation of IKK beta as therapeutic target in airway inflammatory disease by adenoviral-mediated delivery of dominant-negative IKK beta to pulmonary epithelial cells. Br.J.Pharmacol. **145**:114-122.

16. **Chang, T. H., C. L. Liao, and Y. L. Lin**. 2006. Flavivirus induces interferon-beta gene expression through a pathway involving RIG-I-dependent IRF-3 and PI3K-dependent NF-kappaB activation. Microbes.Infect. **8**:157-171.

17. **Chariot, A., A. Leonardi, J. Muller, M. Bonif, K. Brown, and U. Siebenlist**. 2002. Association of the adaptor TANK with the I kappa B kinase (IKK) regulator NEMO connects IKK complexes with IKK epsilon and TBK1 kinases. J.Biol.Chem. **277**:37029-37036.

18. **Chen, L. f., S. A. Williams, Y. Mu, H. Nakano, J. M. Duerr, L. Buckbinder, and W. C. Greene**. 2005. NF-{kappa}B RelA Phosphorylation Regulates RelA Acetylation. Mol Cell Biol **25**:7966-7975.

19. **Choudhary, S., S. Boldogh, R. P. Garofalo, M. Jamaluddin, and A. R. Brasier**. 2005. RSV influences NF-κB dependent gene expression through a

novel pathway involving MAP3K14/NIK expression and nuclear complex formation with NF-κB2. J Virol **79**:8948-8959.

20. **Civas, A., P. Genin, P. Morin, R. Lin, and J. Hiscott**. 2006. Promoter organization of the interferon-A genes differentially affects virus-induced expression and responsiveness to TBK1 and IKKepsilon. J.Biol.Chem. **281**:4856-4866.

21. **Claudio, E., K. Brown, S. Park, H. Wang, and U. Siebenlist**. 2002. BAFF-induced NEMO-independent processing of NF-kappa B2 in maturing B cells. Nat Immunol. **3**:958-965.

22. **Collins, P. L., M. G. Hill, E. Camargo, H. Grosfeld, R. Chanock, and B. R. Murphy**. 1995. Production of infectious human respiratory syncytial virus from cloned cDNA confirms an essential role for the transcription elongation factor from the 5' proximal open reading frame of the M2 mRNA in gene expression and provides a capability for vaccine development. Proc Natl Acad Sci USA **92**:11567.

23. **Collins, P. L., Y. T. Huang, and G. W. Wertz**. 1984. Identification of a tenth mRNA of respiratory syncytial virus and assignment of polypeptides to the 10 viral genes. J Virol **49**:572-578.

24. **Connors, M., N. A. Giese, A. B. Kulkarni, C. Y. Firestone, H. C. Morse, III, and B. R. Murphy**. 1994. Enhanced pulmonary histopathology induced by respiratory syncytial virus (RSV) challenge of formalin-inactivated RSV-immunized BALB/c mice is abrogated by depletion of interleukin-4 (IL-4) and IL-10. J Virol. **68**:5321-5325.

25. **Coope, H. J., P. G. Atkinson, B. Huhse, M. Belich, J. Janzen, M. J. Holman, and S. C. Ley**. 2002. CD40 regulates the processing of NF-kappaB2 p100 to p52. EMBO J. **21**:5375-5385.

26. **Courtois, G., A. Smahi, and A. Israel**. 2001. NEMO/IKK gamma: linking NF-kappa B to human disease. Trends Mol Med **7**:427-430.

27. **Darnell, J. E., Jr.** 1997. STATS and gene regulation. Science **277**:1630-1635.

28. **de Bouteiller, O., E. Merck, U. A. Hasan, S. Hubac, B. Benguigui, G. Trinchieri, E. E. Bates, and C. Caux**. 2005. Recognition of double-stranded RNA by human toll-like receptor 3 and downstream receptor signaling requires multimerization and an acidic pH. J.Biol.Chem. **280**:38133-38145.

29. **Dejardin, E., N. M. Droin, M. Delhase, E. Haas, Y. Cao, C. Makris, Z. W. Li, M. Karin, C. F. Ware, and D. R. Green**. 2002. The Lymphotoxin-[beta]

Receptor Induces Different Patterns of Gene Expression via Two NF-[kappa]B Pathways. Immunity **17**:525-535.

30. **Der, S. D., A. Zhou, B. R. G. Williams, and R. H. Silverman**. 1998. Identification of genes differentially regulated by interferon α , β or γ using oligonucleotide arrays. Proc Natl Acad Sci USA **95**:15623-15628.

31. **DiDonato, J. A., M. Hayakawa, D. M. Rothwarf, E. Zandl, and M. Karin**. 1997. A cytokine-responsive IkB kinase that activates the transcription factor NF-kB. Nature **388**:548-554.

32. **Ebbert, J. O. and A. H. Limper**. 2005. Respiratory syncytial virus pneumonitis in immunocompromised adults: clinical features and outcome. Respiration **72**:263-269.

33. **Ehl, S., R. Bischoff, T. Ostler, S. Vallbracht, J. Schulte-Monting, A. Poltorak, and M. Freudenberg**. 2004. The role of Toll-like receptor 4 versus interleukin-12 in immunity to respiratory syncytial virus. Eur.J.Immunol. **34**:1146-1153.

34. **Eisenhut, M.** 2006. Extrapulmonary manifestations of severe respiratory syncytial virus infection--a systematic review. Crit Care **10**:R107.

35. **Emeny, J. M. and M. J. Morgan**. 1979. Regulation of the interferon system: evidence that Vero cells have a genetic defect in interferon production. J.Gen.Virol. **43**:247-252.

36. **Faisca, P., D. B. Tran Anh, A. Thomas, and D. Desmecht**. 2006. Suppression of pattern-recognition receptor TLR4 sensing does not alter lung responses to pneumovirus infection. Microbes.Infect. **8**:621-627.

37. **Foy, E., K. Li, R. Sumpter, Jr., Y. M. Loo, C. L. Johnson, C. Wang, P. M. Fish, M. Yoneyama, T. Fujita, S. M. Lemon, and M. Gale, Jr.** 2005. Control of antiviral defenses through hepatitis C virus disruption of retinoic acid-inducible gene-I signaling. Proc Natl Acad Sci U S A **102**:2986-2991.

38. **Foy, E., K. Li, C. Wang, R. Sumpter, Jr., M. Ikeda, S. M. Lemon, and M. Gale, Jr.** 2003. Regulation of interferon regulatory factor-3 by the hepatitis C virus serine protease. Science **300**:1145-1148.

39. **Fredericksen, B. L. and M. Gale, Jr.** 2006. West Nile virus evades activation of interferon regulatory factor 3 through RIG-I-dependent and -independent pathways without antagonizing host defense signaling. J.Virol. **80**:2913-2923.

40. **Gagro, A., M. Tominac, V. Krsulovic-Hresic, A. Bace, M. Matic, V. Drazenovic, G. Mlinaric-Galinovic, E. Kosor, K. Gotovac, I. Bolanca, S. Batinica, and S. Rabatic**. 2004. Increased Toll-like receptor 4 expression in

infants with respiratory syncytial virus bronchiolitis. Clin.Exp.Immunol. **135**:267-272.

41. **Garofalo, R. and P. L. Ogra**. 1996. Mechanisms of mucosal immunopathology in respiratory syncytial virus infection *In* M. Kagnoff and H. Kiyono (ed.), Essentials of Mucosal Immunology. Academic Press, San Diego.

42. **Garofalo, R., M. Sabry, M. Jamaluddin, R. K. Yu, A. Casola, P. L. Ogra, and A. R. Brasier**. 1996. Transcriptional activation of the interleukin-8 gene by RSV infection in alveolar epithelial cells: Nuclear translocation of the Rel A transcription factor as a mechanism producing airway mucosal inflammation. J Virol **70**:8773-8781.

43. **Garofalo, R. and H. Haeberle**. 2000. Epithelial regulation of innate immunity to respiratory syncytial virus. Am J Respir Cell Mol Biol **23**:581-585.

44. **Garoufalis, E., I. Kwan, R. Lin, A. Mustafa, N. Pepin, A. Roulston, J. Lacoste, and J. Hiscott**. 1994. Viral induction of the human beta interferon promoter: Modulation of transcription by NF-kB/rel proteins and interferon regulatory factors. J Virol **68**:4707-4715.

45. **Garrison, M. M., D. A. Christakis, E. Harvey, P. Cummings, and R. L. Davis**. 2000. Systemic corticosteroids in infant bronchiolitis: A meta-analysis. Pediatrics **105**:E44.

46. **Ghildyal, R., J. Mills, M. Murray, N. Vardaxis, and J. Meanger**. 2002. Respiratory syncytial virus matrix protein associates with nucleocapsids in infected cells. J Gen.Virol. **83**:753-757.

47. **Ghosh, S. and D. Baltimore**. 1990. Activation in vitro of NF-kappa B by phosphorylation of its inhibitor I kappa B. Nature **344**:678-682.

48. **Gilmore, T. D. and M. Herscovitch**. 2006. Inhibitors of NF-kappaB signaling: 785 and counting. Oncogene **25**:6887-6899.

49. **Goebel, J., B. Estrada, J. Quinonez, N. Nagji, D. Sanford, and R. C. Boerth**. 2000. Prednisolone plus albuterol versus albuterol alone in mild to moderate bronchiolitis. Clin Pediatr (Phila) **39**:213-220.

50. **Graham, B. S., J. A. Rutigliano, and T. R. Johnson**. 2002. Respiratory syncytial virus immunobiology and pathogenesis. Virology **297**:1-7.

51. **Grosfeld, H., M. G. Hill, and P. L. Collins**. 1995. RNA replication by Respiratory Syncytial Virus (RSV) is directed by the N,P,and L proteins; Transcription also occurs under these conditions but requires RSV superinfection for efficient synthesis of full-length mRNA. J Virol **69**:5677-5686.

52. **Groskreutz, D. J., M. M. Monick, L. S. Powers, T. O. Yarovinsky, D. C. Look, and G. W. Hunninghake**. 2006. Respiratory syncytial virus induces TLR3 protein and protein kinase R, leading to increased double-stranded RNA responsiveness in airway epithelial cells. J Immunol **176**:1733-1740.

53. **Guerguerian, A. M., M. Gauthier, M. H. Lebel, C. A. Farrell, and J. Lacroix**. 1999. Ribavirin in ventilated respiratory syncytial virus bronchiolitis. A randomized, placebo-controlled trial. Am J Respir Crit Care Med **160**:829-834.

54. **Guo, B. and G. Cheng**. 2007. Modulation of the interferon antiviral response by the TBK1/IKKi adaptor protein TANK. J Biol Chem **282**:11817-11826.

55. **Haeberle, H., A. Casola, Z. Gatalica, S. Petronella, H.-J. Dieterich, P. B. Ernst, A. R. Brasier, and R. P. Garofalo**. 2004. IκB kinase is a critical regulator of chemokine expression and lung inflammation in respiratory syncytial virus infection. J Virol **78**:2232-2241.

56. **Hai, T., M. L. Yeung, T. G. Wood, Y. Wei, S. Yamaoaka, Z. Gatalica, K.-T. Jeang, and A. R. Brasier**. 2006. An Alternative Splice Product of IκB Kinase (IKK)-γ, IKK γ−Δ, Differentially Mediates Cytokine And HTLV-I Tax Induced NF-κB Activation. J Virol **80**:4227-4241.

57. **Harris, J. and D. Werling**. 2003. Binding and entry of respiratory syncytial virus into host cells and initiation of the innate immune response. Cell Microbiol. **5**:671-680.

58. **Haynes, L. M., D. D. Moore, E. A. Kurt-Jones, R. W. Finberg, L. J. Anderson, and R. A. Tripp**. 2001. Involvement of toll-like receptor 4 in innate immunity to respiratory syncytial virus. J.Virol. **75**:10730-10737.

59. **Hiscott, J., R. Lin, P. Nakhaei, and S. Paz**. 2006. MasterCARD: a priceless link to innate immunity. Trends Mol.Med. **12**:53-56.

60. **Hiscott, J., P. Pitha, P. Genin, H. Nguyen, C. Heylbroeck, Y. Mamane, M. Algarte, and R. Lin**. 1999. Triggering the interferon response: the role of IRF-3 transcription factor. J Interferon Cytokine Res **19**:1-13.

61. **Horvai, A., L. Xu, and e. Korzus**. 1997. Nuclear integration of JAK/STAT and RAS/AP-1 signaling by CBP and p300. Proc Natl Acad Sci USA **94**:1074-1079.

62. **Hu, W. H., X. M. Mo, W. M. Walters, R. Brambilla, and J. R. Bethea**. 2004. TNAP, a novel repressor of NF-kappaB-inducing kinase, suppresses NF-kappaB activation. J.Biol.Chem. **279**:35975-35983.

63. **Huang, Y. T., P. L. Collins, and G. W. Wertz**. 1985. Characterization   of the 10 proteins of human respiratory syncytial virus: identification of a fourth envelope-associated protein. Virus Res. **2**:157-173.

64. **Jamaluddin, M., A. Casola, R. P. Garofalo, Y. Han, T. Elliott, P. L. Ogra, and A. R. Brasier**. 1998. The major component of IkBa proteolysis occurs independently of the proteasome pathway in Respiratory Syncytial Virus-infected pulmonary epithelial cells. J Virol **72**:4849-4857.

65. **Jamaluddin, M., S. Wang, R. Garofalo, T. Elliott, A. Casola, S. Baron, and A. R. Brasier**. 2001. INFb mediates coordinate expression of antigen-processing genes in RSV infected pulmonary epithelial cells. Am J.Physiol.Lung Cell Mol Physiol **280**:L248-L257.

66. **Jin, D. Y., V. Giordano, K. V. Kibler, H. Nakano, and K. T. Jeang**. 1999. Role of adapter function in oncoprotein-mediated activation of NF-kappaB. Human T-cell leukemia virus type I Tax interacts directly with IkappaB kinase gamma. J.Biol.Chem. **274**:17402-17405.

67. **Johnson, C. L. and M. Gale, Jr.** 2006. CARD games between virus and host get a new player. Trends Immunol. **27**:1-4.

68. **Kang, D. C., R. V. Gopalkrishnan, Q. Wu, E. Jankowsky, A. M. Pyle, and P. B. Fisher**. 2002. mda-5: An interferon-inducible putative RNA helicase with double-stranded RNA-dependent ATPase activity and melanoma growth-suppressive properties. Proc.Natl.Acad.Sci.U.S.A **99**:637-642.

69. **Kanno, T., G. Franzoso, and U. Siebenlist**. 1994. Human T-cell leukemia virus type I Tax-protein-mediated activation of NF-kappa B from p100 (NF-kappa B2)-inhibited cytoplasmic reservoirs. Proc.Natl.Acad.Sci.U.S.A **91**:12634-12638.

70. **Kato, H., S. Sato, M. Yoneyama, M. Yamamoto, S. Uematsu, K. Matsui, T. Tsujimura, K. Takeda, T. Fujita, O. Takeuchi, and S. Akira**. 2005. Cell Type-Specific Involvement of RIG-I in Antiviral Response. Immunity **23**:19-28.

71. **Kato, H., O. Takeuchi, S. Sato, M. Yoneyama, M. Yamamoto, K. Matsui, S. Uematsu, A. Jung, T. Kawai, K. J. Ishii, O. Yamaguchi, K. Otsu, T. Tsujimura, C. S. Koh, C. Reis e Sousa, Y. Matsuura, T. Fujita, and S. Akira**. 2006. Differential roles of MDA5 and RIG-I helicases in the recognition of RNA viruses. Nature **441**:101-105.

72. **Kawai, T., K. Takahashi, S. Sato, C. Coban, H. Kumar, H. Kato, K. J. Ishii, O. Takeuchi, and S. Akira**. 2005. IPS-1, an adaptor triggering RIG-I- and Mda5-mediated type I interferon induction. Nat Immunol **6**:981-988.

73. **Kayagaki, N., M. Yan, D. Seshasayee, H. Wang, W. Lee, D. M. French, I. S. Grewal, A. G. Cochran, N. C. Gordon, J. Yin, M. A. Starovasnik, and V. M. Dixit**. 2002. BAFF/BLyS receptor 3 binds the B cell survival factor BAFF ligand through a discrete surface loop and promotes processing of NF-kappaB2. Immunity. **17**:515-524.

74. **Kim, H. W., J. G. Canchola, and C. D. Brandt**. 1969. Respiratory syncytial virus disease infants despite prior administration of antigenic inactivated vaccine. Am J Epidemiol **89**:422-434.

75. **Kim, T. K. and T. Maniatis**. 1997. The mechanism of transcriptional synergy of an in vitro assembled interferon-beta enhanceosome. Mol.Cell **1**:119-129.

76. **Kim, Y. S., S. A. Nedospasov, and Z. G. Liu**. 2005. TRAF2 plays a key, nonredundant role in LIGHT-lymphotoxin beta receptor signaling. Mol Cell Biol **25**:2130-2137.

77. **Kotelkin, A., I. M. Belyakov, L. Yang, J. A. Berzofsky, P. L. Collins, and A. Bukreyev**. 2006. The NS2 protein of human respiratory syncytial virus suppresses the cytotoxic T-cell response as a consequence of suppressing the type I interferon response. J.Virol. **80**:5958-5967.

78. **Kovacsovics, M., F. Martinon, O. Micheau, J. L. Bodmer, K. Hofmann, and J. Tschopp**. 2002. Overexpression of Helicard, a CARD-containing helicase cleaved during apoptosis, accelerates DNA degradation. Curr.Biol. **12**:838-843.

79. **Kumar, H., T. Kawai, H. Kato, S. Sato, K. Takahashi, C. Coban, M. Yamamoto, S. Uematsu, K. J. Ishii, O. Takeuchi, and S. Akira**. 2006. Essential role of IPS-1 in innate immune responses against RNA viruses. J.Exp.Med. **203**:1795-1803.

80. **Kurt-Jones, E. A., L. Popova, L. Kwinn, L. M. Haynes, L. P. Jones, R. A. Tripp, E. E. Walsh, M. W. Freeman, D. T. Golenbock, L. J. Anderson, and R. W. Finberg**. 2000. Pattern recognition receptors TLR4 and CD14 mediate response to respiratory syncytial virus. Nat Immunol **1**:398-401.

81. **Leader, S. and K. Kohlhase**. 2002. Respiratory syncytial virus-coded pediatric hospitalizations, 1997 to 1999. Pediatric Infectious Disease Journal **21**:629-632.

82. **Lee, M. S., R. E. Walker, and P. M. Mendelman**. 2005. Medical burden of respiratory syncytial virus and parainfluenza virus type 3 infection among US children. Implications for design of vaccine trials. Hum.Vaccin. **1**:6-11.

83. **Leung, A. K., J. D. Kellner, and H. D. Davies**. 2005. Respiratory syncytial virus bronchiolitis. J Natl Med Assoc. **97**:1708-1713.

84. **Li, K., Z. Chen, N. Kato, M. Gale, Jr., and S. M. Lemon**. 2005. Distinct Poly(I-C) and Virus-activated Signaling Pathways Leading to Interferon-{beta} Production in Hepatocytes. J.Biol.Chem. **280**:16739-16747.

85. **Liao, G., M. Zhang, E. W. Harhaj, and S. C. Sun**. 2004. Regulation of the NF-kappaB-inducing kinase by tumor necrosis factor receptor-associated factor 3-induced degradation. J.Biol.Chem. **279**:26243-26250.

86. **Lin, R., C. Heylbroeck, P. M. Pitha, and J. Hiscott**. 1998. Virus-dependent phosphorylation of the IRF-3 transcription factor regulates nuclear translocation, transactivation potential, and proteasome-mediated degradation. Mol.Cell Biol. **18**:2986-2996.

87. **Liu, P., M. Jamaluddin, K. Li, R. P. Garofalo, A. Casola, and A. R. Brasier**. 2007. Retinoic acid-inducible gene I mediates early antiviral response and toll-like receptor 3 expression in respiratory syncytial virus-infected airway epithelial cells. J Virol **81**:1401-1411.

88. **Liu, T., S. Castro, A. R. Brasier, M. Jamaluddin, R. P. Garofalo, and A. Casola**. 2004. Reactive oxygen species mediate virus-induced STAT activation: role of tyrosine phosphatases. J.Biol.Chem. **279**:2461-2469.

89. **Lu, R., W. C. Au, W. S. Yeow, N. Hageman, and P. M. Pitha**. 2000. Regulation of the promoter activity of interferon regulatory factor-7 gene. Activation by interferon snd silencing by hypermethylation. J.Biol.Chem. **275**:31805-31812.

90. **Luftig, M. A., E. Cahir-McFarland, G. Mosialos, and E. Kieff**. 2001. Effects of the NIK aly mutation on NF-kappaB activation by the Epstein-Barr virus latent infection membrane protein, lymphotoxin beta receptor, and CD40. J.Biol.Chem. **276**:14602-14606.

91. **Malinin, N. L., M. P. Boldin, A. V. Kovalenko, and D. Wallach**. 1997. MAP3K-related kinase involved in NF-kappaB induction by TNF, CD95 and IL-1. Nature **385**:540-544.

92. **Marie, I., J. E. Durbin, and D. Levy**. 1998. Differential viral induction of distinct interferon-alpha genes by positive feedback through interferon regulatory factor-7. EMBO J. **17**:6660-6669.

93. **Marsh, G. A. and G. A. Tannock**. 2005. The role of reverse genetics in the development of vaccines against respiratory viruses. Expert.Opin Biol Ther. **5**:369-380.

94. **Matsumoto, M., K. Funami, M. Tanabe, H. Oshiumi, M. Shingai, Y. Seto, A. Yamamoto, and T. Seya**. 2003. Subcellular localization of Toll-like receptor 3 in human dendritic cells. J.Immunol. **171**:3154-3162.

95. **Matsuyama, T., T. Kimura, M. Kitagawa, K. Pfeffer, T. Kawakami, N. Watanabe, T. M. Kundig, R. Amakawa, K. Kishihara, A. Wakeham, and .** 1993. Targeted disruption of IRF-1 or IRF-2 results in abnormal type I IFN gene induction and aberrant lymphocyte development. Cell **75**:83-97.

96. **May, M. J., F. D'Acquisto, L. A. Madge, J. Glockner, J. S. Pober, and S. Ghosh**. 2000. Selective inhibition of NF-kB activation by a peptide that blocks the interaction of NEMO with the IkB kinase complex. Science **289**:1550-1554.

97. **Meert, K. L., A. P. Sarnaik, M. J. Gelmini, and M. W. Lieh-Lai**. 1994. Aerosolized ribavirin in mechanically ventilated children with respiratory syncytial virus lower respiratory tract disease: a prospective, double-blind, randomized trial. Crit Care Med **22**:566-572.

98. **Mercurio, F., J. A. DiDonato, C. Rosette, and M. Karin**. 1993. p105 and p98 precursor proteins play an active role in NF-kB-mediated signal transduction. Genes Dev **7**:705-718.

99. **Mercurio, F., B. W. Murray, a. Shevchenko, B. L. Bennett, D. B. Young, J. W. Li, G. Pascual, A. Motiwala, H. Zhu, M. Mann, and A. M. Manning**. 1999. IkappaB kinase (IKK)-associated protein 1, a common component of the heterogeneous IKK complex. Mol Cell Biol **19**:1526-1538.

100. **Meylan, E., J. Curran, K. Hofmann, D. Moradpour, M. Binder, R. Bartenschlager, and R. Tschopp**. 2005. Cardif is an adaptor protein in the RIG-I antiviral pathway and is targeted by hepatitis C virus. Nature **437**:1167-1172.

101. **Meylan, E., K. Burns, K. Hofmann, V. Blancheteau, F. Martinon, M. Kelliher, and J. Tschopp**. 2004. RIP1 is an essential mediator of Toll-like receptor 3-induced NF-[kappa]B activation. Nat Immunol **5**:503-507.

102. **Mink, M. A., D. S. Stec, and P. L. Collins**. 1991. Nucleotide sequences of the 3' leader and 5' trailer regions of human respiratory syncytial virus genomic RNA. Virology **185**:615-624.

103. **Monick, M. M., T. O. Yarovinsky, L. S. Powers, N. S. Butler, A. B. Carter, G. Gudmundsson, and G. W. Hunninghake**. 2003. Respiratory syncytial virus up-regulates TLR4 and sensitizes airway epithelial cells to endotoxin. J.Biol.Chem. **278**:53035-53044.

104. **Nanbo, A., K. Inoue, K. Adachi-Takasawa, and K. Takada**. 2002. Epstein-Barr virus RNA confers resistance to interferon-alpha-induced apoptosis in Burkitt's lymphoma. EMBO J. **21**:954-965.

105. **Naumann, M., A. Nieters, E. N. Hatada, and C. Scheidereit**. 1993. NF-kappa B precursor p100 inhibits nuclear translocation and DNA binding of NF-kappa B/rel-factors. Oncogene **8**:2275-2281.

106. **O'Neill, L. A. and A. G. Bowie**. 2007. The family of five: TIR-domain-containing adaptors in Toll-like receptor signalling. Nat.Rev.Immunol. **7**:353-364.

107. **O'Neill, L. A., K. A. Fitzgerald, and A. G. Bowie**. 2003. The Toll-IL-1 receptor adaptor family grows to five members. Trends Immunol. **24**:286-290.

108. **Olmsted, R. A. and P. L. Collins**. 1989. The 1A protein of respiratory syncytial virus is an integral membrane protein present as multiple, structurally distinct species. J Virol. **63**:2019-2029.

109. **Opitz, B., M. Vinzing, V. van Laak, B. Schmeck, G. Heine, S. Gunther, R. Preissner, H. Slevogt, P. D. N'Guessan, J. Eitel, T. Goldmann, A. Flieger, N. Suttorp, and S. Hippenstiel**. 2006. Legionella pneumophila induces IFN beta in lung epithelial cells via IPS-1 and IRF3, which also control bacterial replication. J.Biol.Chem. **281**:36173-36179.

110. **Pande, V. and M. J. Ramos**. 2005. NF-kappaB in human disease: current inhibitors and prospects for de novo structure based design of inhibitors. Curr.Med.Chem. **12**:357-374.

111. **Pestka, S., C. D. Krause, and M. R. Walter**. 2004. Interferons, interferon-like cytokines, and their receptors. Immunol Rev **202**:8-32.

112. **Pichlmair, A., O. Schulz, C. P. Tan, T. I. Naslund, P. Liljestrom, F. Weber, and C. Reis e Sousa**. 2006. RIG-I-Mediated Antiviral Responses to Single-Stranded RNA Bearing 5'-Phosphates. Science **314**:997-1001.

113. **Pilar Orive, F. J., F. J. Casado, M. A. Garcia Teresa, N. A. Rodriguez, O. E. Quiroga, L. F. Cambra, J. J. Melendo, E. A. Ruiz, J. A. Soult Rubio, M. C. Calvo, and J. L. Teja Barbero**. 1998. [Acute respiratory infections in pediatric intensive care units. A multicenter prospective study]. An Esp.Pediatr **48**:138-142.

114. **Prince, G. A., S. J. Curtis, K. C. Yim, and D. D. Porter**. 2001. Vaccine-enhanced respiratory syncytial virus disease in cotton rats following immunization with Lot 100 or a newly prepared reference vaccine. J Gen.Virol. **82**:2881-2888.

115. **Randolph, A. G. and E. E. Wang**. 1996. Ribavirin for respiratory syncytial virus lower respiratory tract infection. A systematic overview. Arch.Pediatr Adolesc.Med **150**:942-947.

116. **Rodriguez, W. J., H. W. Kim, C. D. Brandt, R. J. Fink, P. R. Getson, J. Arrobio, T. M. Murphy, V. McCarthy, and R. H. Parrott**. 1987. Aerosolized ribavirin in the treatment of patients with respiratory syncytial virus disease. Pediatr Infect Dis J **6**:159-163.

117. **Rothwarf, D. M., E. Zandi, G. Natoli, and M. Karin**. 1998. IKK-gamma is an essential regulatory subunit of the IkappaB kinase complex. Nature **395**:297-300.

118. **Rudd, B. D., J. J. Smit, R. A. Flavell, L. Alexopoulou, M. A. Schaller, A. Gruber, A. A. Berlin, and N. W. Lukacs**. 2006. Deletion of TLR3 alters the pulmonary immune environment and mucus production during respiratory syncytial virus infection. J Immunol **176**:1937-1942.

119. **Rudd, B. D., E. Burstein, C. S. Duckett, X. Li, and N. W. Lukacs**. 2005. Differential Role for TLR3 in Respiratory Syncytial Virus-Induced Chemokine Expression. J.Virol. **79**:3350-3357.

120. **Saha, S. K., E. M. Pietras, J. Q. He, J. R. Kang, S.-Y. Liu, G. Oganesyan, A. Shahangian, B. Zarnegar, T. L. Shiba, Y. Wang, and G. Cheng**. 2006. Regulation of antiviral responses by a direct and specific interaction between TRAF3 and Cardif. EMBO J **25**:3237-3263.

121. **Sasai, M., M. Shingai, K. Funami, M. Yoneyama, T. Fujita, M. Matsumoto, and T. Seya**. 2006. NAK-associated protein 1 participates in both the TLR3 and the cytoplasmic pathways in type I IFN induction. J Immunol **177**:8676-8683.

122. **Sasaki, C. Y., T. J. Barberi, P. Ghosh, and D. L. Longo**. 2005. Phosphorylation of RelA/p65 on Serine 536 Defines an I{kappa}B{alpha}-independent NF-{kappa}B Pathway. J.Biol.Chem. **280**:34538-34547.

123. **Sato, M., N. Hata, M. Asagiri, T. Nakaya, T. Taniguchi, and N. Tanaka**. 1998. Positive feedback regulation of type I IFN genes by the IFN-inducible transcription factor IRF-7. FEBS Lett. **441**:106-110.

124. **Sato, M., N. Tanaka, N. Hata, E. Oda, and T. Taniguchi**. 1998. Involvement of the IRF family transcription factor IRF-3 in virus-induced activation of the IFN-beta gene. FEBS Lett. **425**:112-116.

125. **Scheinman, R. I., A. A. Beg, and A. S. Baldwin, Jr.** 1993. NF-kappa B p100 (Lyt-10) is a component of H2TF1 and can function as an I kappa B-like molecule. Mol.Cell Biol. **13**:6089-6101.

126. **Schindler, C., D. E. Levy, and T. Decker**. 2007. JAK-STAT Signaling: From Interferons to Cytokines. J.Biol.Chem. **282**:20059-20063.

127. **Schmidt, A. C., T. R. Johnson, P. J. Openshaw, T. J. Braciale, A. R. Falsey, L. J. Anderson, G. W. Wertz, J. R. Groothuis, G. A. Prince, J. A. Melero, and B. S. Graham**. 2004. Respiratory syncytial virus and other pneumoviruses: a review of the international symposium--RSV 2003. Virus Res. **106**:1-13.

128. **Schmidt, C., B. Peng, Z. Li, G. M. Sclabas, S. Fujioka, J. Niu, M. Schmidt-Supprian, D. B. Evans, J. L. Abbruzzese, and P. J. Chiao**. 2003. Mechanisms of Proinflammatory Cytokine-Induced Biphasic NF-[kappa]B Activation. Molecular Cell **12**:1287-1300.

129. **Schroder, M. and A. G. Bowie**. 2005. TLR3 in antiviral immunity: key player or bystander? Trends Immunol. **26**:462-468.

130. **Sen, G. C. and S. N. Sarkar**. 2005. Hitching RIG to action. Nat Immunol **6**:1074-1076.

131. **Senftleben, U., Y. Cao, G. Xiao, F. R. Greten, G. Krahn, G. Bonizzi, Y. Chen, Y. Hu, A. Fong, S. C. Sun, and M. Karin**. 2001. Activation by IKKalpha of a Second, Evolutionary Conserved, NF-kappa B Signaling Pathway. Science **293**:1495-1499.

132. **Seth, R. B., L. Sun, C. K. Ea, and Z. J. Chen**. 2005. Identification and Characterization of MAVS, a Mitochondrial Antiviral Signaling Protein that Activates NF-[kappa]B and IRF3. Cell **122**:669-682.

133. **Sharma, S., B. R. tenOever, N. Grandvaux, G. P. Zhou, R. Lin, and J. Hiscott**. 2003. Triggering the interferon antiviral response through an IKK-related pathway. Science **300**:1148-1151.

134. **Shikama, Y., M. Yamada, and T. Miyashita**. 2003. Caspase-8 and caspase-10 activate NF-kappaB through RIP, NIK and IKKalpha kinases. Eur.J.Immunol. **33**:1998-2006.

135. **Siebenlist, U., G. Franzoso, and K. Brown**. 1994. Structure, regulation and function of NF-kB. Annu.Rev.Cell Biol. **10**:405-455.

136. **Smith, D. W., L. R. Frankel, L. H. Mathers, A. T. Tang, R. L. Ariagno, and C. G. Prober**. 1991. A controlled trial of aerosolized ribavirin in infants receiving mechanical ventilation for severe respiratory syncytial virus infection. N.Engl.J Med **325**:24-29.

137. **Spann, K. M., K. C. Tran, B. Chi, R. L. Rabin, and P. L. Collins**. 2004. Suppression of the Induction of Alpha, Beta, and Gamma Interferons by the NS1

and NS2 Proteins of Human Respiratory Syncytial Virus in Human Epithelial Cells and Macrophages. J.Virol. **78**:4363-4369.

138. **Spann, K. M., K. C. Tran, and P. L. Collins**. 2005. Effects of Nonstructural Proteins NS1 and NS2 of Human Respiratory Syncytial Virus on Interferon Regulatory Factor 3, NF-{kappa}B, and Proinflammatory Cytokines. J.Virol. **79**:5353-5362.

139. **Stec, D. S., M. G. Hill, III, and P. L. Collins**. 1991. Sequence analysis of the polymerase L gene of human respiratory syncytial virus and predicted phylogeny of nonsegmented negative-strand viruses. Virology **183**:273-287.

140. **Sugrue, R. J., C. Brown, G. Brown, J. Aitken, and R. H. McL**. 2001. Furin cleavage of the respiratory syncytial virus fusion protein is not a requirement for its transport to the surface of virus-infected cells. J.Gen.Virol. **82**:1375-1386.

141. **Sun, S. C., P. A. Ganchi, C. Beraud, D. W. Ballard, and W. C. Greene**. 1994. Autoregulation of the NF-kappa B transactivator RelA (p65) by multiple cytoplasmic inhibitors containing ankyrin motifs. Proc Natl Acad Sci USA **91**:1346-1350.

142. **Tal, G., A. Mandelberg, I. Dalal, K. Cesar, E. Somekh, A. Tal, A. Oron, S. Itskovich, A. Ballin, S. Houri, A. Beigelman, O. Lider, G. Rechavi, and N. Amariglio**. 2004. Association between common Toll-like receptor 4 mutations and severe respiratory syncytial virus disease. J.Infect.Dis. **189**:2057-2063.

143. **Tanabe, M., M. Kurita-Taniguchi, K. Takeuchi, M. Takeda, M. Ayata, H. Ogura, M. Matsumoto, and T. Seya**. 2003. Mechanism of up-regulation of human Toll-like receptor 3 secondary to infection of measles virus-attenuated strains. Biochem.Biophys.Res.Commun. **311**:39-48.

144. **Taniguchi, T., K. Ogasawara, A. Takaoka, and N. Tanaka**. 2001. IRF family of transcription factors as regulators of host defense. Annu.Rev.Immunol. **19**:623-655.

145. **Teng, M. N. and P. L. Collins**. 1998. Identification of the respiratory syncytial virus proteins required for formation and passage of helper-dependent infectious particles. J Virol. **72**:5707-5716.

146. **Thompson, A. J. and S. A. Locarnini**. 2007. Toll-like receptors, RIG-I-like RNA helicases and the antiviral innate immune response. Immunol.Cell Biol.

147. **Thompson, W. W., D. K. Shay, E. Weintraub, L. Brammer, N. Cox, L. J. Anderson, and K. Fukuda**. 2003. Mortality associated with influenza and respiratory syncytial virus in the United States. JAMA **289**:179-186.

148. **Tian, B. and A. R. Brasier**. 2003. Identification of a nuclear factor kappa B-dependent gene network. Recent Prog.Horm Res **58**:95-130.

149. **Tian, B., Y. Zhang, B. A. Luxon, R. P. Garofalo, A. Casola, M. Sinha, and A. R. Brasier**. 2002. Identification Of NF-κB Dependent Gene Networks In Respiratory Syncytial Virus-Infected Cells. J Virol **76**:6800-6814.

150. **Tissari, J., J. Siren, S. Meri, I. Julkunen, and S. Matikainen**. 2005. IFN-alpha enhances TLR3-mediated antiviral cytokine expression in human endothelial and epithelial cells by up-regulating TLR3 expression. J.Immunol. **174**:4289-4294.

151. **Ueba, O.** 1978. Respiratory syncytial virus: I. concentration and purification of the infectious virus. Acta.Med.Okayama **32**:265-272.

152. **van der Sluijs, K. F., E. L. van, M. Nijhuis, R. Schuurman, S. Florquin, H. M. Jansen, R. Lutter, and P. T. van der**. 2003. Toll-like receptor 4 is not involved in host defense against respiratory tract infection with Sendai virus. Immunol.Lett. **89**:201-206.

153. **Veerappan, A. and A. Kumar**. 1996. Role of steroids in croup and beta agonists in bronchiolitis. Indian J Pediatr **63**:577-581.

154. **Vermeulen, L., G. De Wilde, P. Van Damme, W. Vanden Berghe, and G. Haegeman**. 2003. Transcriptional activation of the NF-kappaB p65 subunit by mitogen- and stress-activated protein kinase-1 (MSK1). EMBO J **22**:1313-1324.

155. **Wingender, E., P. Dietze, H. Karas, and R. Knuppel**. 1996. TRANSFAC: a database on transcription factors and their DNA binding sites. Nucleic Acids Res. **24**:238-241.

156. **Xiao, G. and S. C. Sun**. 2000. Negative regulation of the nuclear factor kappa B-inducing kinase by a cis-acting domain. J.Biol.Chem. **275**:21081-21085.

157. **Xiao, G., A. Fong, and S. C. Sun**. 2004. Induction of p100 Processing by NF-{kappa}B-inducing Kinase Involves Docking I{kappa}B Kinase {alpha} (IKK{alpha}) to p100 and IKK{alpha}-mediated Phosphorylation. J.Biol.Chem. **279**:30099-30105.

158. **Xiao, G., E. W. Harhaj, and S. C. Sun**. 2001. NF-[kappa]B-Inducing Kinase Regulates the Processing of NF-[kappa]B2 p100. Molecular Cell **7**:401-409.

159. **Xu, L. G., Y. Y. Wang, K. J. Han, L. Y. Li, Z. Zhai, and H. B. Shu**. 2005. VISA Is an Adapter Protein Required for Virus-Triggered IFN-b Signaling. Molecular Cell **19**:727-740.

160. **Yamaoka, S., G. Courtois, C. Bessia, S. T. Whiteside, R. Weil, F. Agou, H. E. Kirk, R. J. Kay, and A. Israel**. 1998. Complementation cloning of NEMO, a component of the IkB kinase complex essential for NF-kB activation. Cell **93**:1231-1240.

161. **Ye, J., X. Xie, L. Tarassishin, and M. S. Horwitz**. 2000. Regulation of the NF-kappaB activation pathway by isolated domains of FIP3/IKKgamma, a component of the IkappaB-alpha kinase complex. J.Biol.Chem. **275**:9882-9889.

162. **Yin, L., L. Wu, H. Wesche, C. D. Arthur, J. M. White, D. V. Goeddel, and R. D. Schreiber**. 2001. Defective lymphotoxin-beta receptor-induced NF-kappaB transcriptional activity in NIK-deficient mice. Science **291**:2162-2165.

163. **Yoneyama, M., W. Suhara, Y. Fukuhara, M. Fukuda, E. Nishida, and T. Fujita**. 1998. Direct triggering of the type I interferon system by virus infection: activation of a transcription factor complex containing IRF-3 and CBP/p300. EMBO J. **17**:1087-1095.

164. **Yoneyama, M., M. Kikuchi, T. Natsukawa, N. Shinobu, T. Imaizumi, M. Miyagishi, K. Taira, S. Akira, and T. Fujita**. 2004. The RNA helicase RIG-I has an essential function in double-stranded RNA-induced innate antiviral responses. Nat Immunol **5**:730-737.

165. **Zandi, E. and M. Karin**. 1999. Bridging the gap: composition, regulation, and physiological function of the IkappaB kinase complex. Mol.Cell Biol. **19**:4547-4551.

166. **Zhang, W., H. Yang, X. Kong, S. Mohapatra, H. Juan-Vergara, G. Hellermann, S. Behera, R. Singam, R. F. Lockey, and S. S. Mohapatra**. 2005. Inhibition of respiratory syncytial virus infection with intranasal siRNA nanoparticles targeting the viral NS1 gene. Nat.Med. **11**:56-62.

167. **Zhang, Y., M. Jamaluddin, B. Tian, S. Wang, A. Casola, R. P. Garofalo, and A. R. Brasier**. 2003. Ribavirin treatment upregulates anti-viral gene expression via the IFN-stimulated response element in RSV infected epithelial cells. J Virol **78**:5933-5947.

168. **Zhang, Y., B. A. Luxon, A. Casola, R. P. Garofalo, M. Jamaluddin, and A. R. Brasier**. 2001. Expression Of RSV-Induced Chemokine Gene Networks In Lower Airway Epithelial Cells Revealed By cDNA Microarrays. J Virol **75**:9044-9058.

169. **Zhao, T., L. Yang, Q. Sun, M. Arguello, D. W. Ballard, J. Hiscott, and R. Lin**. 2007. The NEMO adaptor bridges the nuclear factor-kappaB and interferon regulatory factor signaling pathways. Nat.Immunol. **8**:592-600.

170. **Zheng, S., M. C. Brown, and S. M. Taffet**. 1993. Lipopolysaccharide stimulates both nuclear localization of the nuclear factor kappa B 50-kDa subunit and loss of the 105-kDa precursor in RAW264 macrophage-like cells. J.Biol.Chem. **268**:17233-17239.

171. **Zhong, H., R. E. Voll, and S. Ghosh**. 1998. Phosphorylation of NF-kB p65 by PKA stimulates transcriptional activity by promoting a novel bivalent interaction with the coactivator CBP/p300. Molecular Cell **1**:661-671.

172. **Zhong, H., M. J. May, E. Jimi, and S. Ghosh**. 2002. The Phosphorylation Status of Nuclear NF-[kappa]B Determines Its Association with CBP/p300 or HDAC-1. Molecular Cell **9**:625-636.

VITA

Ping Liu was born on Noverber 11, 1974 to Zhenru Li and Guiqi Liu.   While at graduate school, Ping is very active in his acdemic education.   Ping published two papers as the first author and wrote a book chapter on the study of respiratory syncytial virus. He also did several important presentations and posters in local and national conferences.

Ping can be contacted at 232 South Woods Mill Roads, Chesterfield, MO

Education

M.D., July 2000, The Beijing University of Traditional Chinese Medicine, Beijing, China

Publications

Liu P., Jamaluddin M., Li K., Garofalo RP., Casola A., Brasier AR.. Retinoic acid-inducible gene I mediates early antiviral response and Toll-like receptor 3 expression in respiratory syncytial virus-infected airway epithelial cells. Journal of Virology. 2007, Feb; 81(3):1401-11.

Liu P., Li K., Garofalo RP., Casola A., Brasier AR.. RSV-induces RelA release from cytoplasmic 100 kDa NF-κB2 complexes via a novel retinoic acid inducible gene-I-NF-κB inducing kinase (NIK) signaling pathway. (Submitted)

Brasier AR., Liu P., Tian B., Sanjeev C. Signaling pathways in the host cell response to RSV infection. Host Gene Responses to RNA Viral Infection. (In press)

Haaland D., Sinclair M., Tian B., Liu P., Brasier AR.. (2007, September). Hypespectral confocal fluorescence imaging of cells. Poster presented at: Society of Photo-Optical Instrumentation Engineering (SPIE); Boston, MA